Temperature-Time Modeling of Spent Fuel Cladding in Dry Storage Casks

Spent Fuel and Waste Disposition

Prepared for
US Department of Energy
Spent Fuel and Waste Science and Technology

David J. Richmond
Ben J. Jensen, Justin Clarity
Megan E. Higley, Nicholas Kucinski

March 31, 2024

M3SF-24PN010203025
PNNL-35805

SUMMARY

This report uses thermal and decay heat modeling to investigate spent fuel performance and the potential for spent nuclear fuel (SNF) cladding to anneal in dry storage conditions. Annealing is an important feature to investigate in SNF cladding because it has a direct relationship to cladding response in storage, transportation, and disposal conditions. Annealed SNF cladding may have lower yield strength than as-discharged SNF cladding, which is a consideration for SNF performance under external loads. The potential for annealing and the effects on SNF cladding performance are the driver for this work, however, are outside of the scope of this report.

The modeling focused on three representative storage systems, the TN-32B, MAGNASTOR with a Transportable Storage Canister (TSC)-37 canister, and NUHOMS Advanced Horizontal Storage Module (AHSM) with a 32PTH2 canister. This covers the vertical dual-purpose, vertical ventilated, and horizontal ventilated casks, respectively. Decay heat modeling using high and low enrichment assemblies was used to bound the decay heat curves that might be expected in dry storage. To bound the temperature relationship, the storage casks were modeled starting at the design basis heat loads with heat decaying through time. Although the results are bounding there is not an attempt to maximize conservatism, rather the intent is to form a reasonable upper limit on temperature that will be broadly applicable to the U.S. cask fleet. This will allow materials testing to focus on relevant conditions for annealing that may affect the U.S. spent fuel inventory.

The results show a clear dependence on heat load pattern in time in Figure S-1 and Figure S-2. This dependence is due to the different assembly decay heat curves for different assemblies in casks with non-uniform decay heat patterns. It shows the need for careful decay heat modeling when examining in service SNF cladding temperatures that are less than the cask design basis heat load. The body of the report shows percent cladding area above multiple cutoff temperatures of 275°C, 300°C and 350 °C. These results can be used to inform testing and conclusions about SNF cladding performance through time and the potential for cladding annealing during dry storage.

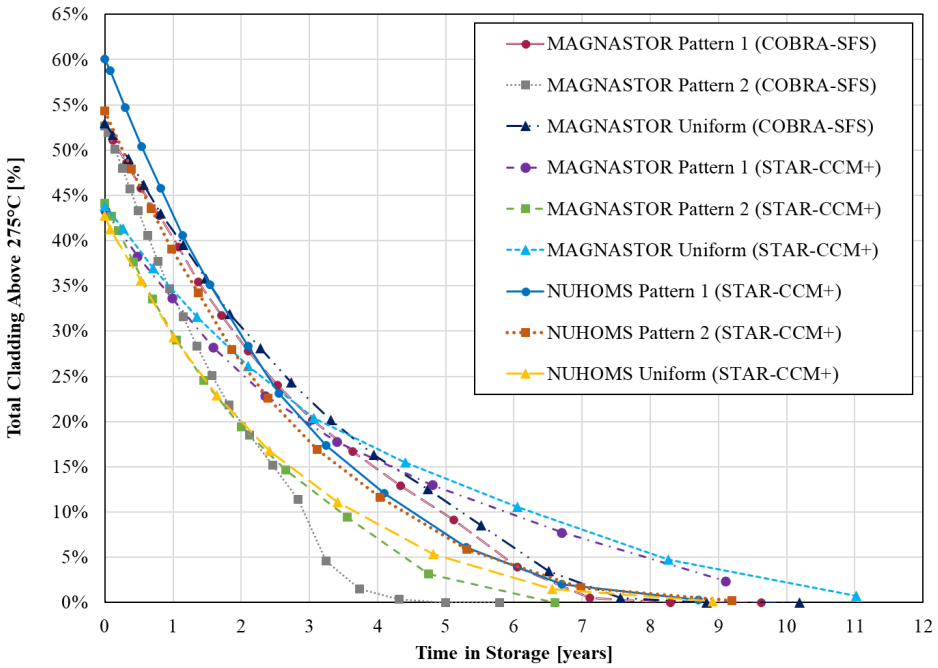

Figure S-1. Time in Storage vs Percentage Cladding above 275 °C

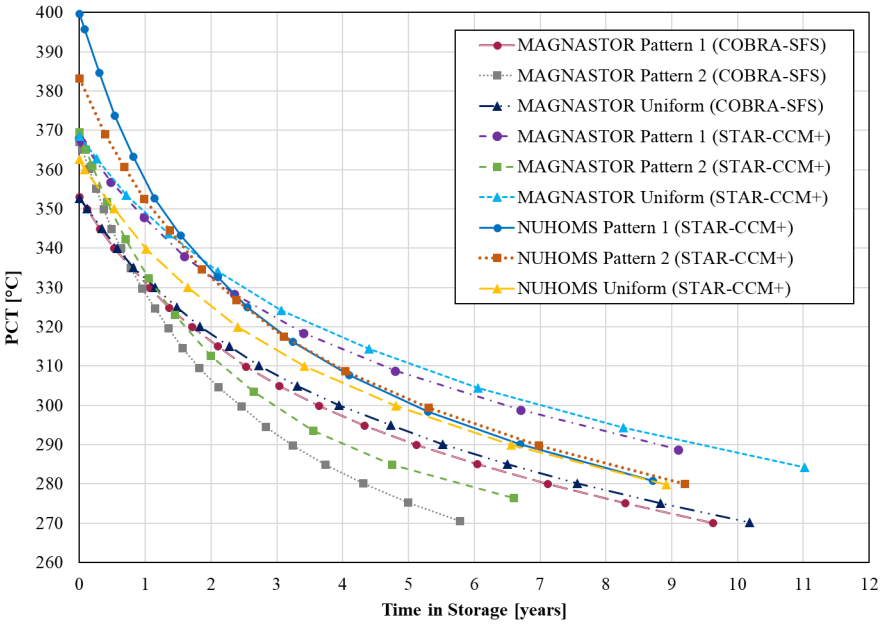

Figure S-2. Time in Storage vs. PCT

ACKNOWLEDGEMENTS

The authors would like to acknowledge the important review work of Sarah Suffield and Steve Ross for reviewing this report, the Department of Energy Spent Fuel and Waste Science and Technology program for sponsoring this work, and Brady Hanson and Ricardo Torres for their technical guidance and project management assistance.

This page is intentionally left blank.

CONTENTS

LIST OF FIGURES

LIST OF TABLES

ACRONYMS

BWR	boiling water reactor
DOE	US Department of Energy
HEHB	High Enrichment High Burnup
HLZC	heat loading zone configuration
ISFSI	independent spent fuel storage installation
LELB	Low Enrichment Low Burnup
MCT	minimum cladding temperature
MTU	Metric Tons of Uranium
PCT	peak cladding temperature
PNNL	Pacific Northwest National Laboratory
PWR	pressurized water reactor
SFWST	Spent Fuel and Waste Science and Technology
SNF	spent nuclear fuel
UDB	Unified Database

This page is intentionally left blank.

TEMPERATURE-TIME MODELING OF SPENT FUEL CLADDING IN DRY STORAGE CASKS

1. INTRODUCTION

The purpose of this modeling work is to inform test parameters for the Department of Energy (DOE) Spent Fuel and Waste Science and Technology (SFWST) sibling pin testing campaign. Early materials testing of sibling pins shows that there is the potential for spent nuclear fuel (SNF) cladding to anneal in dry storage conditions. The extent of SNF cladding annealing would be affected by the temperature and the time fuel is stored at this temperature. Annealing is an important feature to investigate in SNF cladding because it has a direct relationship to cladding response in storage, transportation, and disposal conditions. Annealed SNF cladding may have lower yield strength than as-discharged SNF cladding, which is a consideration for SNF performance under external loads. The potential for annealing and the effects on SNF cladding performance are the driver for this work, however, are outside of the scope of this report.

This report is focused on thermal modeling of normal storage conditions in spent fuel storage casks. The primary goal is to characterize the time-temperature relationship for SNF cladding in dry storage through a variety of metrics. One key metric that will be discussed is percent cladding surface area above a cutoff temperature. This is important because it can be used to understand the amount of cladding and fuel assemblies that may be at risk for annealing. The cutoff temperature at which annealing may occur requires more research to define and as such this report will examine multiple potentially relevant temperature cutoffs. The models used are representative of conditions in the dry storage fleet in the United States (U.S.) and research was done to define the decay heat curve with respect to time that would be reasonable for pressurized water reactor (PWR) fuel assemblies. The storage casks modeled were the TN-32B, the MAGNASTOR™ with TSC-37 canister, and NUHOMS AHSM with a 32PTH2. This covers the vertical dual-purpose, vertical ventilated, and horizontal ventilated casks, respectively. Decay heat modeling using high and low enrichment assemblies was used to bound the decay heat curves that might be expected in dry storage. To bound the temperature relationship, the storage casks were modeled starting at the design basis heat loads with heat decaying through time. Although the results are bounding there is not an attempt to maximize conservatism, rather the intent is to form a reasonable upper limit on temperature that will be broadly applicable to the U.S. cask fleet. This will allow materials testing to focus on relevant conditions for annealing that may affect the U.S. SNF inventory.

This page is intentionally left blank.

2. MODELING APPROACH

Estimating the extent of SNF cladding annealing requires an interdisciplinary modeling approach. In this case: nuclear, materials, and thermal specialties were employed to determine the decay heats applied to thermal models and temperature results that may be of interest for materials testing. Three cask designs were selected for thermal modeling to cover every major category of cask in use in the U.S. Sections 2.1 – 2.4 discuss the casks and modeling process. After cask designs were selected, decay heat was modeled for loading patterns that cover the design basis through 100 years after initial storage. Models of enrichment, burnup, and reactor operating conditions were selected to bound typical storage conditions and comparisons are provided in Section 2.5.

2.1 Cask Design Selection

The three cask types used most often in the U.S. are bolted dual-purpose, vertical ventilated, and horizontal ventilated. There is also an increasing use of underground ventilated designs, however, the thermal behavior of these designs are similar to vertical ventilated casks. This makes the TN-32B, MAGNASTOR, and NUHOMS designs relevant to model and capture a wide array of thermal behavior. Each system used in this report is modeled with a PWR fuel configuration. This generally generates more bounding temperatures and has direct application to the sibling pin test campaign, since the sibling pins are pulled from PWR fuel assemblies used in a Westinghouse type plant. All the casks were modeled with Westinghouse 17×17 OFA fuel designs. The 17×17 design tends to be thermally limiting and design variations within 17×17 assemblies like those seen from more modern Framatome and Westinghouse designs have minimal impact on SNF thermal performance.

2.1.1 TN-32B

The TN-32B is a bolted lid dual purpose cask designed by Orano-TN (Transnuclear Inc. 2012). It holds 32 PWR assemblies and has a maximum heat load of 32.7 kW. This heat load is uniformly distributed across the 32 assemblies which results in 1020 W heat load per assembly. There are no preferential heat load maps for the TN-32B unlike the other two cask designs studied in this report. The general structure consists of a stainless steel inner cavity with a stainless steel and aluminum basket. Shielding is provided by the steel and aluminum body structure along with an integral resin neutron shield. The internal atmosphere is helium with a 2.2 atm absolute pressure as the design pressurization. Primary heat transfer in the casks is via conduction out of the basket and through the walls of the casks where it is removed to the environment via radiation and convection. Figure 1 shows an example of a TN-32B in its storage configuration outside.

Figure 1. TN32B Cask in Storage (note: extra equipment is non-standard for data collection)

2.1.2 MAGNASTOR TSC-37

The NAC MAGNASTOR (NAC International 2015, Fort, Michener et al., 2016) is a vertical ventilated cask consisting of a welded canister and concrete overpack. It can hold boiling water reactor (BWR) or PWR assemblies. In this case a TSC-37 PWR canister is modeled. This design relies on conduction through the basket and internal helium circulation to remove heat from the fuel to the canister surface. At that point, the overpack has an annulus with inlet and outlet vents to provide primary heat rejection through convection to the environment. The primary shielding is provided by the concrete structure of the overpack and the canister/overpack lid structure. The design basis heat load for the TSC-37 is 35.5 kW for all heat loading zone configurations (HLZC). Figure 2 shows a diagram of the MAGNASTOR canister in its overpack.

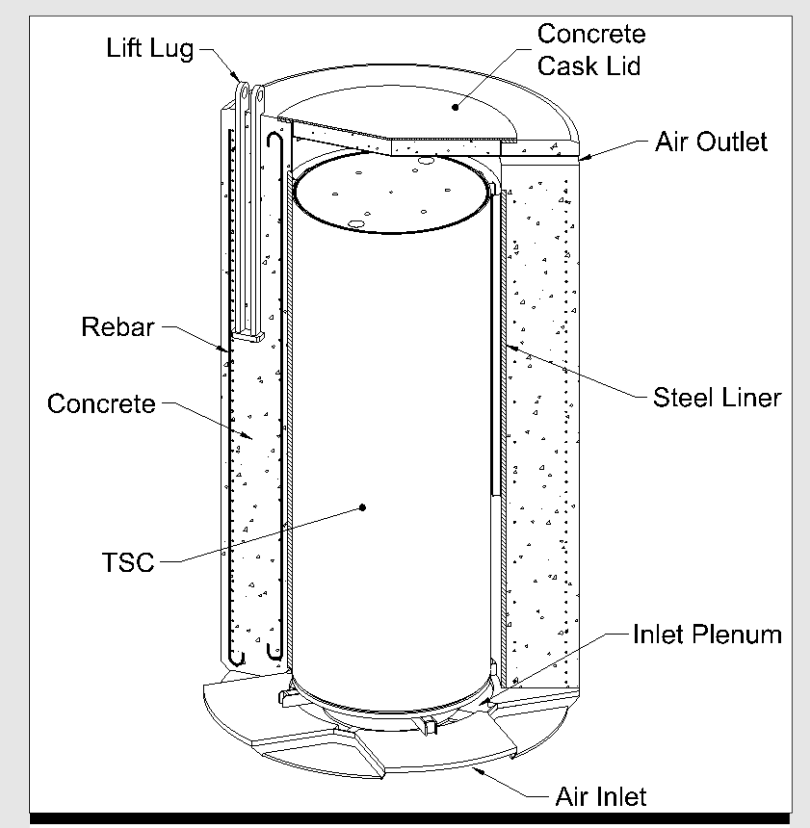

Figure 2. MAGNASTOR diagram (not to scale)

2.1.2.1 MAGNASTOR Load Maps

The MAGNASTOR loading maps are presented in Figure 3 and Table 1. Three different configurations are analyzed in this report.

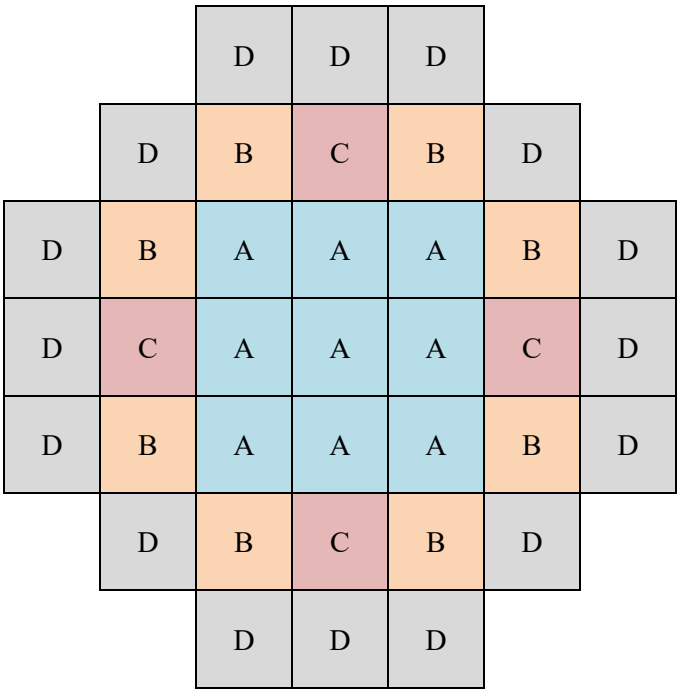

Figure 3. MAGNASTOR Heal load zone map

Table 1. MAGNASTOR Design basis heat loading pattern (NAC International 2015)

	Zone A [W/assembly]	Zone B [W/assembly]	Zone C [W/assembly]	Zone D [W/assembly]
Uniform	959	959	959	959
HLZC 1	922	1200	1200	800
HLZC 2	513	1300	1800	830
Number of Assemblies	9	8	4	16

2.1.3 NUHOMS HSMH 32PTH2

The NUHOMS design by Orano-TN is a horizontal storage module which can accept welded stainless-steel canisters of varying assembly types. The 32PTH2 canister is similar to many deployed canisters and holds 32 PWR assemblies. The design is very similar to the 32PTH canister except for minor differences in canister wall thickness. In the NUHOMS HSMH (horizontal storage module) the maximum heat load is dependent on the HLZC. The total decay heat load for the uniform, HLZC 1, and HLZC 2 are 32.0 kW, 37.2 kW, and 35.2 kW, respectively. Canisters are loaded in the front of the storage module horizontally and heat rejection is provided though conduction through the basket to the canister wall where ventilation airflow moves it to the environment. Shielding is provided by the large, shielded vault door and the concrete structure of the module.

2.1.3.1 Load Maps

Three different heat load configurations are modeled in the 32PTH2 canister and are presented in tabular and graphical form in Table 2 and Figure 4.

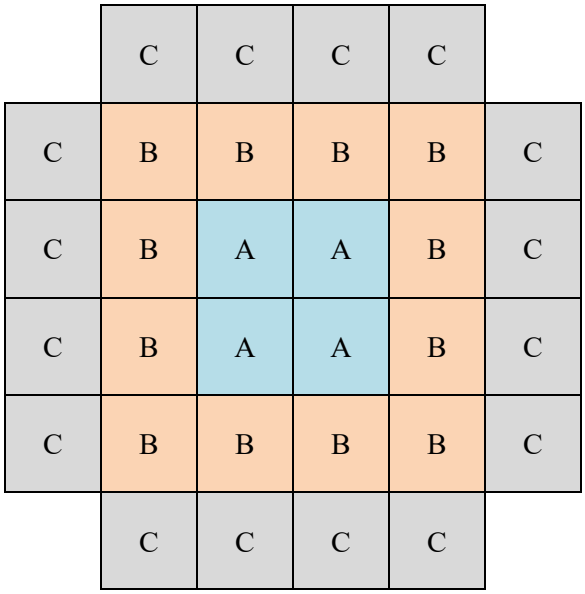

Figure 4. NUHOMS 32PTH2 canister heat loading zone configuration map

Table 2. NUHOMS 32PTH2 heat loading zone configurations (Transnuclear Inc. 2006)

	Zone A [W/Assembly]	Zone B [W/Assembly]	Zone C [W/Assembly]	Total Decay Heat [kW]
Uniform	1000	1000	1000	32.0
HLZC 1	800	1500	1000	37.2
HLZC 2	900	1300	1000	35.2
Number of Assemblies	4	12	16	

2.2 Modeling Conservatism and Uncertainty

The focus of this modeling is to produce temperatures and decay heats that are near the top of a realistic range seen in the field, not to produce the highest possible temperatures. To accomplish this, decay heat modeling uses conservative assumptions of burnup, enrichment, and reactor operating conditions. However, there is no assumption that all assemblies will be at the maximum burnup or enrichment allowable because this is not realistic to what is currently loaded into dry storage in the U.S. or what will be loaded in the near and medium term. Similarly, ambient temperature boundary and solar conditions are analyzed with relatively moderate temperatures, not the maximum. By assuming the casks are loaded to the design basis at the start of their storage life there is an inherent conservatism to the results. This is because constraints such as uncertainty in decay heat analysis and availability of fuel for loading make it impossible to load a cask to the actual design basis heat load in the field.

Formal uncertainty analysis was not conducted for all of the thermal models. Because the modeling is used for scoping and there is no experimental comparison, a full uncertainty analysis would be of limited value. Experience shows reasonable uncertainties on peak cladding temperatures (PCTs) will be on the order of ±15 °C. (Richmond, Suffield et al., 2022).

2.3 Thermal Code Selection

STAR-CCM+ (Siemens Industries Digital Software 2022) and COBRA-SFS (Richmond, Hom et al. 2023) were used to model casks in this report. Both of these codes have been used extensively for thermal modeling by the DOE SFWST program and there is a validation pedigree associated with these modeling tools. The validation is primarily through the High Burnup Demonstration Research Project Cask and the 1980s TAN facility testing, along with other small scale validation tests (Richmond, Hom et al., 2023). STAR-CCM+ is a general purpose computational fluid dynamics code and COBRA-SFS is a purpose-built thermal analysis code with specific features to spent fuel storage and transportation casks. COBRA-SFS uses a finite difference formulation to model each fuel assembly in detail. This allows individual rod temperatures to be modeled and a direct representation of temperatures at cladding surfaces to be output. The STAR-CCM+ models use a porous media model to represent the fuel assemblies. The porous media model approximates the thermal conductivity and flow resistance of the fuel assemblies as a homogenous material which improves runtime. Although this does not provide direct modeling of the clad surface temperature, methods are used to relate the porous region temperatures to clad surface temperatures based on the location and area weighting of temperature results. Different codes were used to model the different cask designs. Where possible, multiple codes are used as a confirmatory modeling approach even if not all results are shown in this report. Table 3 shows which casks were modeled with each code.

Table 3. Thermal Code Comparison

Model	COBRA-SFS	STAR-CCM+ Porous
TN-32B	YES	YES
MAGNASTOR TSC-37	YES	YES
NUMHOMS HSMH 32PTH2	NO	YES

2.4 Boundary Condition Selection

The modeling in this report uses steady state models. This makes any change in boundary conditions a highly direct effect. Most importantly, the ambient temperature selected has a nearly one to one correlation with PCTs in most models. This is compared to transient modeling where boundary condition changes can cause delayed cladding temperature changes. Solar insolation can have some effect, especially on bolted casks, but is not a large contributor to temperature because of its relatively low power compared to the heat load of the fuel and the relatively large size of a spent fuel cask. In a ventilated system, the effect is even less pronounced because the primary boundary heat transfer surface of the canister is not exposed to the sun. In this way, the overpack acts as a shade allowing direct cooling from outside air. An ambient outside temperature of 25°C (77°F) was chosen as a relatively warm average air temperature to model. This chosen temperature is in line with the overall philosophy of conservative but not overly bounding model choices. Solar insolation was selected as the average insolation from North Anna, Virginia (Richmond and Jensen 2022). This provides conditions that are approximately average for the continental United States based on latitude. The ground temperature is modeled at marginally different locations in different models. In some cases, it is the soil surface temperature and in others it is the temperature below the concrete independent spent fuel storage installation (ISFSI) pad which may be multiple feet thick in a typical deployment. In either case, 10 °C is a reasonable estimate in the continental United States. Because the ground temperature is a heat sink temperature in these models it would be an over estimation to model it at the air temperature. The assumed temperature boundary conditions are summarized in Table 4.

Table 4. Model Boundary Conditions

Ambient Air Temp (°C)	25
Ground Temp (°C)	10
Side Solar (W/m^2)	175
Top Solar (W/m^2)	338

2.5 Decay Heat

The cladding temperature analyses in this report were performed for various cask designs, each with different possible loading patterns. The temperature results are directly dependent on assembly decay heat. The design basis heat load of the cask provides a starting point for heat loading, but to understand the change in time more sophisticated analysis is needed. This section provides the data used to analyze decay heat through time and also compares to in -service casks using the STANDARDS (Stefanovic, Banerjee et al., 2023) database.

2.5.1 Decay Heat Limits

The allowable contents section of a storage cask Final Safety Analysis Report limits the decay heat of the cask. Typically, these limits are imposed for each storage location within the basket. Decay heat limits from different loading patterns and cask designs were used in the cladding temperature analyses. The cask designs, loading patterns, and associated decay heat limits used in this analysis are described in Section 2.1.

2.5.2 Selection of Assembly Characteristics

A goal of this work was to examine the variability in evolution of thermal characteristics of cask systems as a function of time following loading. To provide a variety of time-dependent decay heat trajectories, an envelope of fuel characteristics was examined. Management of nuclear fuel has evolved from early operation where low enriched assemblies were used and low discharge burnups were achieved to modern reactor operation where higher initial fuel enrichments are used and higher discharge burnups are achieved. The amount of cooling time necessary to meet the decay heat limits storage casks will be longer for high enrichment/high burnup (HEHB) assemblies than it will be for low enrichment/low burnup (LELB) assemblies. Additionally, once the assembly decay heat meets the limit for storage, the rate of decrease of decay heat with cooling time will vary between the LELB and HEHB groups.

To develop reasonable estimates good combinations of enrichment and burnup should be used for the LELB and HEHB fuel. Information from the unified database (UDB) (Banerjee, Clarity et al., 2023) was used for these estimates. The data used here are for Westinghouse 17 × 17 assembly with the 0.374-inch fuel rod outer diameter because they represent the largest group of fuel in the U.S. inventory (Banerjee, Clarity et al., 2023). Examples of these fuel types are assemblies with GC-859 type codes W1717WL, W1717B, W1717WVH, W1717WR, and W1717WR2, all of which have initial uranium loadings of approximately 460 kgU. To simplify the discussion of these fuel types, they will collectively be referred to as W1717WL because this was the first such type in the set. To develop appropriate combinations of enrichment and burnup, low and high enrichment ranges of 1.5 – 2.5 wt. % and 4.0 – 5.0 wt. % were selected and the averages of the enrichments and the burnups of the W1717WL fuel from the UDB were calculated. The enrichment and burnup of the LELB fuel was found to be 2.11 wt. % and 19,401 MWd/MTU and the enrichment and burnup of the HEHB fuel was found to be 4.40 wt. % and 47,737

MWd/MTU. The LELB and HEHB data sets and average enrichments and burnups are depicted in Figure 5.

To further explore the potential variability in potential thermal trajectories, the conditions under which the fuel was depleted to discharge burnups was varied. The STANDARDS tool has two sets of operating history assumptions available, which are referred to as conservative and nominal. The conservative assumptions include operating parameters which harden the neutron spectrum during depletion and lead to increased generation of actinides. The nominal assumptions include parameters that are intended to be representative of a typical assembly during depletion. The increased actinide composition of the fuel results in increased decay heat for an assembly for a given burnup and enrichment, particularly for longer cooling times. For the W1717WL the conservative operating history parameters include depletion with 24 Pyrex burnable absorber rods, a soluble boron concentration of 1000 ppm, and a moderator density of 0.67 g/cm^3. The nominal operating history assumptions assume no burnable absorber is present, a soluble boron concentration of 800 ppm, and a moderator density of 0.71 g/cm^3. All calculations assumed two 18-month cycles of irradiation. The LELB and HEHB conservative and nominal calculation parameters are summarized in Table 5.

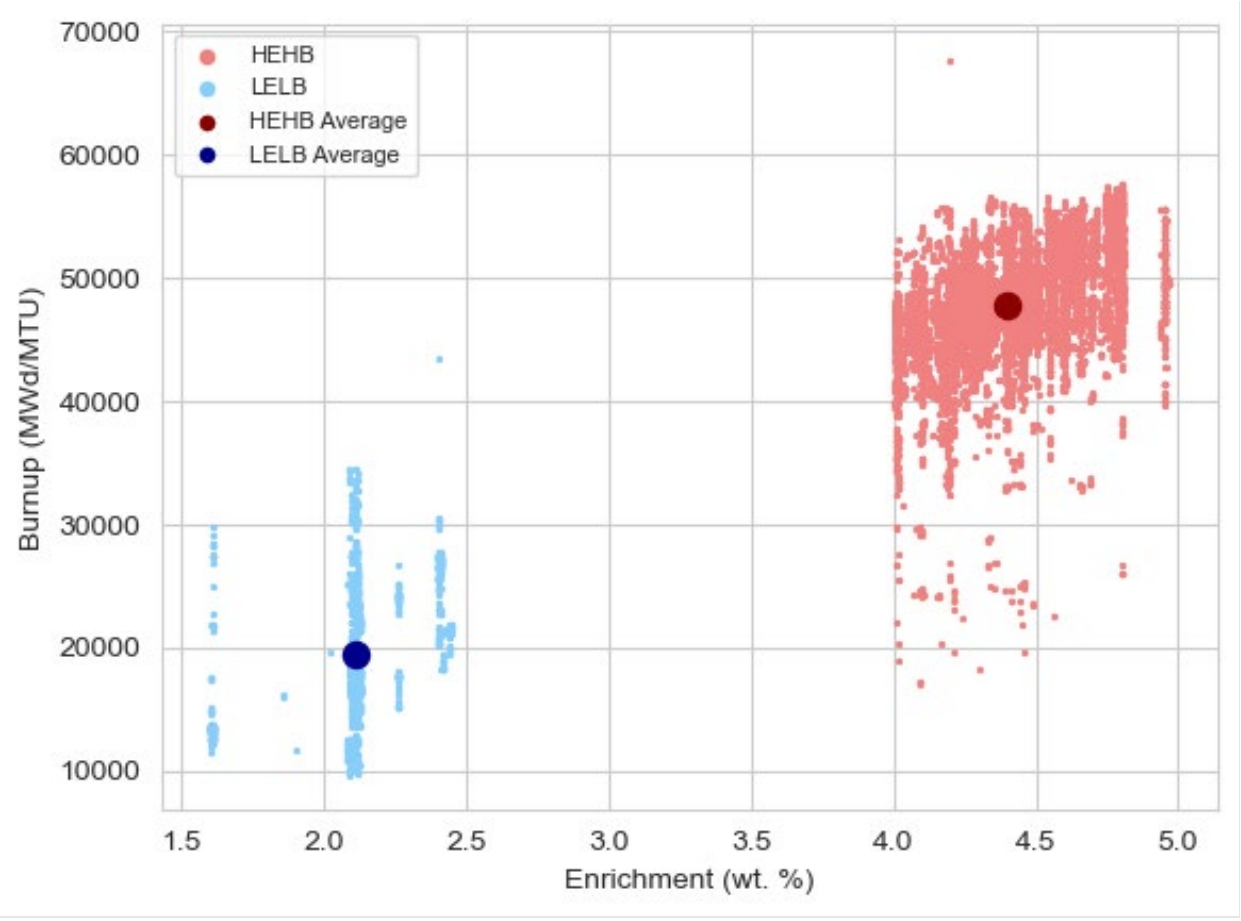

Figure 5. Plot of LELB and HEHB fuel set burnups versus enrichments.

Table 5. Summary of parameters used for the decay heat calculations with LELB and HEHB fuel types and the conservative and nominal depletion conditions.

	LELB Fuel		HEHB Fuel	
Parameter	**Nominal**	**Conservative**	**Nominal**	**Conservative**
Assembly Type	W1717WL			
Initial Uranium Mass (kgU)	460	460	460	460
Initial Enrichment (wt %)	2.11	2.11	4.40	4.40
Max Burnup (MWd/MTHM)	19401	19401	47734	47734
Burnable Absorber Loading	None	24 Pyrex Rods	None	24 Pyrex Rods
Moderator Density (g/cm^3)	0.71	0.67	0.71	0.67
Soluble Boron Concentration (ppm)	800	1000	800	1000

2.5.3 Decay Heat Analysis Methods

To determine decay heat trajectories for each of the fuel assembly decay heat limits as discussed in Section 2.1, a three-step process was followed.

1. The first step in the process was to generate decay heat as a function of cooling time following reactor discharge for each combination of fuel type and depletion conditions.
2. The second step was to determine when an assembly would be eligible for storage, termed here as the in-service time.
3. And the third step mapped the decay heats as a function of post-discharge cooling time onto the in-service timeline by interpolating the calculated decay heats.

The STANDARDS SNF Data and Analysis System was used to automate depletion and decay heat calculations for each of the LELB and HEHB fuel types with both the conservative and nominal depletion calculations. STANDARDS uses the ORIGAMI module of the SCALE 6.2.4 code (Wieselquist, Lefebvre et al., 2020, Williams, Skutnik et al., 2020) to calculate the decay heats and performs calculations using pre-generated ORIGEN cross-section libraries for each set of depletion conditions. Decay heat calculations were performed for the first 140 years following reactor discharge so that in-service timelines of up to 100 years can be generated for the thermal analyses.

The in-service decay heats for the LELB and HEHB were calculated by using linear interpolation to map the post-reactor decay heat data onto the cask in-service timeline. First, the post-reactor cooling time was calculated followed by subsequent in-service decay heats at fixed times. The post in-service cooling times are calculated in quarter year increments for the first two years, half-year increments up to five years, one year increments up to 10 years, two year increments up to 20 years, five year increments up to 60 years and 10 year increments up to 100 years of total in-service cooling time.

To illustrate this process, an example is provided in Figure 6 and Figure 7 for a representative assembly heat load limit of 800 Watts. Figure 6 shows the assembly decay heats calculated as a function of post-reactor cooling time for the LELB and HEHB fuel each with the conservative and nominal operating history assumptions. The decay heat values cross the 800 W threshold at 9.2 and 8.3 years for the HEHB conservative and nominal cases, and cross at 2.8 and 2.7 years for the LELB conservative and nominal cases. The interpolated decay heats over the in-service period are plotted in Figure 7 showing the decay heat trajectories over the first 100 years of dry storage.

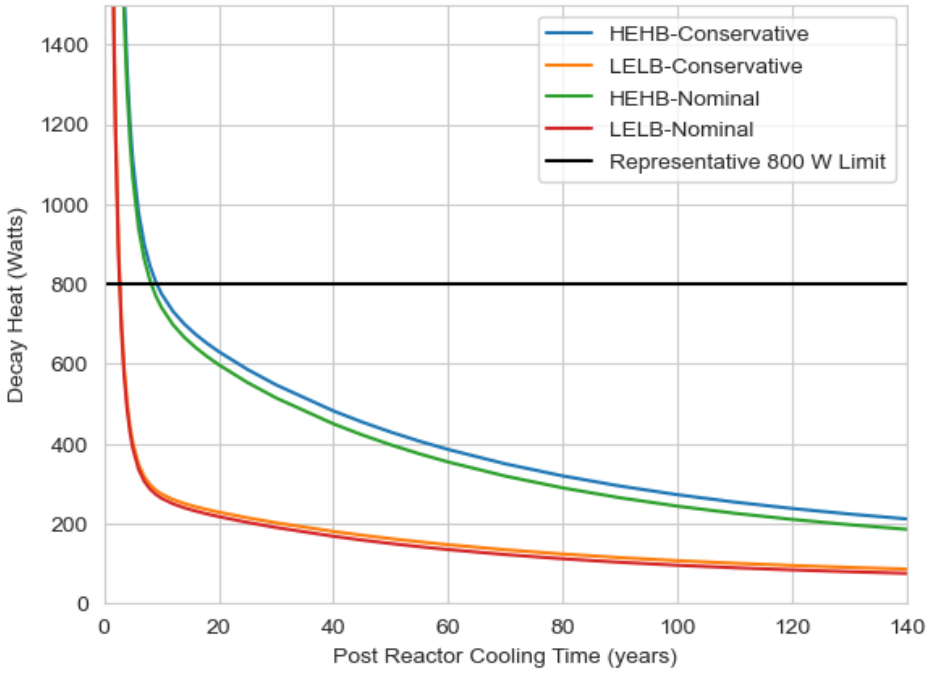

Figure 6. Assembly decay heat as a function of cooling time for each assembly type and depletion condition set, compared to a representative 800-watt limit.

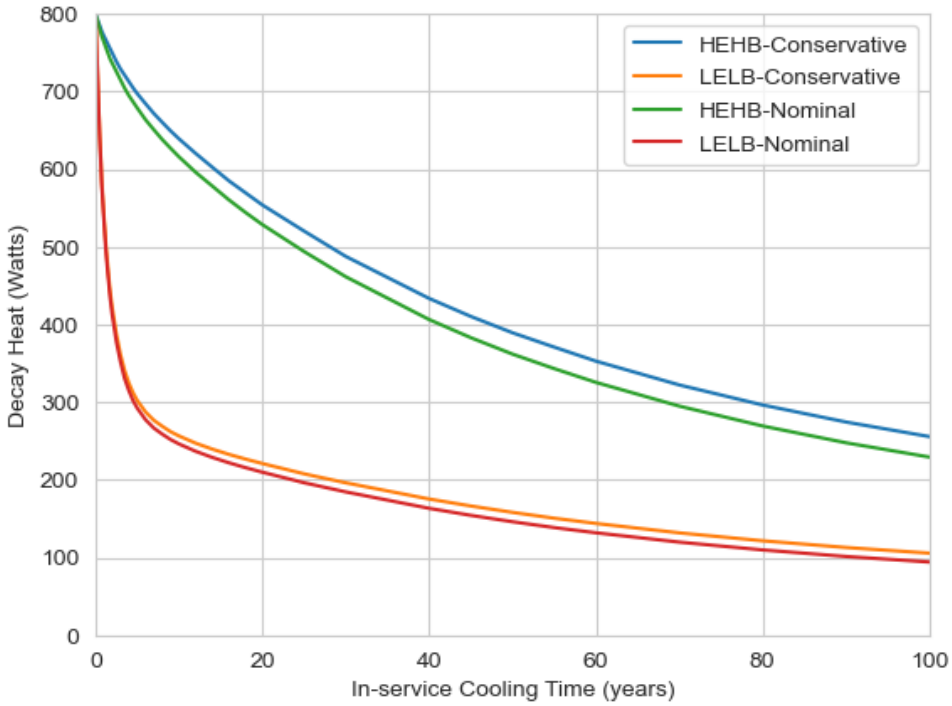

Figure 7. Assembly decay heat as a function of cooling time for each assembly type and depletion condition set, compared to a representative 800-watt limit.

2.5.4 As-Loaded Canister Decay Heat Analysis

The decay heat values discussed in Section 2.5.3 are based on the storage decay heat limits imposed in the certificate of compliance. Many fuel assemblies which are loaded into dry storage have lower decay heats. This section provides a comparison of the decay heats calculated for casks in their as-loaded configuration as a function of in-service cooling time. The same methods used to calculate the decay heats were used as is discussed in Section 2.5.3, however, the enrichment, burnup, and cooling time of each assembly are considered.

A comparison of the design basis and as-loaded decay heat curves is shown in Figure 8 for the TN-32 cask design. The individual cell heat load limits for the TN-32 are 1020 Watts, which is used to develop the in-service decay heat trajectories for each of the fuel types and then multiplied by 32. Among the three sites using TN-32 casks, a total of 64 casks were included in this comparison. The results in Figure 8 show that the as-loaded decay heats roughly vary between the HEHB and LELB curves for the majority of the first 100 years of storage. It is notable that the LELB fuel decay heat is significantly higher than the actual as-loaded decay heat for the first few years of storage.

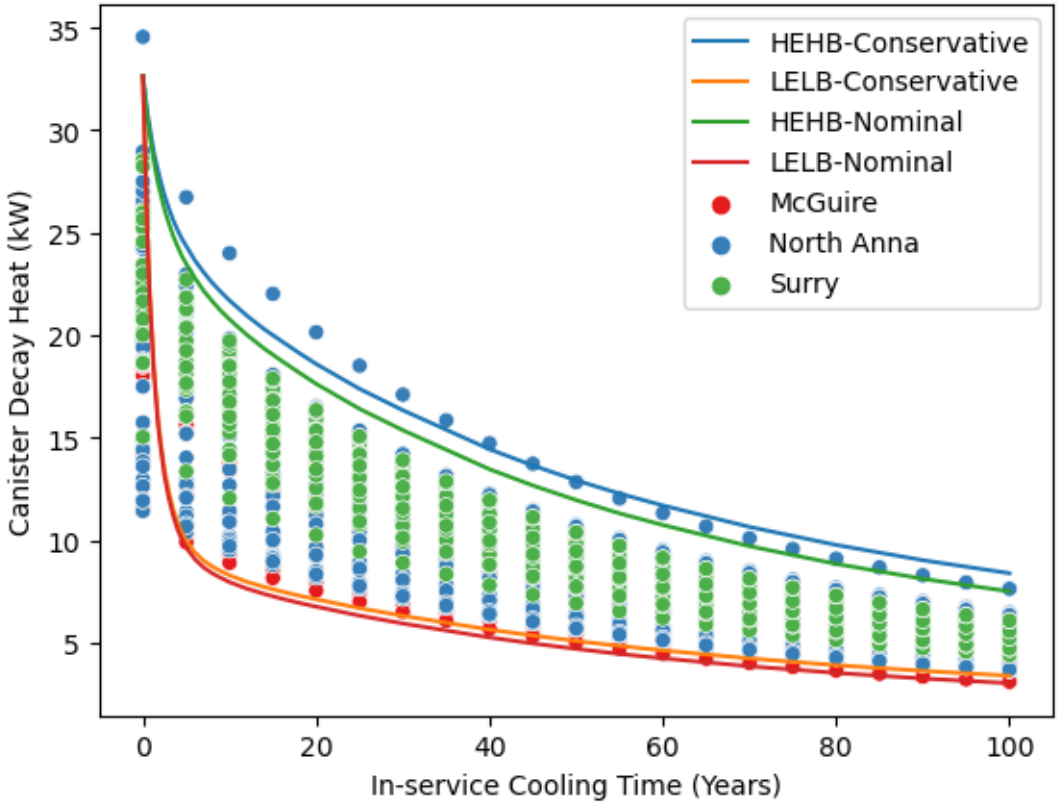

Figure 8. Comparison of the TN-32 design basis and as-loaded decay heats.

Comparisons of the design basis and as-loaded decay heat curves for the MAGNASTOR cask design are shown for the uniform, HLZC 1, and HLZC 2 loading patterns in Figure 9, Figure 10, and Figure 11, respectively. The individual cell heat load limits for the MAGNASTOR are provided in Section 2.1.2.1. Among the four sites using MAGNASTOR casks, a total of 116 casks were included in these comparisons. The results in these figures show that the as-loaded decay heats roughly vary between the HEHB and LELB curves for the majority of the first 100 years of storage. The LELB decay heat is significantly higher than the actual as-loaded decay heat for the first few years of storage. For the non-

uniform heat load patterns, some as-loaded canisters were cooler than LELB for a majority of the cooling times analyzed.

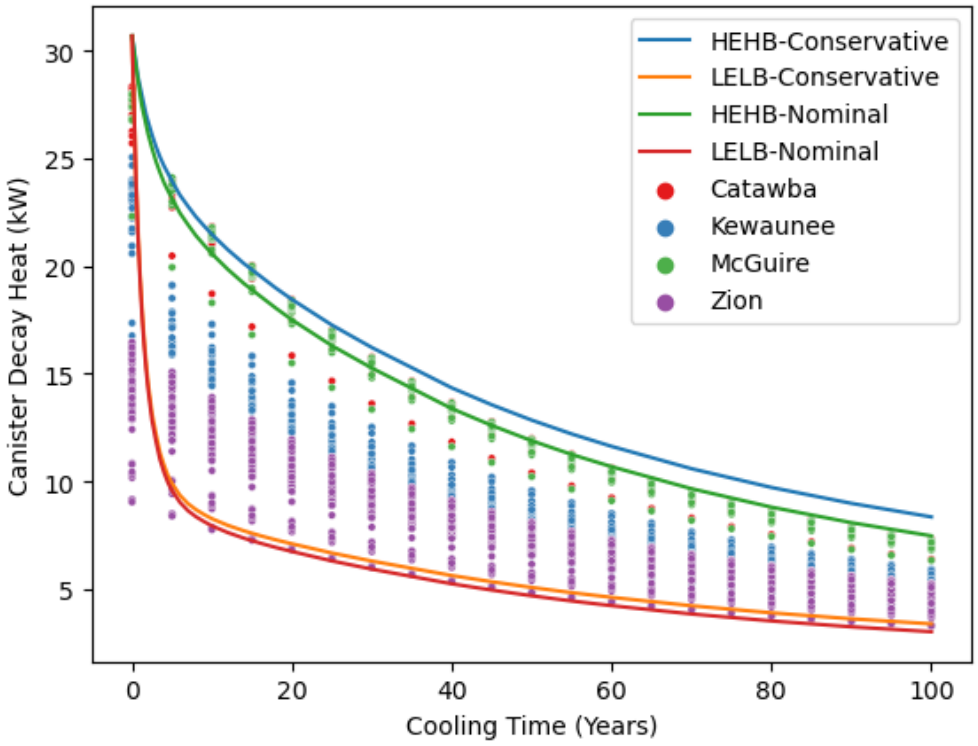

Figure 9. Comparison of the MAGNASTOR uniform loading pattern and as-loaded decay heats.

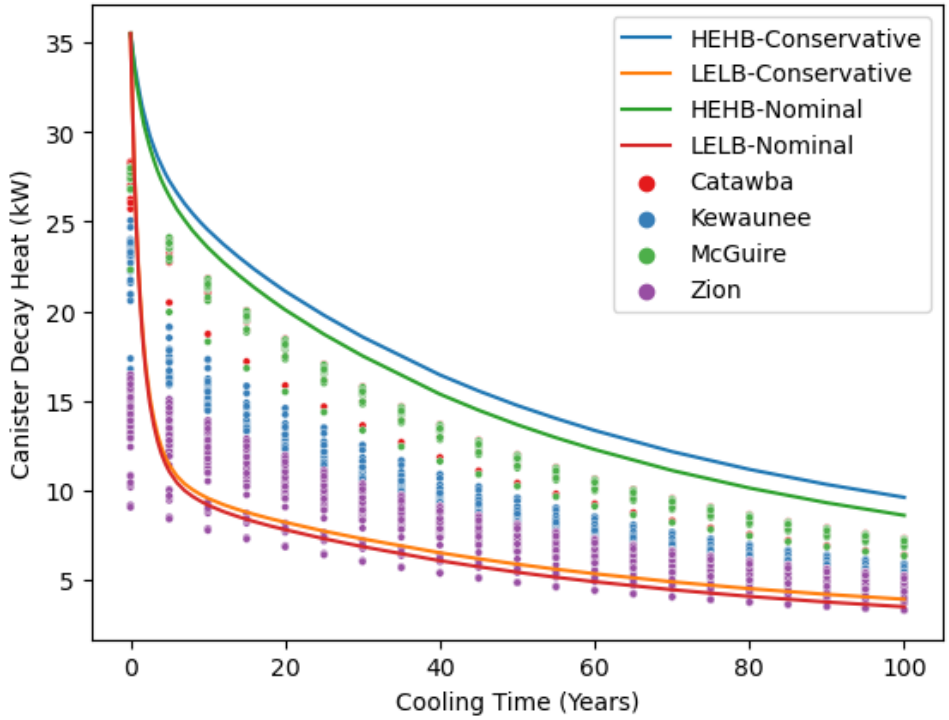

Figure 10. Comparison of the MAGNASTOR HLZC 1 and as-loaded decay heats.

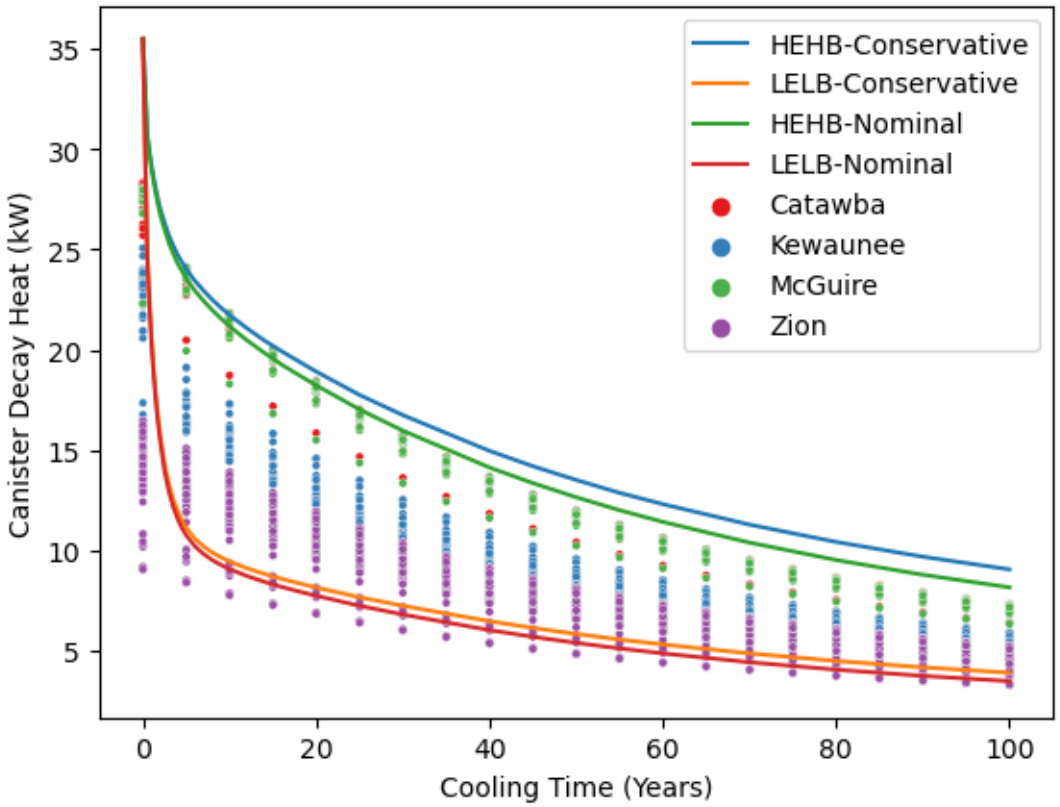

Figure 11. Comparison of the MAGNASTOR HLZC 2 and as-loaded decay heats.

Comparisons of the design basis and as-loaded decay heat curves for the NUHOMS 32PTH cask design are shown for the uniform, HLZC 1, and HLZC 2 loading patterns in Figure 12, Figure 13, and Figure 14, respectively. The individual cell heat load limits for the NUHOMS are provided in Section 2.1.3.1. Among the seven sites using NUHOMS casks, a total of 181 casks were included in these comparisons. The results in these figures show that the as-loaded decay heats roughly vary between the HEHB and LELB curves for the majority of the first 100 years of storage. The LELB decay heat is significantly higher than the actual as-loaded decay heat for the first few years of storage.

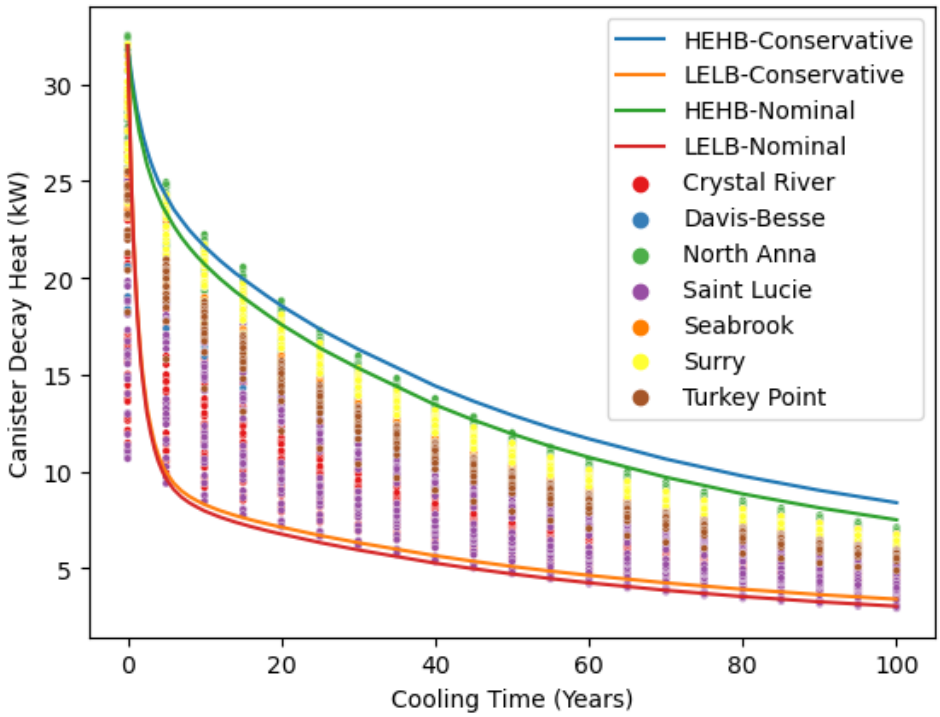

Figure 12. Comparison of the NUHOMS uniform loading pattern and as-loaded decay heats.

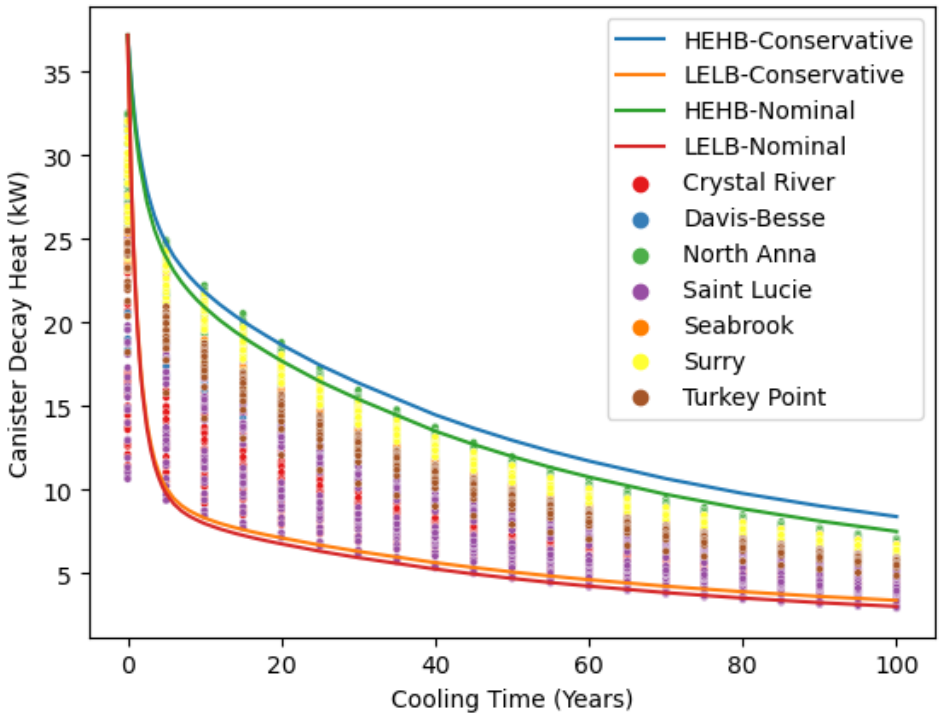

Figure 13. Comparison of the NUHOMS HLZC 1 and as-loaded decay heats.

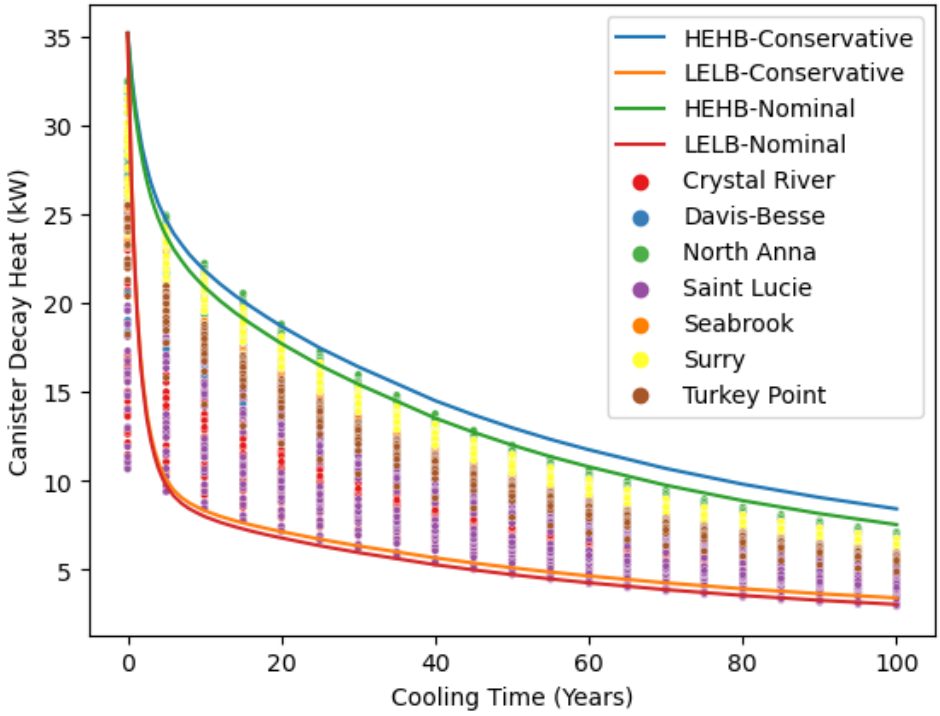

Figure 14. Comparison of the NUHOMS HLZC 2 and as-loaded decay heats.

Based on the evaluation of the HEHB and LELB curves against the as loaded canisters, the HEHB conservative curves were used for all the results evaluated with the thermal models in this report. This curve was chosen for two reasons. First, HEHB decay heat curves will provide a conservative estimate of potential annealing and second, it is more relevant to modern fuel that is likely to be higher enrichment and burnup and loaded earlier after discharge.

This page is intentionally left blank.

3. RESULTS

This section presents results from modeling each cask design with their respective heat loads. Results are also broken down by code. These results are summarized in tables, histograms, box plots, maps of per assembly values, and axial cladding temperatures. The maps of per assembly values contain PCT and percentage of cladding above 275°C.

The histogram plots contain cladding temperature distributions for all assemblies in the respective system, the assembly containing the PCT, and assembly with the minimum average cladding temperature. Note, the minimum average cladding temperature is different from the minimum clad temperature (MCT). MCT is based off a point value and minimum average cladding temperature is the average value of cladding in a particular assembly. The reason MCT is not used is because it is often the same assembly as PCT in vertical cask models and doesn't reflect the coldest assembly. The assembly containing the PCT will be referred to as the PCT assembly. The minimum average cladding temperature assembly is determined by averaging the cladding temperature in each assembly in the respective system for the current storage time and selecting the assembly with the lowest average temperature.

Figure 15 shows a diagram explaining the symbols of a box and whisker plot. For each model and heat loading zone configuration, a box plot is included. The box plot provides a summary of the PCT, MCT, median cladding temperature, temperature at which 25% of cladding is below, and temperature at which 75% of the cladding is below. Also included in these plots are horizontal lines at 275°C, 300°C, and 350°C. These temperatures are important thresholds for annealing over long periods of time.

Maps of the PCT and MCT for each assembly are included, along with maps of percentage of cladding over 275°C. These maps are for assembly values, meaning for PCT it is the PCT in the particular assembly. Percent of cladding over 275°C plots are also provided. These are calculated on a per assembly basis, rather than for all assemblies in the canister.

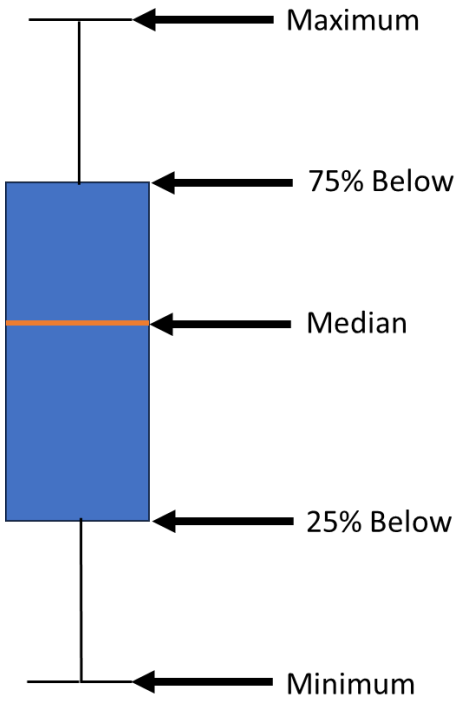

Figure 15. Diagram of box plot symbols

3.1 TN-32 Model Comparisons

3.1.1 COBRA-SFS

Figure 16 shows the temperature distribution of the cladding in the TN-32 system for the uniform heat loading configuration at the design basis heat load and 75% of the design basis heat load. Figure 16 a) and b) show the temperature distribution of the cladding in all of the assemblies in the TN-32 system. Figure 16 c) and d) show the temperature distribution of the cladding only in the assembly with the PCT. Figure 16 e) and f) show cladding temperature distribution of the cladding in the assembly with the lowest average temperature.

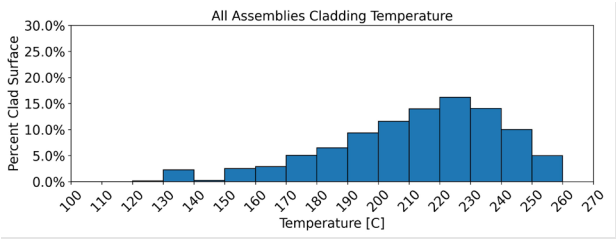

a) Design basis heat load (32.7 kW), all assemblies cladding temperature histogram

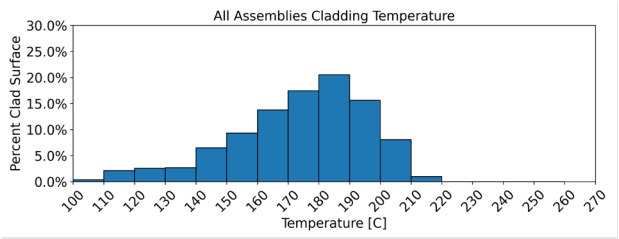

b) 75% of design basis heat load (24.5 kW), all assemblies cladding temperature histogram

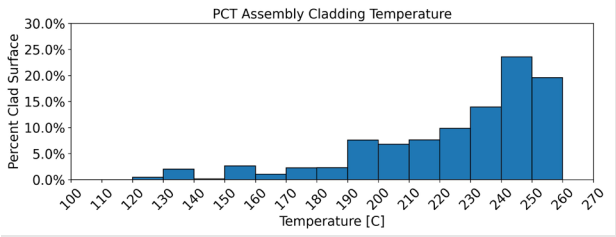

c) Design basis heat load (32.7 kW), assembly containing rod with maximum PCT cladding temperature histogram

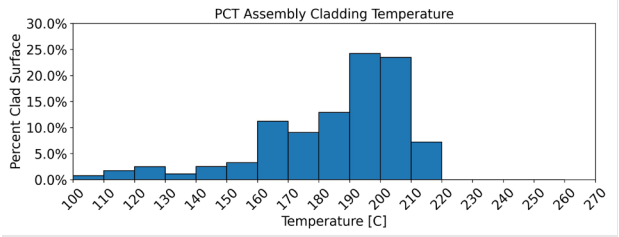

d) 75% of design basis heat load (24.5 kW), assembly containing rod with maximum PCT cladding temperature histogram

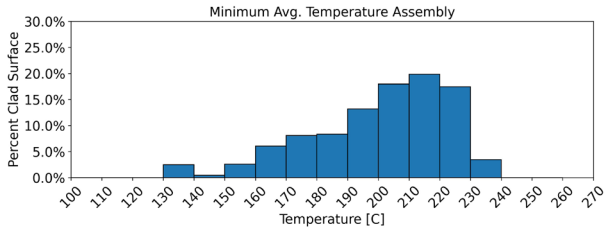

e) Design basis heat load (32.7 kW), minimum average temperature assemblies cladding temperature histogram

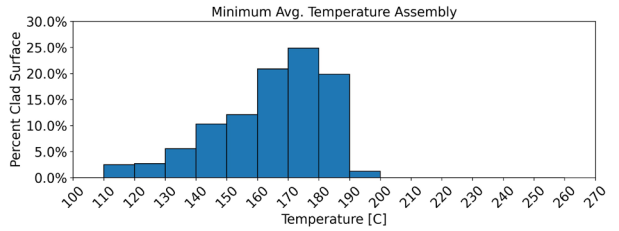

f) 75% of design basis heat load (24.5 kW), minimum average temperature assembly cladding temperature histogram

Figure 16. COBRA-SFS results for the TN-32 system at design basis heat load (32.7 kW), and 75% of design basis heat load (24.5 kW)

Figure 17 shows the axial temperature distribution of the hottest rod in the TN-32 system for both heat loads, the design basis and 75% of the design basis heat load.

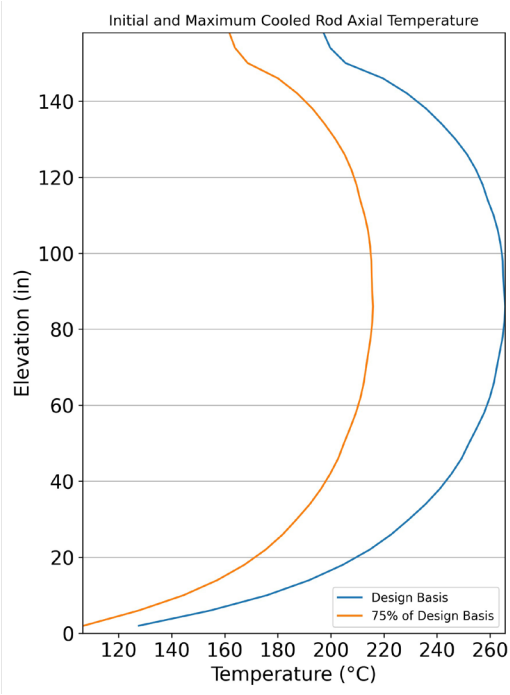

Figure 17. Temperature profiles of rods in a TN-32 with PCT for design basis (32.7 kW)and 75% of design basis (24.5 kW) heat loads

Figure 18 and Figure 19 show a map of the maximum temperature in each assembly. Figure 18 is for the design basis heat load and Figure 19 is at 75% of the design basis heat load.

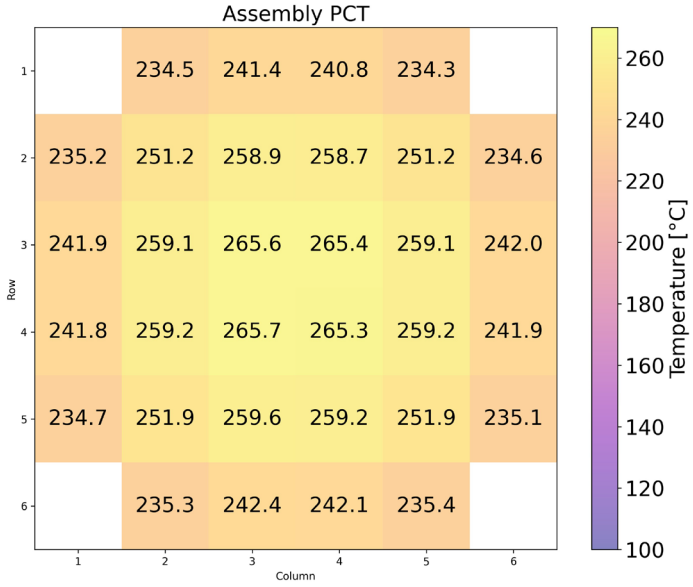

Figure 18. PCT map of TN-32 at the design basis heat load (32.7 kW)

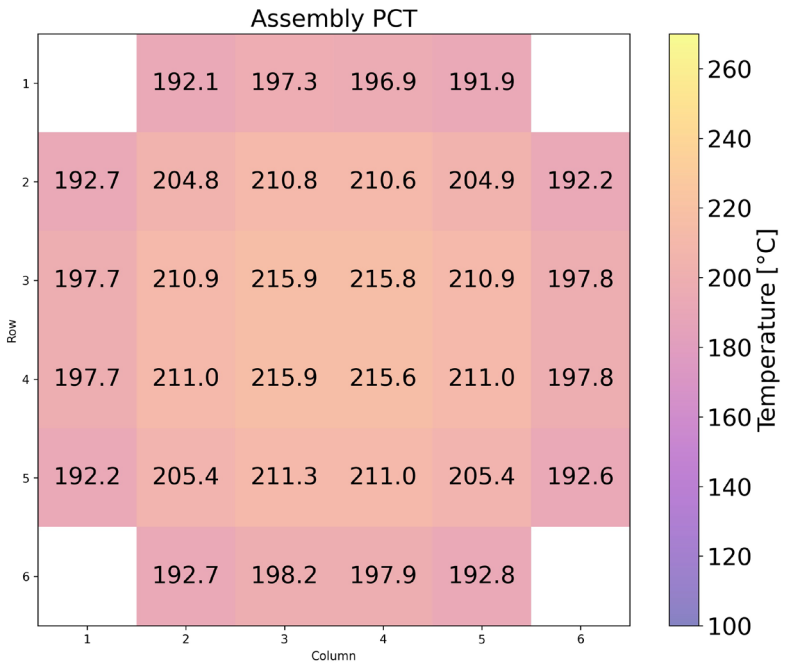

Figure 19. PCT map of TN-32 with 75% of design basis heat load (24.5 kW)

Figure 20 shows a box and whisker plot of the cladding temperatures in the TN-32 system.

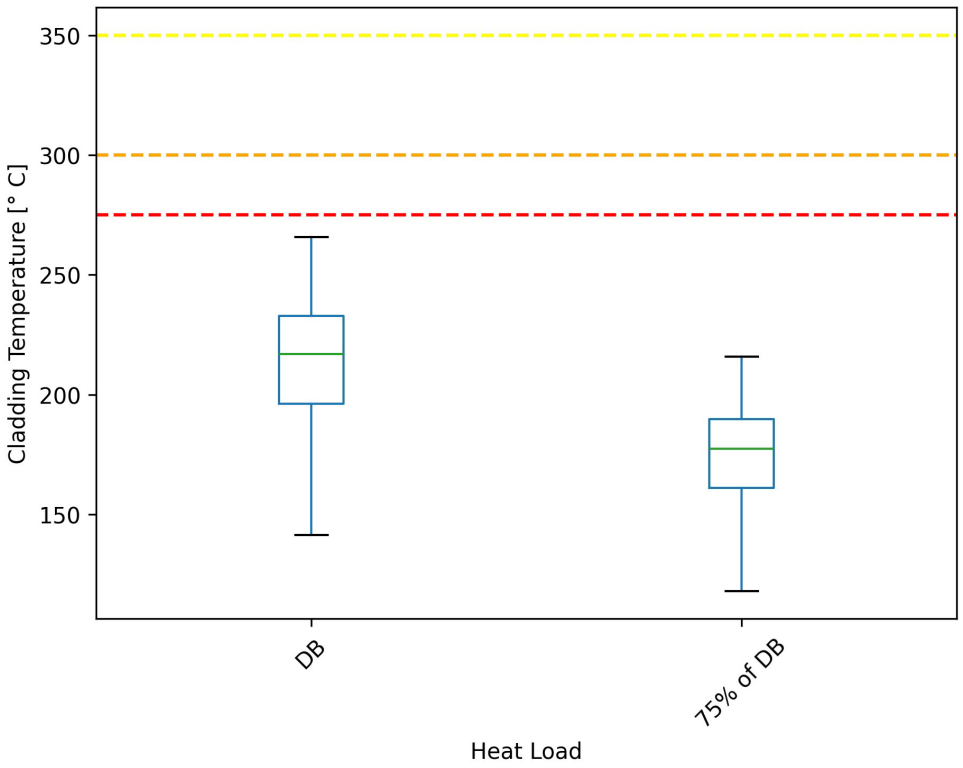

Figure 20. Box plot for COBRA-SFS TN32 model for design basis heat load (32.7 kW) and 75% of design basis heat load (24.5 kW)

3.1.2 STAR-CCM+

Figure 21 shows the cladding temperature histograms of a) total cladding temperature at the design basis heat load, b) PCT containing assembly at the design basis heat load, c) total cladding temperature at coldest simulated heat load, and d) coldest average assembly at the design basis heat load for the TN-32 STAR-CCM+ model. Figure 22 shows the box and whisker plots for both the design basis and 75% of design basis heat loads using the STAR-CCM+ model.

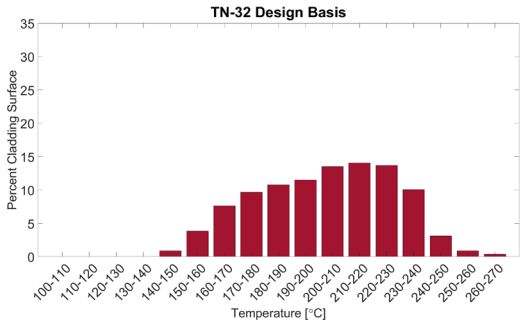

a) Total cladding temperature histogram for design basis heat load (32.7 kW)

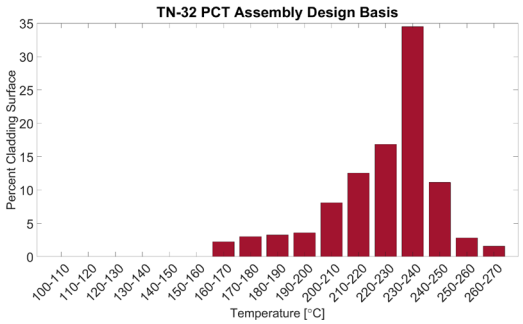

b) PCT assembly cladding temperature histogram for design basis heat load (32.7 kW)

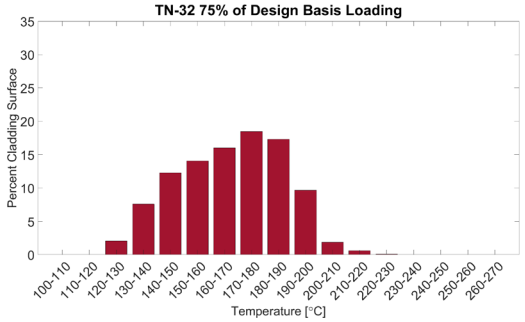

c) Total cladding temperature histogram of 75% for design basis heat load (24.5 kW)

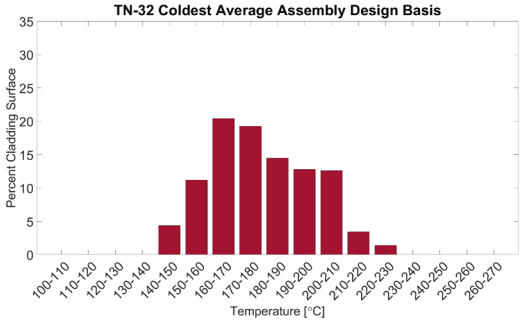

d) Coldest average assembly cladding temperature histogram for design basis heat load (32.7 kW)

Figure 21. Total and select assembly cladding temperature histograms at design basis heat load and final simulated heat load for the TN-32 uniform HLZC from the STAR-CCM+ model

Figure 23 shows a map of locations of the assemblies in the TN-32 model. Each assembly is labeled with its local PCT, and the local percentage of cladding above 275°C, 300°C, and 350°C for the design basis heat load. Figure 24 shows the axial temperature distribution of the hottest rod in the TN-32 system for both heat loads, the design basis and 75% of the design basis heat load.

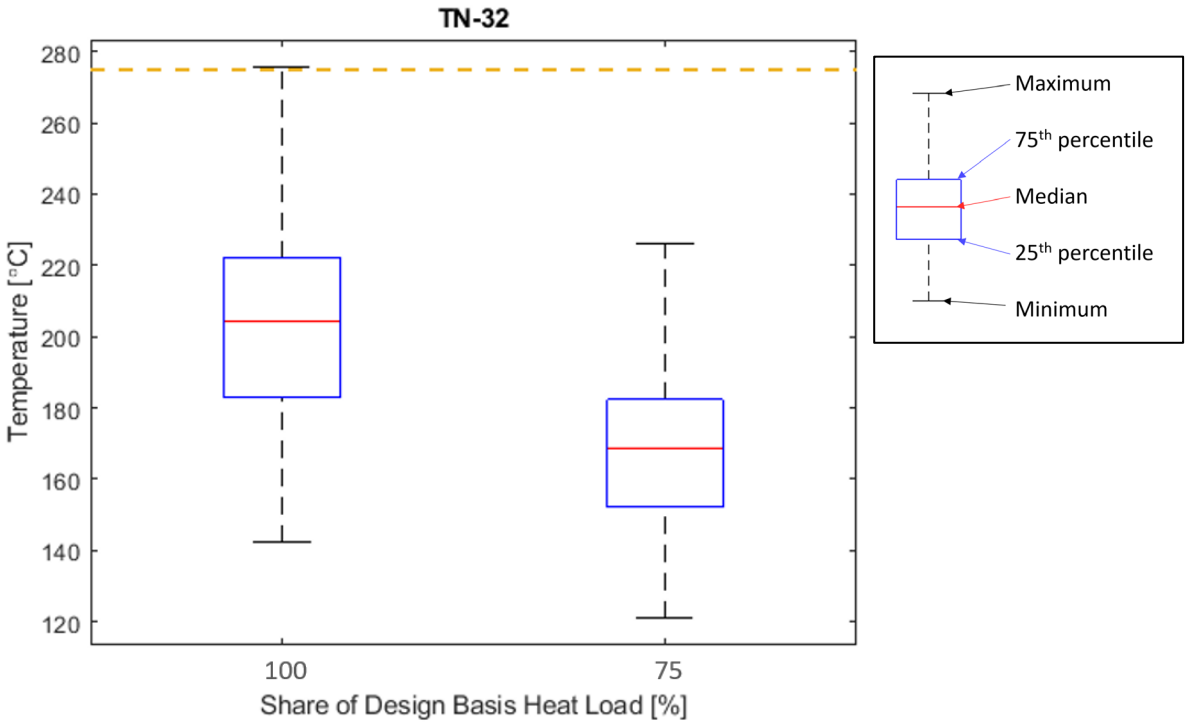

Figure 22. Box plots for the STAR-CCM+ TN-32 model for design basis heat load (32.7 kW) and 75% of design basis heat load (24.5 kW)

.PCT [°C]
Percent above 275°C
Percent above 300°C
Percent above 350°C

	237	251	251	236	
	0%	0%	0%	0%	
	0%	0%	0%	0%	
	0%	0%	0%	0%	
231	256	270	270	255	231
0%	0%	0%	0%	0%	0%
0%	0%	0%	0%	0%	0%
0%	0%	0%	0%	0%	0%
247	266	276	276	266	247
0%	0%	0%	0%	0%	0%
0%	0%	0%	0%	0%	0%
0%	0%	0%	0%	0%	0%
248	266	276	276	266	248
0%	0%	0%	0%	0%	0%
0%	0%	0%	0%	0%	0%
0%	0%	0%	0%	0%	0%
231	256	270	270	255	231
0%	0%	0%	0%	0%	0%
0%	0%	0%	0%	0%	0%
0%	0%	0%	0%	0%	0%
	237	251	251	237	
	0%	0%	0%	0%	
	0%	0%	0%	0%	
	0%	0%	0%	0%	

Figure 23. Assembly map of the STAR-CCM+ TN-32 model with the assembly's PCT, percent of cladding above 275°C, percent of cladding above 300°C, and percent of cladding above 350°C for the design basis heat load (32.7 kW).

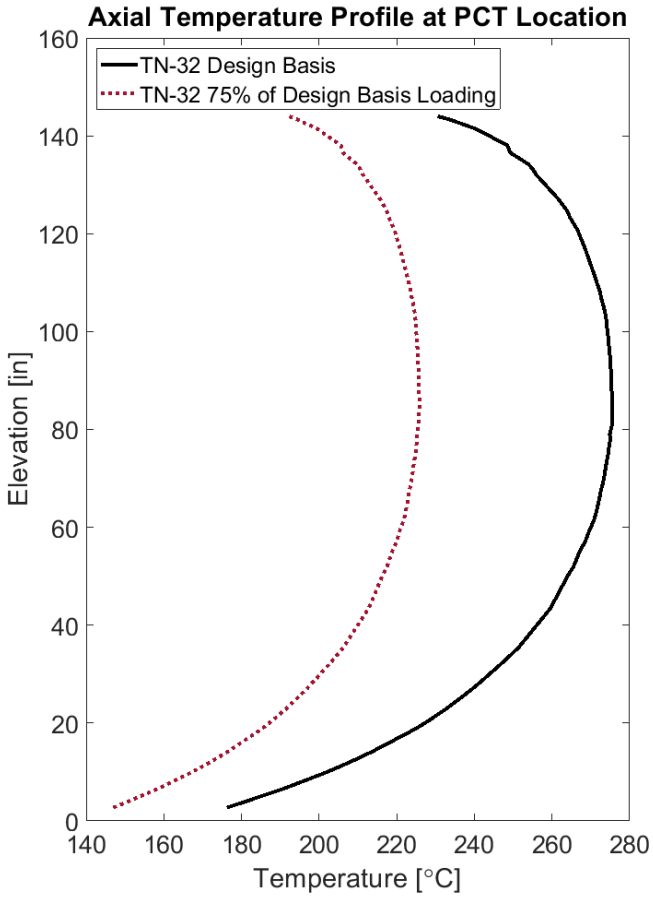

Figure 24. Temperature profiles of rods with PCT for design basis (32.7 kW) and 75% of design basis (24.5 kW) heat loads from the TN-32 STAR-CCM+ model.

3.2 MAGNASTOR TSC-37

For the MAGNASTOR TSC-37 system, three different HLZC with both COBRA-SFS and STAR-CCM+ models are analyzed. The three heat loads are shown previously in Table 1 in conjunction with Figure 3. The uniform and HLZC 1 are fairly similar. HLZC 2 has four assemblies that have a much higher heat load.

3.2.1 COBRA-SFS Results

The results for the COBRA-SFS models of the MAGANSTOR TSC-37 models are in the following sections 3.2.1.1 to 3.2.1.4 for each heat loading zone configuration.

3.2.1.1 Uniform HLZC

Table 6 shows the tabular results for the uniform HLZC for the MAGNASTOR COBRA-SFS model. These results include the time in storage, heat load, PCT, percent cladding above certain temperatures for all assemblies in the cask and for the PCT assembly.

Table 6. MAGNASTOR Uniform HLZC Tabular Data COBRA-SFS Model

Time in Storage		Heat Load		PCT	% Total Cladding Above			PCT Assembly % Cladding Above		
[years]	[months]	[kW]	[% DB]	[°C]	275°C	300°C	350°C	275°C	300°C	350°C
0.0	0.0	35.50	100%	353	53	32.7	0.0	56.9	44.6	1.2
0.1	1.4	35.14	99%	350	52	30.9	0.0	55.9	43.8	0.0
0.3	4.2	34.47	97%	345	49	27.6	0.0	54.0	41.7	0.0
0.6	6.9	33.80	95%	340	46	24.3	0.0	52.2	39.4	0.0
0.8	9.9	33.13	93%	335	43	20.8	0.0	50.2	37.2	0.0
1.2	13.8	32.47	91%	330	40	17.5	0.0	48.1	34.7	0.0
1.5	17.8	31.81	90%	325	36	14.2	0.0	46.1	32.2	0.0
1.8	22.0	31.15	88%	320	32	10.8	0.0	43.7	29.5	0.0
2.3	27.4	30.49	86%	315	28	7.2	0.0	41.4	26.6	0.0
2.7	32.7	29.84	84%	310	24	2.7	0.0	38.8	20.6	0.0
3.3	39.7	29.20	82%	305	20	0.4	0.0	36.2	4.1	0.0
3.9	47.4	28.55	80%	300	16	0.0	0.0	33.3	0.0	0.0
4.7	56.8	27.91	79%	295	13	0.0	0.0	30.4	0.0	0.0
5.5	66.2	27.27	77%	290	9	0.0	0.0	27.5	0.0	0.0
6.5	78.1	26.64	75%	285	4	0.0	0.0	23.7	0.0	0.0
7.6	90.8	26.00	73%	280	1	0.0	0.0	4.6	0.0	0.0
8.8	105.9	25.37	71%	275	0	0.0	0.0	0.0	0.0	0.0
10.2	122.2	24.75	70%	270	0	0.0	0.0	0.0	0.0	0.0

Figure 25 shows the cladding temperature distribution for all assemblies, the PCT assembly, and the minimum average temperature assembly. Also included is the cladding temperature distribution for all assemblies after 10.2 years of storage which results in a PCT of less than 275°C.

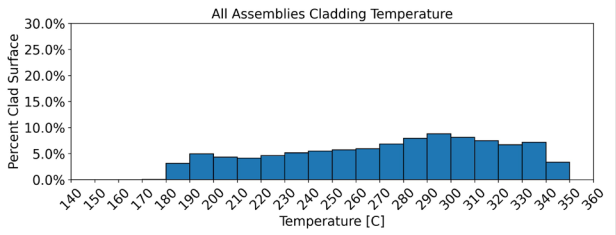

a) Uniform HLZC design basis heat load (initial loading, 35.5 kW)) all assemblies cladding temperature histogram

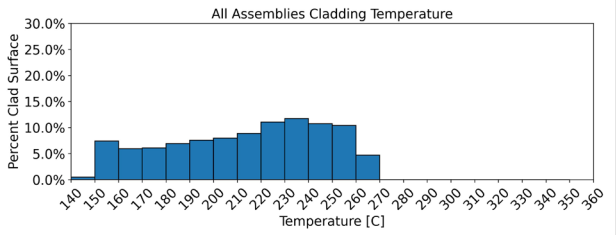

b) Uniform HLZC after 10.2 years of storage (24.75 kW) all assemblies cladding temperature histogram

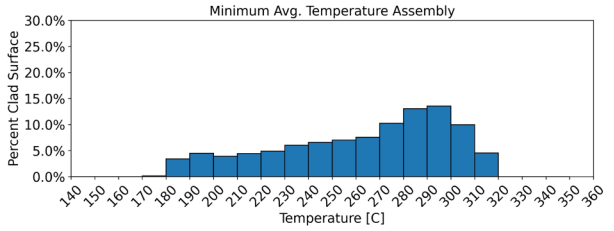

c) Uniform HLZC design basis heat load assembly with lowest average cladding temperature histogram

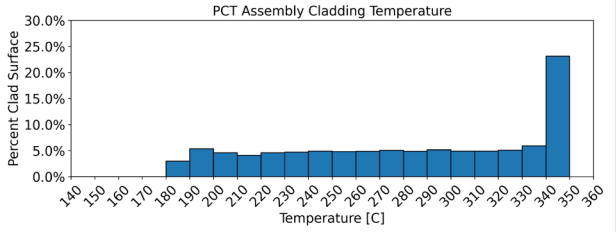

d) Uniform HLZC design basis heat load assembly containing the PCT cladding temperature histogram

Figure 25. Cladding temperature histograms at design basis heat load for MAGNASTOR uniform HLZC from COBRA-SFS model

Figure 26 shows a box and whisker plot for the uniform HLZC for the COBRA-SFS MAGNASTOR model. The horizontal dashed lines are placed at 275°C, 300°C, and 350°C to better visualize the amount of cladding above those temperature thresholds.

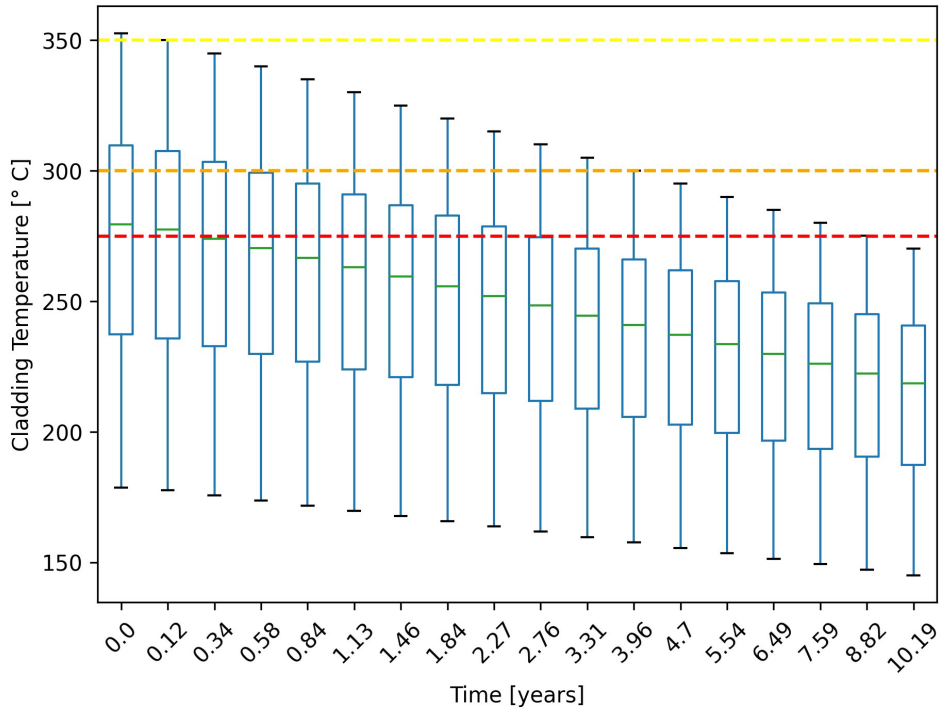

Figure 26. Box plot of Uniform HLZC COBRA-SFS MAGNASTOR Model, red dashed line at 275°C. orange dashed line at 300°C, and yellow dashed line at 350°C

Figure 27 to Figure 30 show the PCT maps, and percentage of cladding above 275°C. Maps for the PCT after 10.2 years of storage which results in PCT less than 275°C are included. Also included is a map of the percentage of cladding above 275°C after 5.5 years of storage. 5.5 years of storage is approximately half the time it takes the fuel to cool from the design basis to less than 275°C PCT.

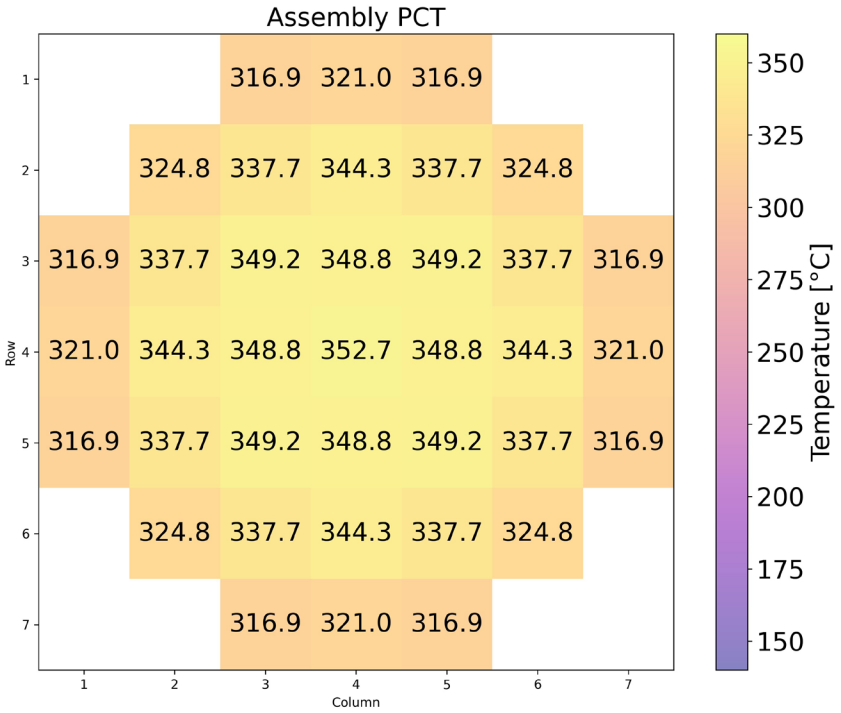

Figure 27. PCT map for MAGNASTOR uniform HLZC design basis heat load (35.5 kW)

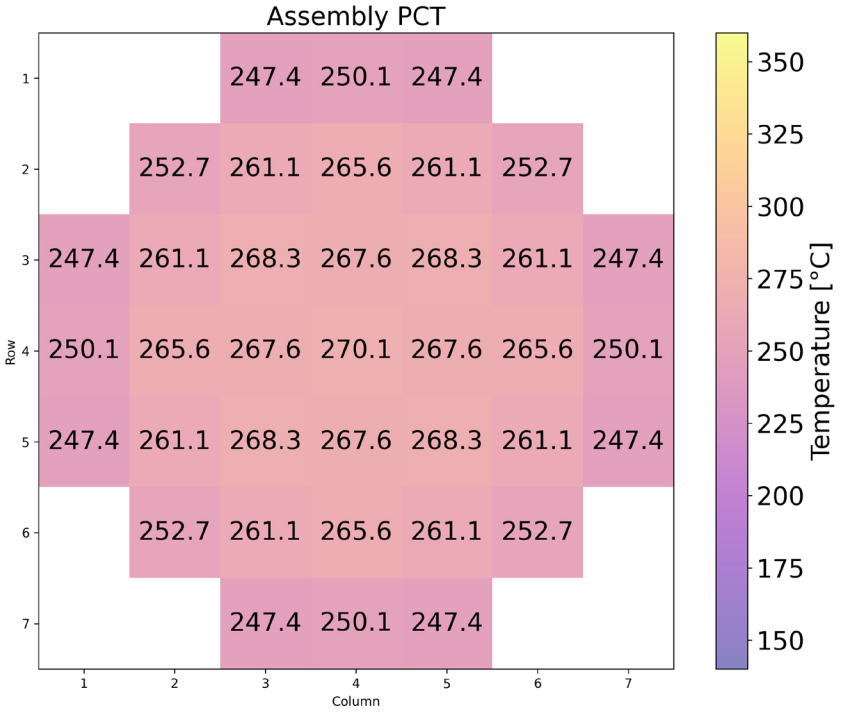

Figure 28. PCT map for MAGNASTOR uniform HLZC after 10.2 years of storage (24.7 kW)

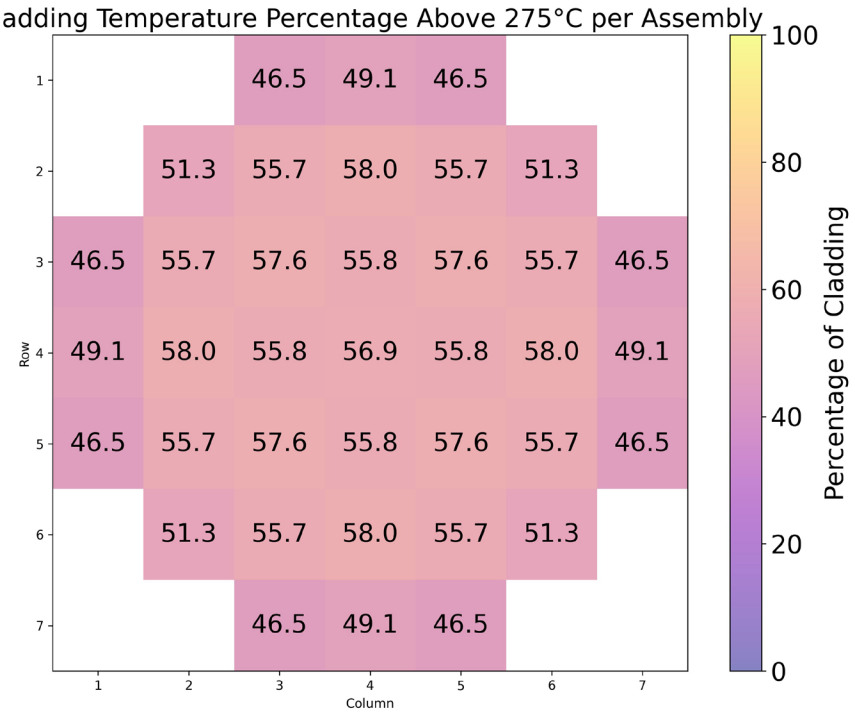

Figure 29. MAGNASTOR uniform HLZC map of percentage of cladding above 275°C per assembly for design basis heat load (35.5 kW)

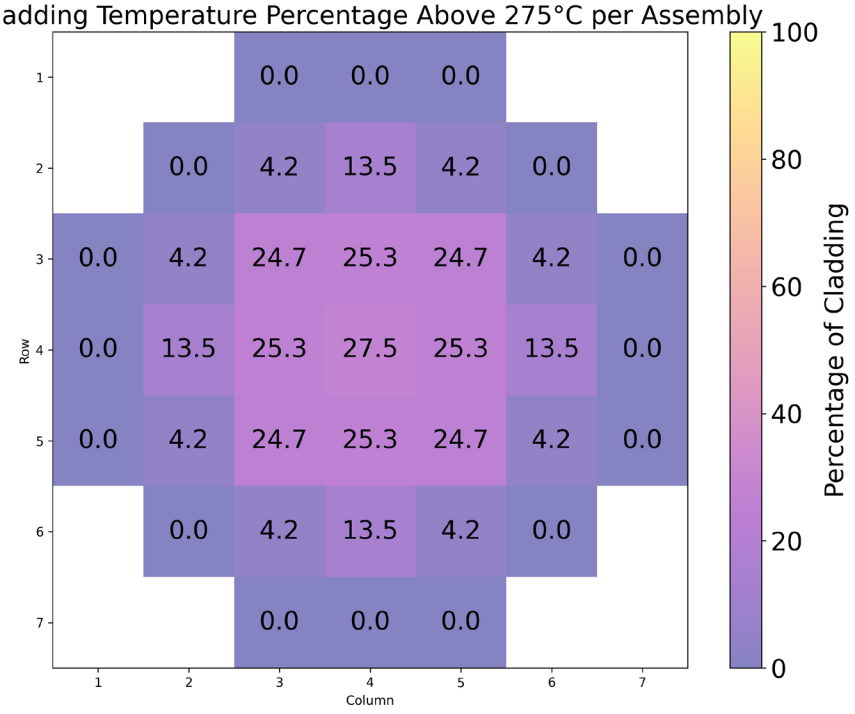

Figure 30. MAGNASTOR uniform HLZC map of percentage of cladding above 275°C per assembly after 5.5 years of storage (27.27 kW)

Figure 31 shows the axial temperature profile of the PCT rod at initial loading, and after it has cooled to be less than 275°C. The vertical lines are included to show the portion of rod that is above 275°C, 300°C, and 350°C.

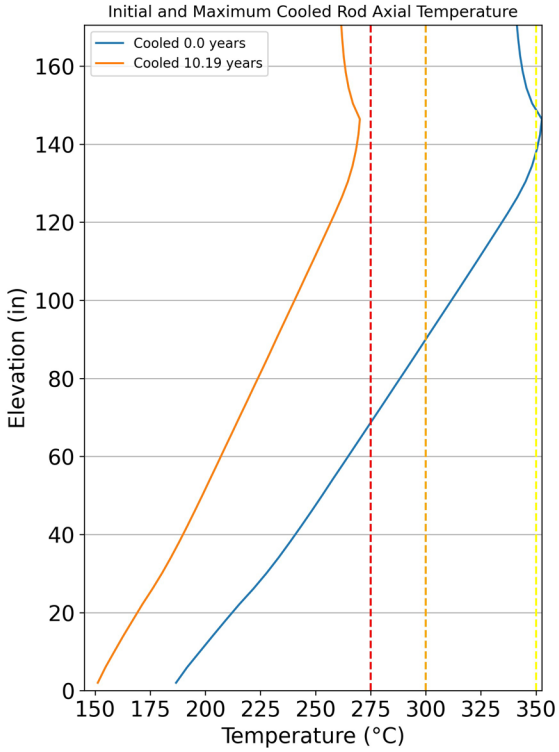

Figure 31. MAGNASTOR uniform HLZC axial temperature profile of hottest rod at the design basis heat load (35.5 kW) and after 10.2 years of storage time (24.75 kW), red dashed line at 275°C, orange dashed line at 300°C, and yellow dashed line at 350°C

3.2.1.2 HLZC 1

Table 7 shows the tabular results for the HLZC 1 for the MAGNASTOR COBRA-SFS model. These results include the time in storage, heat load, PCT, percent cladding above certain temperatures for all assemblies in the cask and the PCT assembly.

Table 7. MAGNASTOR HLZC 1 Tabular Data COBRA-SFS Model

Time in Storage		Heat Load		PCT	% Total Cladding Above			PCT Assembly % Cladding Above		
[years]	[months]	[kW]	[% DB]	[°C]	275°C	300°C	350°C	275°C	300°C	350°C
0.00	0.0	35.49	100%	353.0	52.7	33.3	0.2	56.1	44.4	1.5
0.12	1.4	35.07	98.8%	349.9	51.1	31.2	0	55.1	43.1	0
0.31	3.8	34.40	97%	344.9	48.6	27.8	0	53.4	41.1	0
0.53	6.4	33.72	95%	339.9	45.8	24.6	0	51.4	39.1	0
0.80	9.6	33.05	93%	334.9	42.8	21.4	0	49.5	36.7	0
1.07	12.9	32.39	91%	329.9	39.3	18.4	0	47.5	34.4	0
1.37	16.4	31.71	89%	324.8	35.4	15.3	0	45.4	31.9	0
1.71	20.5	31.07	88%	319.9	31.7	12.2	0	43.3	29.4	0
2.10	25.3	30.41	86%	314.9	27.8	8.4	0	41.0	26.3	0
2.53	30.4	29.73	84%	309.8	24.0	3.1	0	38.4	20.7	0
3.04	36.5	29.12	82%	304.8	20.2	0.5	0	35.9	4	0
3.64	43.7	28.48	80%	299.9	16.7	0	0	33.1	0	0
4.33	52.0	27.81	78%	294.8	12.9	0	0	30.3	0	0
5.12	61.4	27.20	77%	289.9	9.1	0	0	27.3	0	0
6.05	72.6	26.57	75%	285.0	3.9	0	0	23.6	0	0
7.11	85.3	25.92	73%	279.9	0.5	0	0	4.3	0	0
8.29	99.5	25.32	71%	275.1	0.0	0	0	0.0	0	0
9.63	115.5	24.69	70%	270.0	0.0	0	0	0.0	0	0

Figure 32 shows the cladding temperature distribution for all assemblies, the PCT assembly, and minimum average temperature assembly. Also included is the cladding temperature distribution for all assemblies after 9.6 years of storage which results in a PCT of less than 275°C.

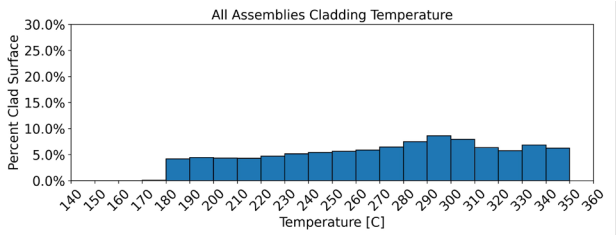

a) HLZC 1 design basis heat load (initial loading, 35.49 kW) all assemblies cladding temperature histogram

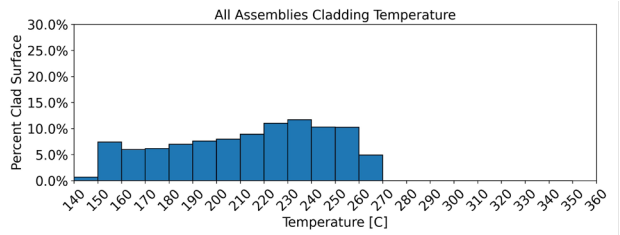

b) HLZC 1 after 9.6 years of storage (24.69 kW) all assemblies cladding temperature histogram

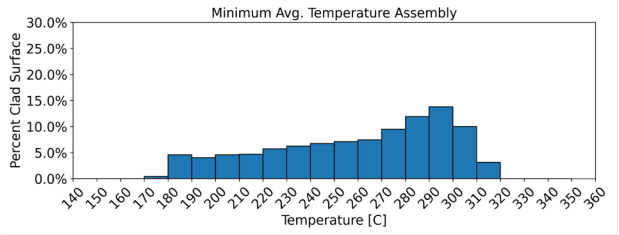

c) HLZC 1 design basis heat load (35.49 kW) assembly with the lowest average cladding temperature histogram

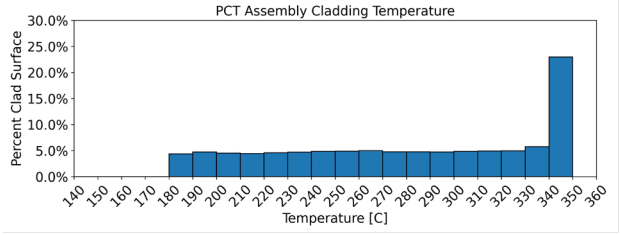

d) HLZC 1 design basis heat load (35.49 kW) assembly containing the PCT cladding temperature histogram

Figure 32. Cladding temperature histograms at Design basis heat load for MAGNASTOR HLZC 1 from COBRA-SFS model

Figure 33 shows a box and whisker plot for HLZC 1 for the COBRA-SFS MAGNASTOR model. The horizontal dashed lines are placed at 275°C, 300°C, and 350°C to better visualize the amount of cladding above those temperature thresholds.

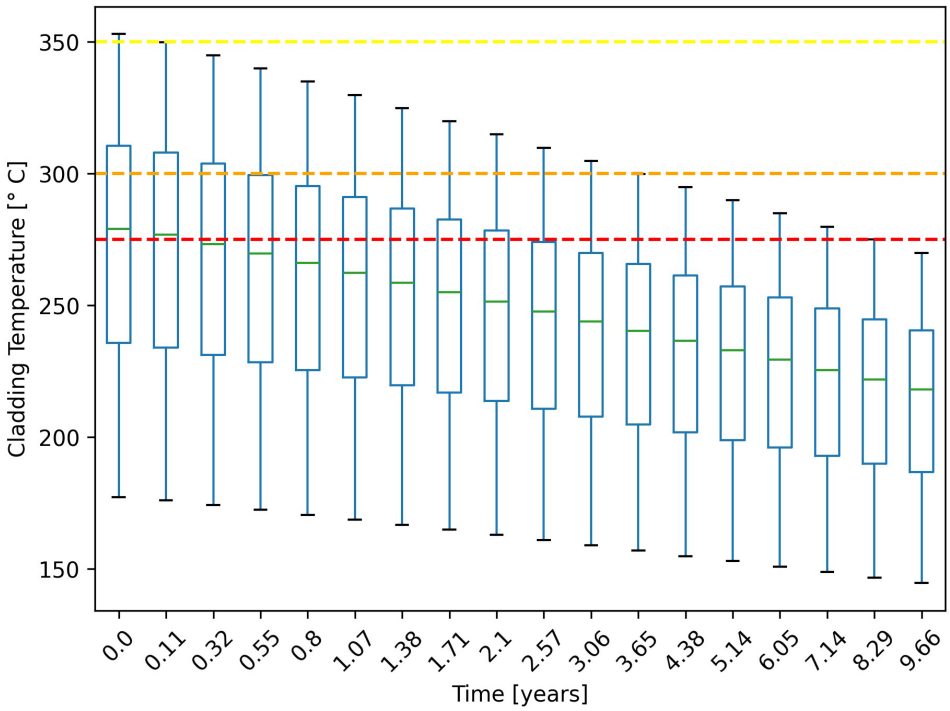

Figure 33. Box plot of HLZC 1 COBRA-SFS MAGNASTOR Model, red dashed line at 275°C. orange dashed line at 300°C, and yellow dashed line at 350°C

Figure 34 to Figure 37 show the PCT maps and percentage of cladding above 275°C. Maps for the PCT after 9.6 years of storage which results in PCT less than 275°C are included. Also included is a map of the percentage of cladding above 275°C after 5.1 years of storage. 5.1 years of storage is approximately half the time it takes the fuel to cool from the design basis to less than 275°C PCT.

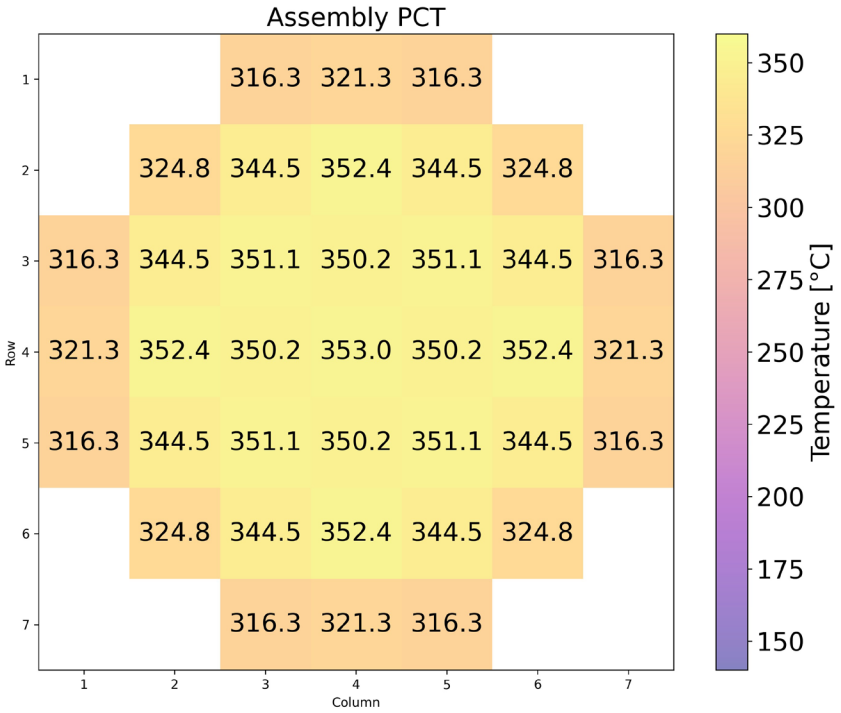

Figure 34. PCT map for MAGNASTOR HLZC 1 design basis heat load (35.49 kW)

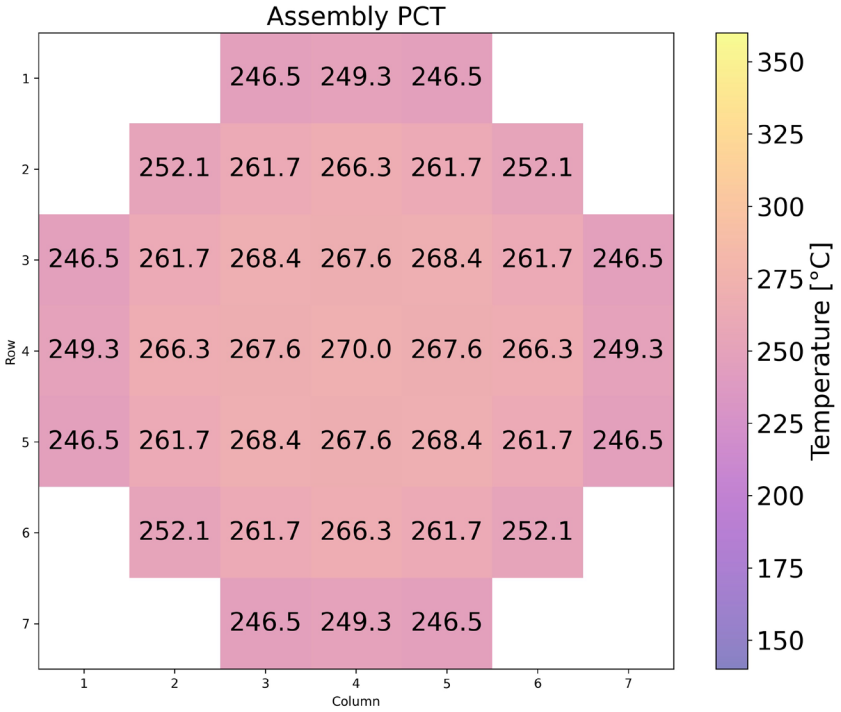

Figure 35. PCT map for MAGNASTOR HLZC 1 after 9.6 years of storage (24.96 kW)

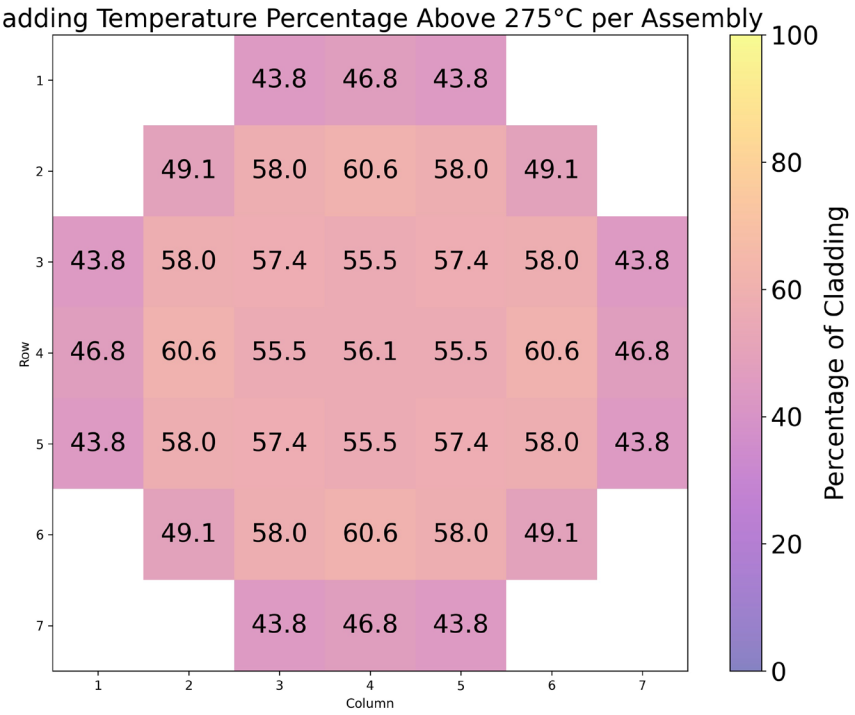

Figure 36. MAGNASTOR HLZC 1 map of percentage of cladding above 275°C per assembly for design basis heat load (35.49 kW)

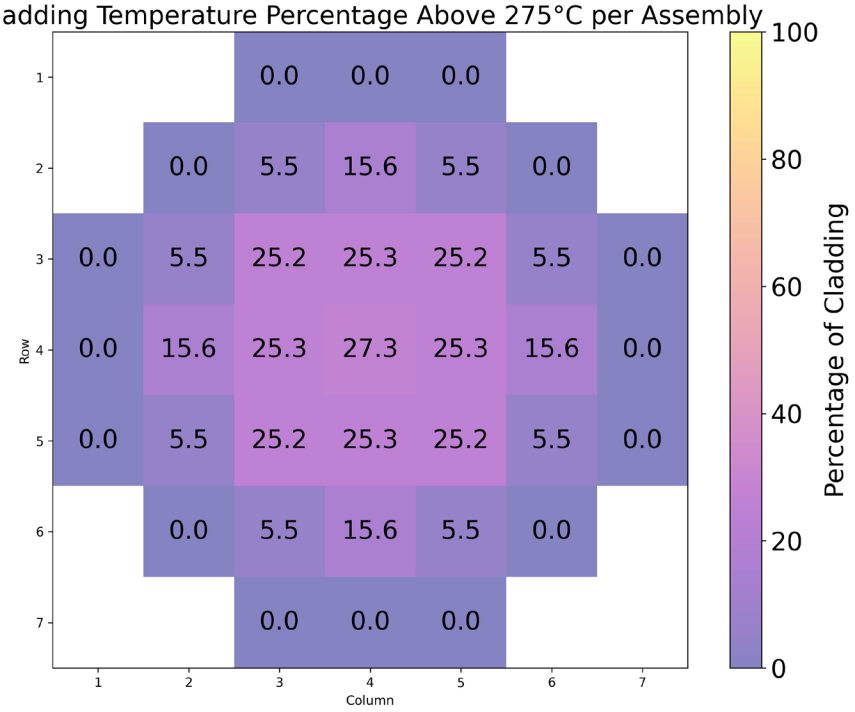

Figure 37. MAGNASTOR HLZC 1 map of percentage of cladding above 275°C per assembly after 5.1 years of storage (27.20 kW)

Figure 38 shows the axial temperature profile of the PCT rod at initial loading, and after it has cooled to be less than 275°C. The vertical lines are included to show the portion of rod that is above 275°C, 300°C, and 350°C.

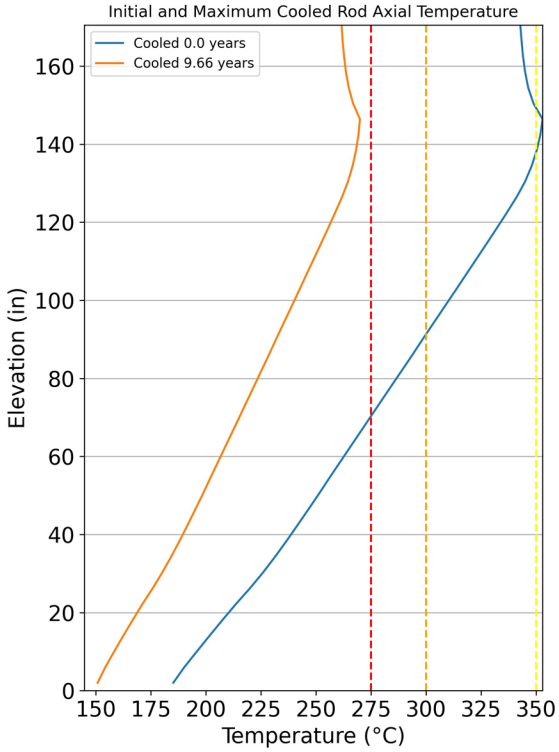

Figure 38. MAGNASTOR HLZC 1 axial temperature profile of hottest rod at the design basis heat load (35.49 kW) and after 9.6 years of storage time (24.69 kW), red dashed line at 275°C, orange dashed line at 300°C, and yellow dashed line at 350°C

3.2.1.3 HLZC 2

Table 8 shows the tabular results for HLZC 2 for the MAGNASTOR COBRA-SFS model. These results include the time in storage, heat load, PCT, percent cladding above certain temperatures for all assemblies in the cask and the PCT assembly.

Table 8. MAGNASTOR HLZC 2 Tabular Data COBRA-SFS Model

Time in Storage		Heat Load		PCT	% Total Cladding Above			PCT Assembly % Cladding Above		
[years]	[months]	[kW]	[% DB]	[°C]	275°C	300°C	350°C	275°C	300°C	350°C
0.00	0.0	35.49	100%	367.0	52.7	33.8	1.2	66.2	54.3	11.5
0.04	0.5	35.27	99%	365.1	51.9	32.8	1	65.6	53.5	9.6
0.15	1.8	34.73	98%	360.1	50.1	30.1	0.6	63.9	51.4	5.5
0.26	3.1	34.19	96%	355.2	48.0	27.4	0.2	62.0	49.3	2.3
0.37	4.4	33.63	95%	349.9	45.7	24.7	0	60.1	47	0
0.49	5.9	33.11	93%	344.8	43.3	22.1	0	58.1	44.4	0
0.63	7.6	32.56	92%	339.9	40.6	19.4	0	56.2	41.9	0
0.78	9.4	32.04	90%	334.9	37.7	16.9	0	54.0	39.3	0
0.95	11.4	31.49	89%	329.7	34.7	14.1	0	51.6	35.6	0
1.15	13.7	30.96	87%	324.7	31.6	11.1	0	49.3	30.9	0
1.35	16.2	30.41	86%	319.6	28.3	4.6	0	46.7	22.7	0
1.57	18.9	29.85	84%	314.5	25.1	2.1	0	43.8	14.5	0
1.82	21.8	29.31	83%	309.4	21.8	0.8	0	41.1	7.7	0
2.12	25.4	28.77	81%	304.5	18.5	0.3	0	38.1	2.8	0
2.46	29.6	28.22	80%	299.6	15.2	0	0	34.7	0	0
2.83	34.0	27.66	78%	294.5	11.4	0	0	28.5	0	0
3.24	38.9	27.13	76%	289.8	4.6	0	0	19.4	0	0
3.74	44.9	26.57	75%	284.9	1.5	0	0	10.3	0	0
4.32	51.8	26.04	73%	280.1	0.4	0	0	3.7	0	0
5.00	60.0	25.48	72%	275.3	0.0	0	0	0.0	0	0
5.79	69.4	24.93	70%	270.6	0.0	0	0	0.0	0	0

Figure 39 shows the cladding temperature distribution for all assemblies, the PCT assembly, and minimum average temperature assembly. Also included is the cladding temperature distribution for all assemblies after 5.8 years of storage which results in a PCT of less than 275°C.

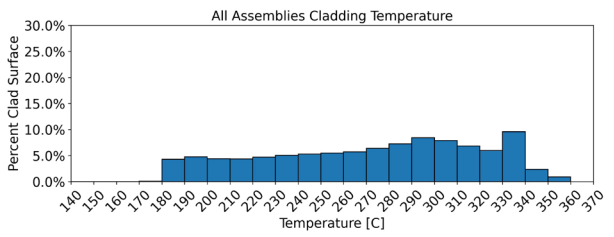

a) HLZC 2 design basis heat load (35.49 kW) all assemblies cladding temperature histogram

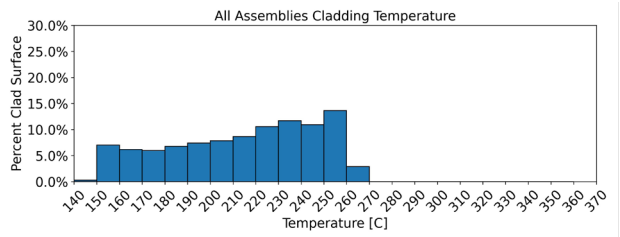

b) HLZC 2 5.8 years after storage (24.93 kW) all assemblies cladding temperature histogram

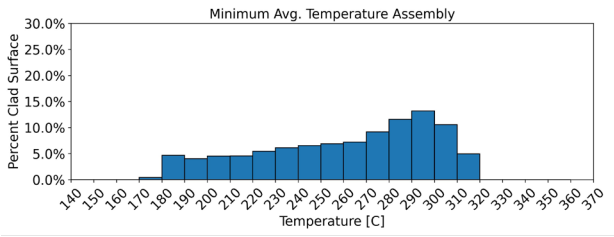

b) HLZC 2 design basis heat load (35.49 kW) assembly with the lowest average cladding temperature histogram

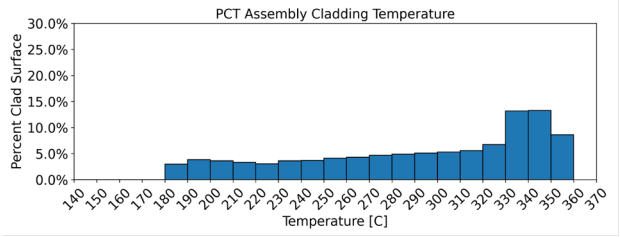

c) HLZC 2 design basis heat load (35.49 kW) assembly containing the PCT cladding temperature histogram

Figure 39. Cladding temperature histograms at design basis heat load for MAGNASTOR HLZC 2 from COBRA-SFS model

Figure 40 shows a box and whisker plot for HLZC 2 for the COBRA-SFS MAGNASTOR model. The horizontal dashed lines are placed at 275°C, 300°C, and 350°C to better visualize the amount of cladding above those temperature thresholds.

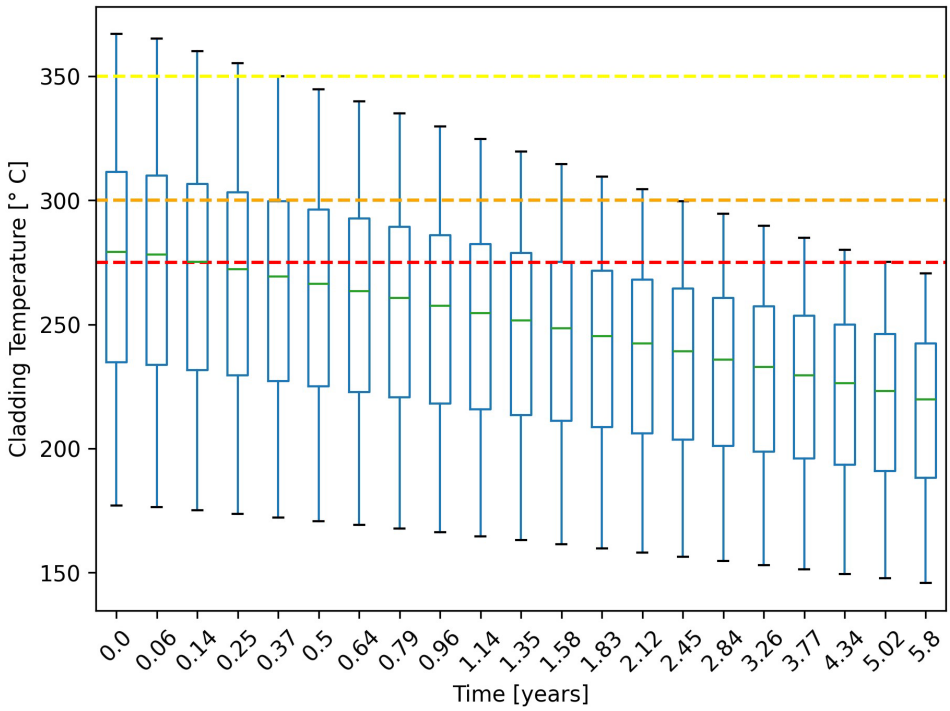

Figure 40. Box plot of HLZC 2 COBRA-SFS MAGNASTOR Model, red dashed line at 275°C. orange dashed line at 300°C, and yellow dashed line at 350°C

Figure 41 to Figure 44 show the PCT maps, and percentage of cladding above 275°C. Maps for the PCT after 5.8 years of storage which results in PCT less than 275°C are included. Also included is a map of the percentage of cladding above 275°C after 3.2 years of storage. 3.2 years of storage is approximately half the time it takes the fuel to cool from the design basis to less than 275°C PCT.

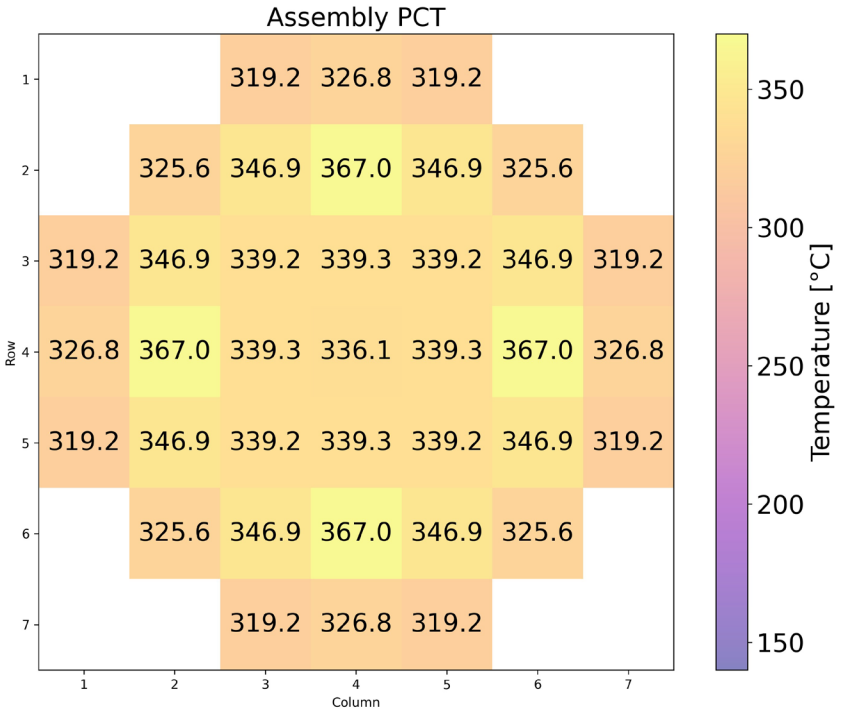

Figure 41. PCT map for MAGNASTOR HLZC 2 design basis heat load (35.49 kW)

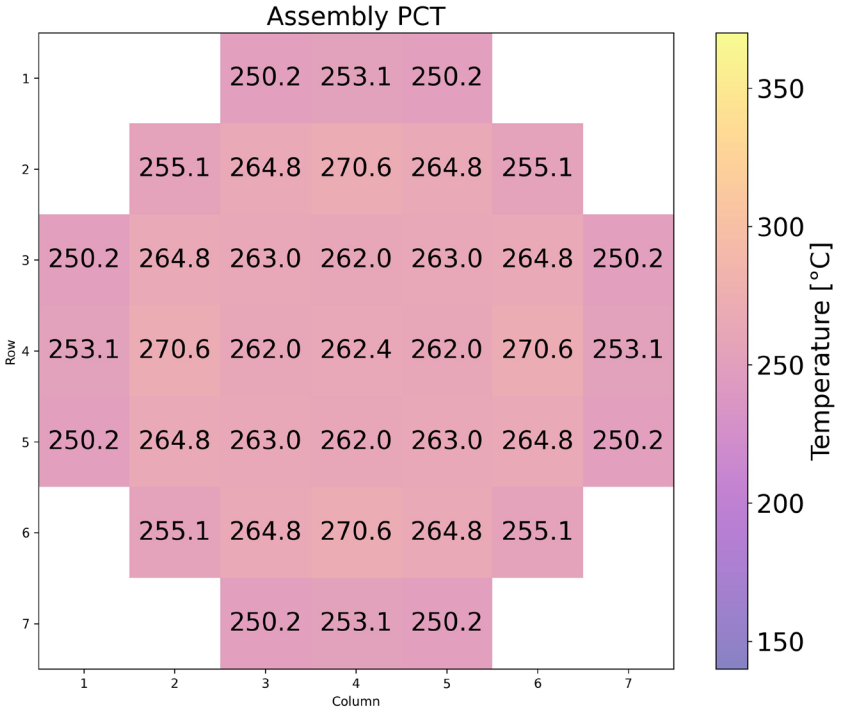

Figure 42. PCT map for MAGNASTOR HLZC 2 after 5.8 years of storage (24.93kW)

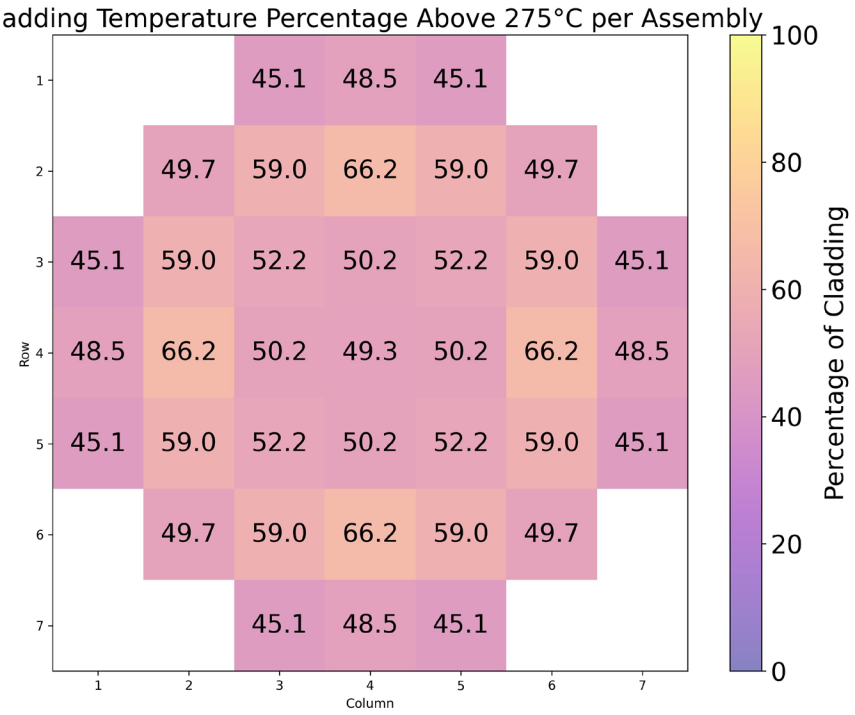

Figure 43. MAGNASTOR HLZC 2 map of percentage of cladding above 275°C per assembly for design basis heat load (35.49 kW)

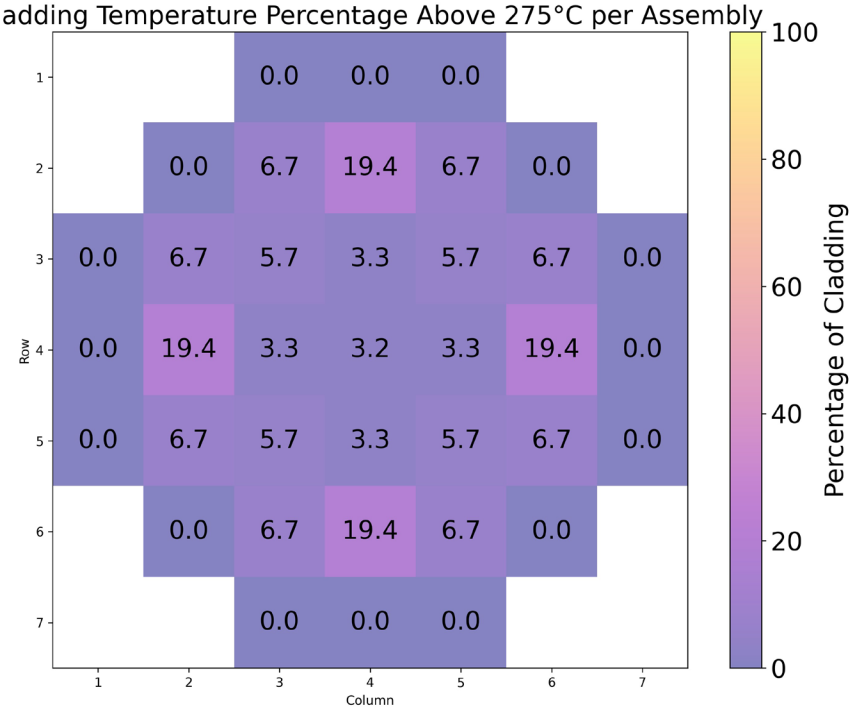

Figure 44. MAGNASTOR HLZC 2 map of percentage of cladding above 275°C per assembly after 3.2 years of storage (27.13 kW)

Figure 45 shows the axial temperature profile of the PCT rod at initial loading and after it has cooled to be less than 275°C. The vertical lines are included to show the portion of rod that is above 275°C, 300°C, and 350°C.

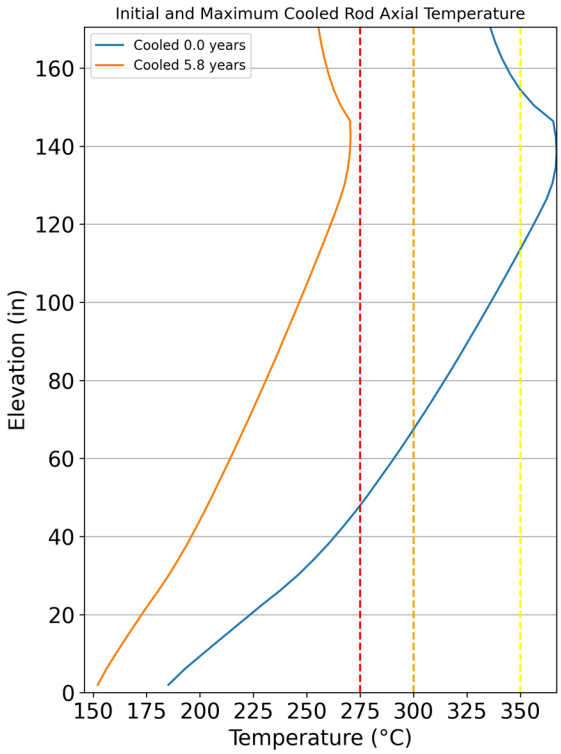

Figure 45. MAGNASTOR HLZC 2 axial temperature profile of hottest rod at the design basis heat load (35.49 kW) and after 5.8 years of storage time (24.93 kW), red dashed line at 275°C, orange dashed line at 300°C, and yellow dashed line at 350°C

3.2.1.4 Summary and Heat Loading Zone Configuration Comparison

The results for the COBRA-SFS MAGNASTOR models are summarized in Figure 46 to Figure 52 for the three heat load zone configurations. Figure 46 shows the PCT decline over the storage time of the fuel. Figure 47 shows the percentage of cladding that is over 275°C over the storage time of the fuel. Figure 48 shows the percentage of cladding over 275°C for the PCT assembly. The following figures Figure 49 to Figure 52 show the percentage of cladding over 300°C and 350°C for all assemblies as well as for just the PCT assembly.

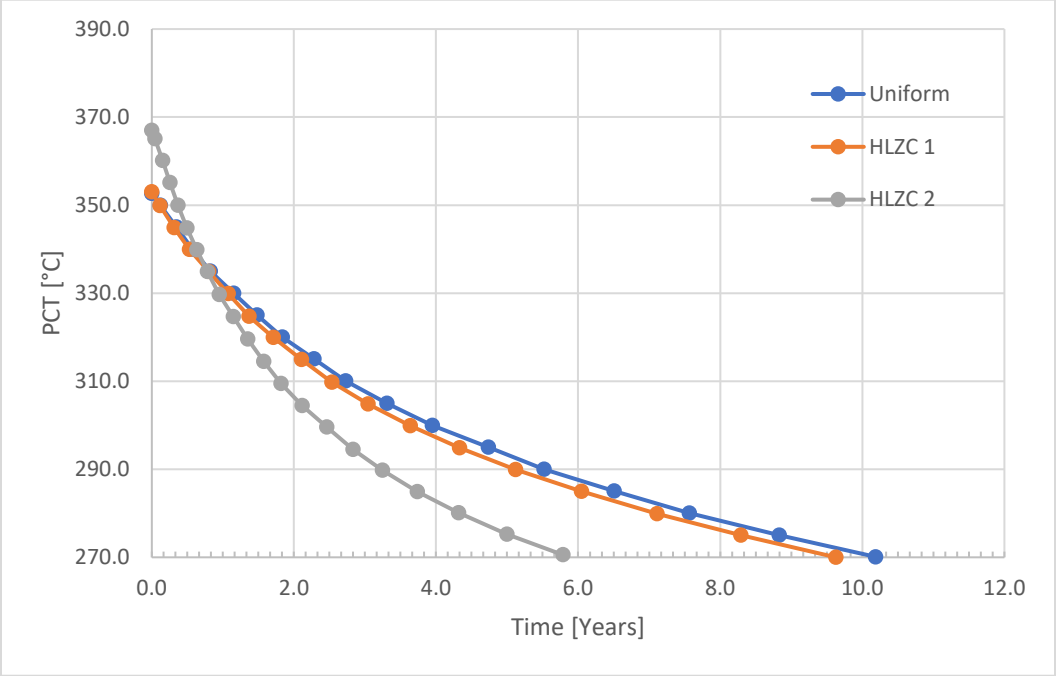

Figure 46. COBRA-SFS MAGNASTOR model PCT vs Time

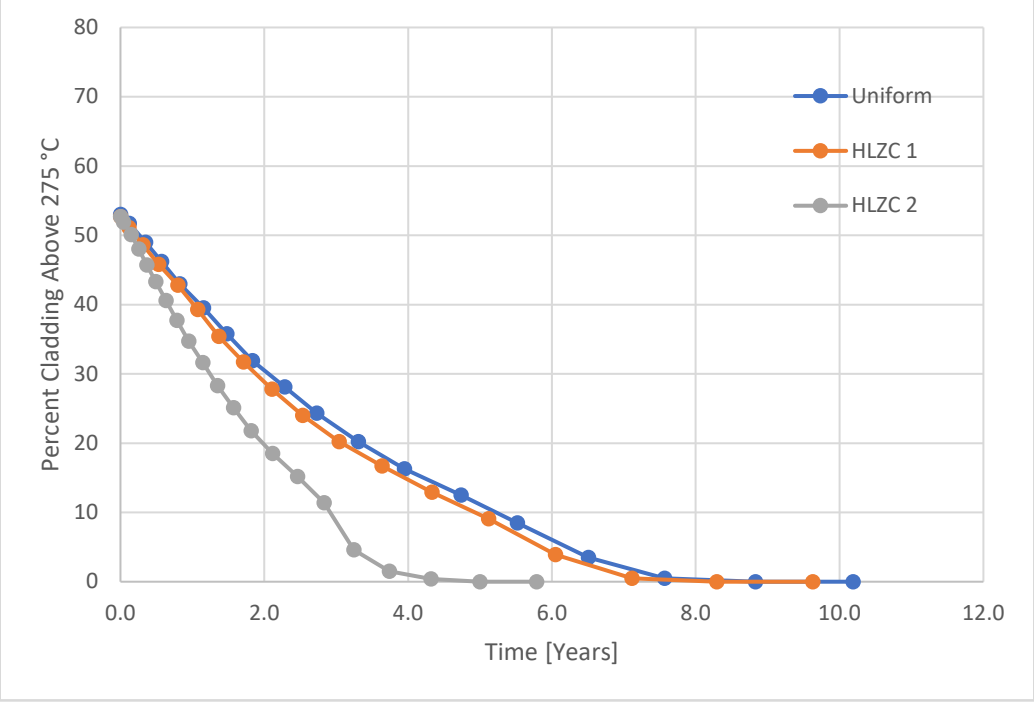

Figure 47. COBRA-SFS MAGNASTOR model percentage of cladding above 275°C vs time

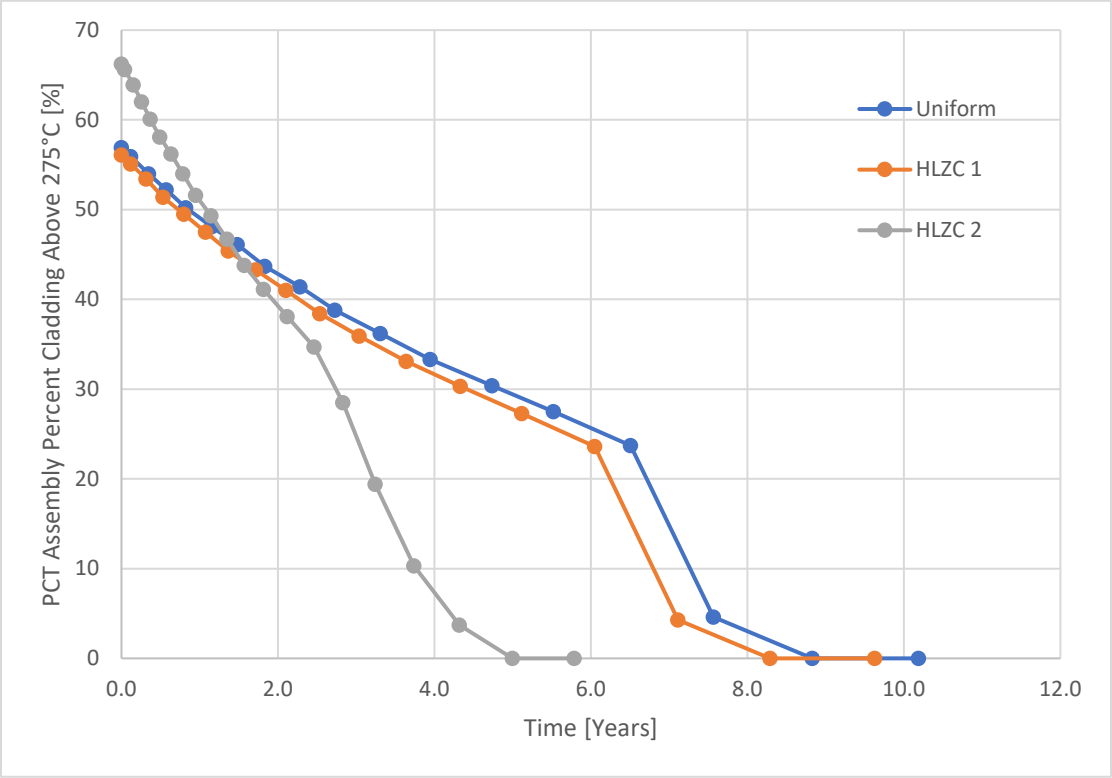

Figure 48. COBRA-SFS MAGNASTOR model percentage of cladding above 275°C in the assembly containing the PCT vs Time

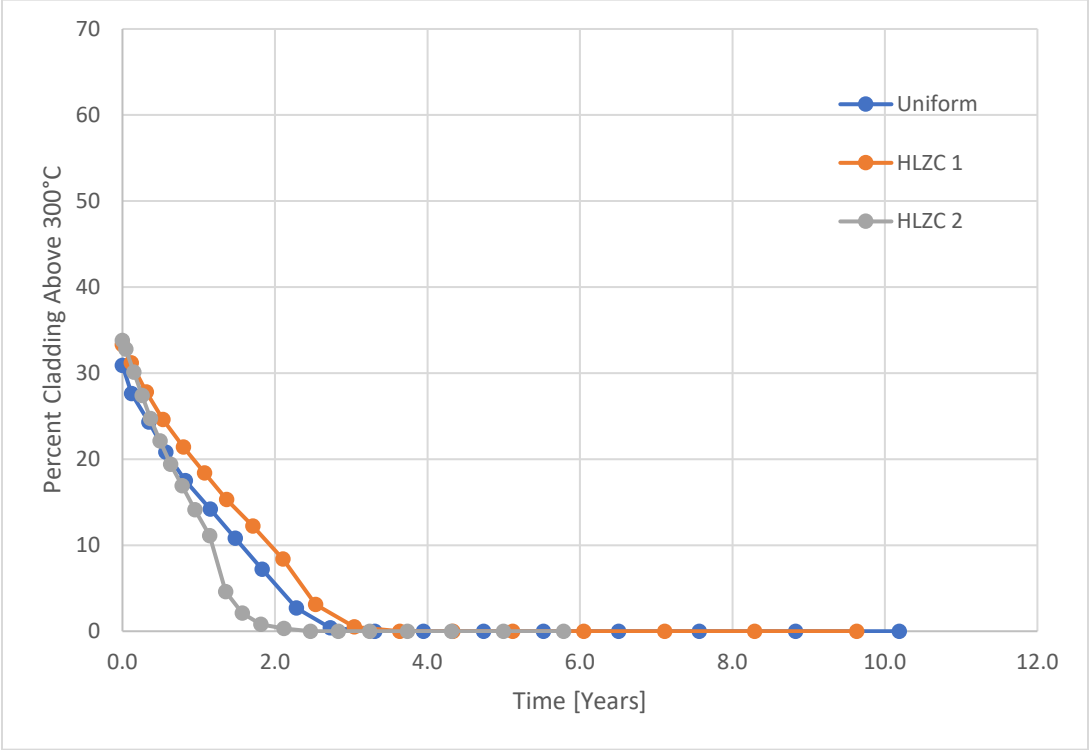

Figure 49. COBRA-SFS MAGNASTOR model percentage of cladding above 300°C vs Time

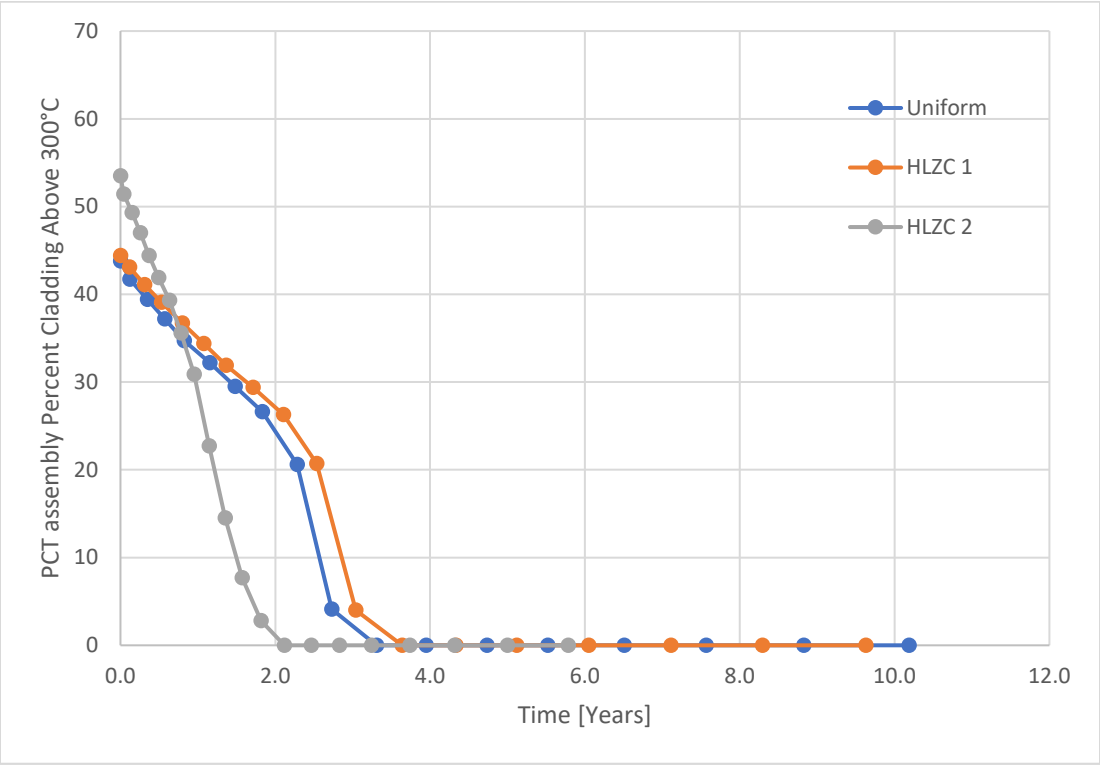

Figure 50. COBRA-SFS MAGNASTOR model percentage of cladding above 300°C in the assembly containing the PCT vs Time

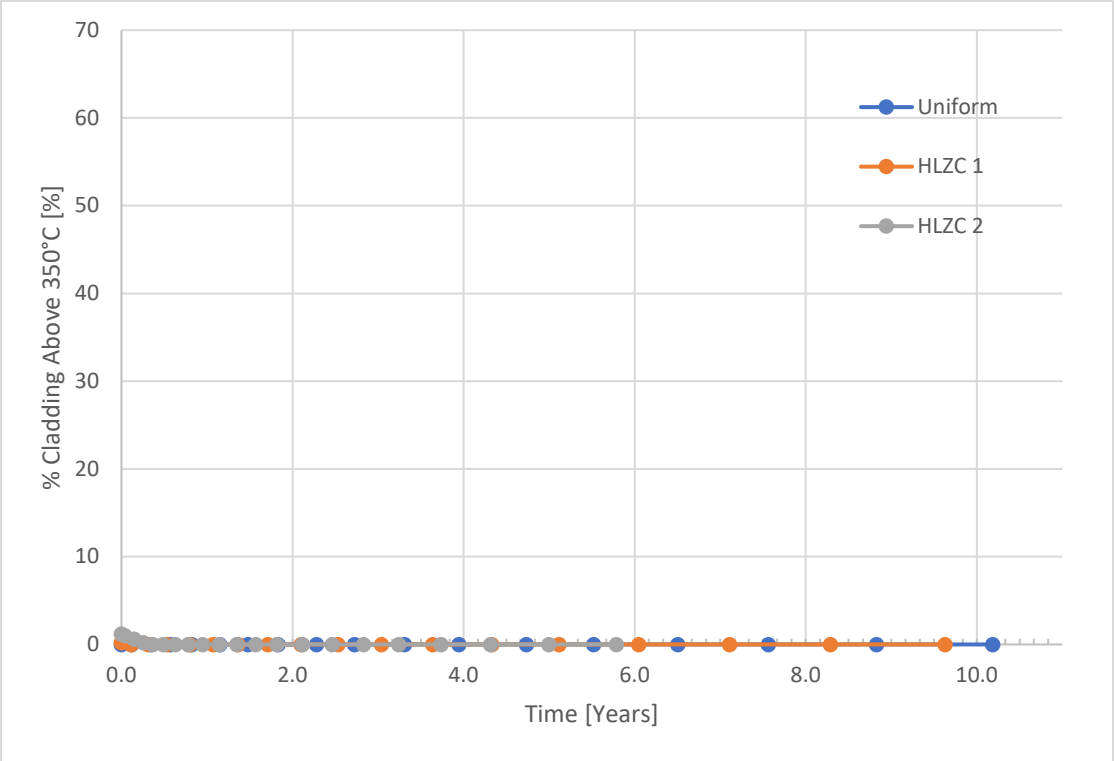

Figure 51. COBRA-SFS MAGNASTOR model percentage of cladding above 350°C vs Time

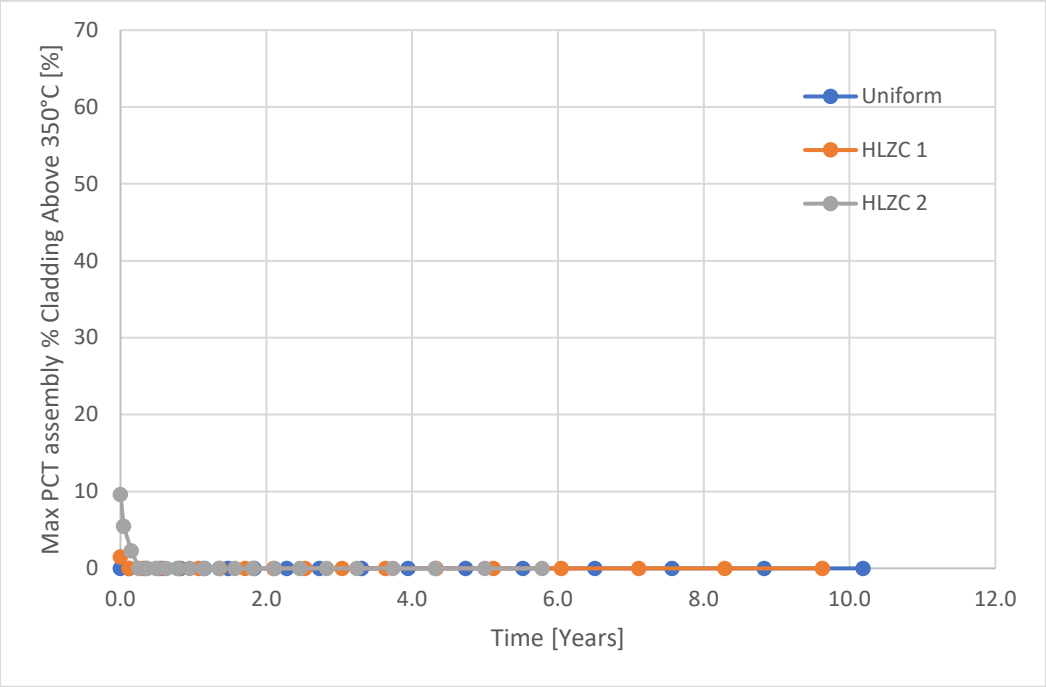

Figure 52. COBRA-SFS MAGNSTOR model percentage of cladding above 350°C in the assembly containing the PCT vs Time

3.2.2 STAR-CCM+ Results

3.2.2.1 Uniform HLZC

Table 9 lists the STAR-CCM+ results for the MAGNASTOR system for the uniform HLZC loading at several storage times. The storage times were chosen as a subset of the COBRA-SFS storage times to produce ~10°C temperature intervals in PCT. The system heat load, the heat load as a percentage of the design basis, the predicted PCT of the loading, the percentage of total cladding above 275°C, 300°C, and 350°C, and the percentage of cladding in the assembly containing the predicted PCT above 275°C, 300°C, and 350°C are listed.

Table 9. MAGNASTOR uniform HLZC tabular data from STAR-CCM+ model

Time in Storage		Heat Load		PCT	% Total Cladding Above			PCT Assembly % Cladding Above		
[years]	[months]	[kW]	[% DB]	[°C]	275°C	300°C	350°C	275°C	300°C	350°C
0.0	0.0	35.5	100.0%	368.5	44%	27%	2%	54%	47%	22%
0.3	3.2	34.7	97.8%	362.8	41%	24%	1%	53%	46%	14%
0.7	8.5	33.4	94.0%	353.5	37%	20%	0%	51%	44%	1%
1.4	16.2	32.1	90.3%	343.8	32%	15%	0%	49%	41%	0%
2.1	25.2	30.8	86.7%	334.0	26%	11%	0%	47%	38%	0%
3.1	36.8	29.5	83.0%	324.1	20%	6%	0%	44%	31%	0%
4.4	52.8	28.2	79.4%	314.4	15%	2%	0%	41%	20%	0%
6.1	72.6	26.9	75.8%	304.4	11%	0%	0%	37%	2%	0%
8.3	99.2	25.6	72.2%	294.3	5%	0%	0%	28%	0%	0%
11.0	132.0	24.4	68.7%	284.3	1%	0%	0%	12%	0%	0%

Figure 53 shows the cladding temperature histograms of a) total cladding temperature at the design basis heat load, b) PCT containing assembly at the design basis heat load, c) total cladding temperature at coldest simulated heat load, and d) coldest average assembly at the design basis heat load for the MAGNASTOR uniform HLZC from the STAR-CCM+ model.

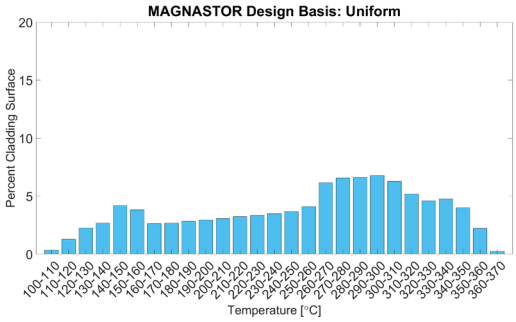

a) Total cladding temperature histogram for design basis heat load (35.5 kW)

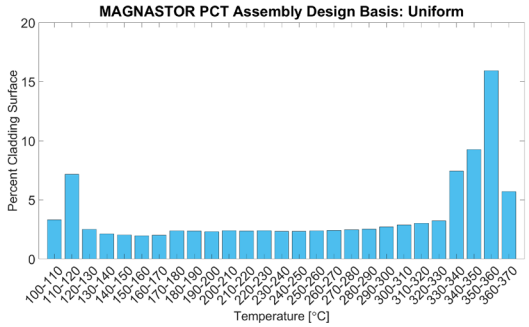

b) PCT assembly cladding temperature histogram for design basis heat load (35.5 kW)

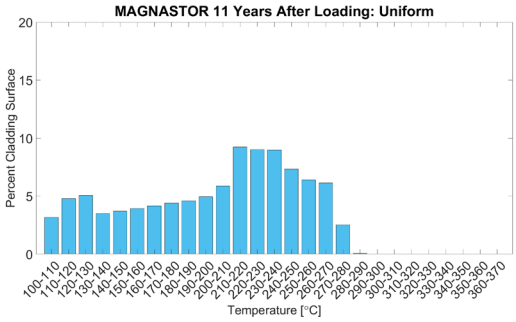

c) Total cladding temperature histogram for final simulated heat load (24.4 kW)

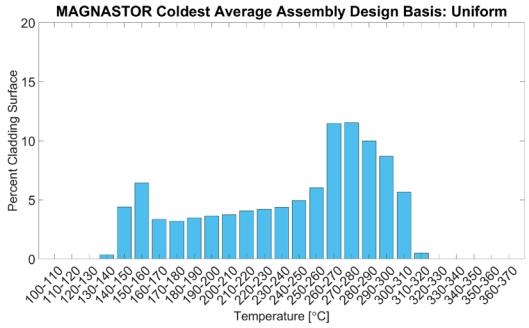

d) Coldest average assembly cladding temperature histogram for design basis heat load (35.5 kW)

Figure 53. Total and select assembly cladding temperature histograms at design basis heat load (35.5 kW) and final simulated heat load (24.4 kW) for the MAGNASTOR uniform HLZC from the STAR-CCM+ model

Figure 54 shows box plots for all the simulated loadings. These plots summarize the maximum (PCT), 75th percentile, median, 25th percentile, and minimum cladding temperatures. Dashed lines for the 275°C, 300°C, and 350°C limits are also shown.

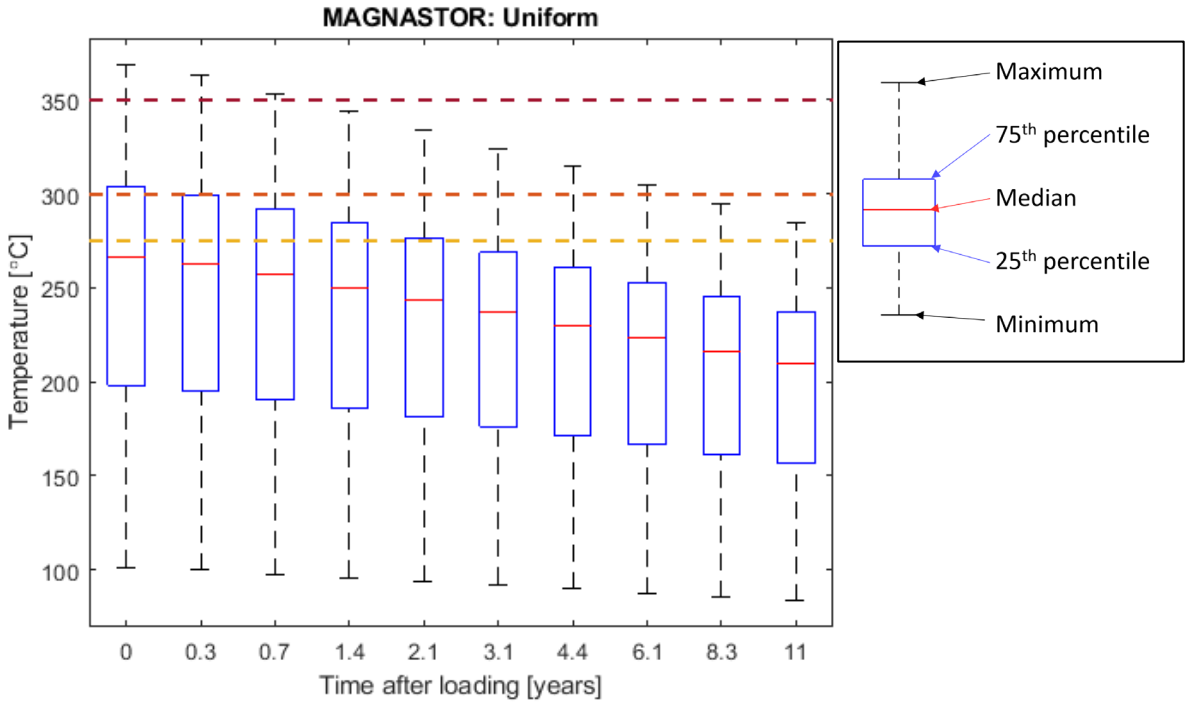

Figure 54. Box plot of uniform HLZC STAR-CCM+ MAGNASTOR model with temperature limits identified with dashed lines

Figure 55 shows a map of locations of the assemblies in the MAGNASTOR model. Each assembly is labeled with its local PCT, and the local percentage of cladding above 275°C, 300°C, and 350°C for the design basis uniform HLZC heat load.

PCT [°C]
Percent above 275°C
Percent above 300°C
Percent above 350°C

		314 30% 6% 0%	322 34% 14% 0%	315 31% 7% 0%		
	327 44% 17% 0%	345 50% 36% 0%	349 53% 44% 0%	345 50% 37% 0%	326 44% 17% 0%	
315 31% 7% 0%	345 50% 36% 0%	358 53% 46% 6%	362 53% 46% 12%	358 54% 46% 7%	345 50% 37% 0%	314 31% 6% 0%
322 33% 14% 0%	349 53% 44% 0%	362 53% 46% 12%	369 54% 47% 22%	362 53% 46% 12%	349 53% 44% 0%	322 34% 15% 0%
314 32% 7% 0%	345 50% 36% 0%	358 54% 46% 6%	362 53% 46% 12%	358 54% 46% 6%	345 50% 36% 0%	315 30% 6% 0%
	326 44% 16% 0%	345 50% 36% 0%	349 53% 44% 0%	345 50% 36% 0%	326 44% 16% 0%	
		315 31% 7% 0%	322 33% 14% 0%	315 30% 6% 0%		

Figure 55. Assembly map with PCT and percent of cladding in each assembly above 275°C, 300°C, and 350°C for the design basis loading (35.5 kW) of the MAGNASTOR uniform HLZC from the STAR-CCM+ model.

Figure 56 shows the axial temperature profiles at the PCT location for the design basis and lowest simulated heat load.

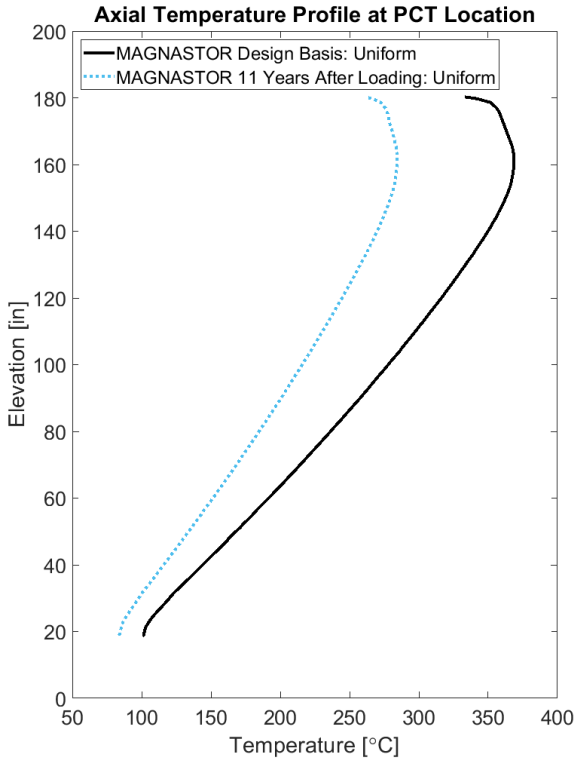

Figure 56. Temperature profiles of rods with PCT for design basis (35.5 kW) and final simulated heat loads (24.4 kW) from STAR-CCM+ MAGNASTOR uniform HLZC model.

3.2.2.2 HLZC 1

Table 10 lists the STAR-CCM+ results for the MAGNASTOR system for the HLZC 1 loading at several storage times. The storage times were chosen as a subset of the COBRA-SFS storage times to produce ~10°C temperature intervals in PCT. The system heat load, the heat load as a percentage of the design basis, the predicted PCT of the loading, the percentage of total cladding above 275°C, 300°C, and 350°C, and the percentage of cladding in the assembly containing the predicted PCT above 275°C, 300°C, and 350°C are listed.

Table 10. MAGNASTOR HLZC 1 tabular data from STAR-CCM+ model

Time in Storage		Heat Load		PCT	% Total Cladding Above			PCT Assembly % Cladding Above		
[years]	[months]	[kW]	[% DB]	[°C]	275°C	300°C	350°C	275°C	300°C	350°C
0.0	0.0	35.5	100.0%	368.1	43%	27%	3%	54%	47%	22%
0.0	0.4	35.4	99.6%	367.0	43%	27%	3%	53%	47%	21%
0.5	5.7	33.9	95.4%	356.8	38%	22%	0%	52%	44%	4%
1.0	11.8	32.6	91.9%	347.8	34%	18%	0%	50%	42%	0%
1.6	19.1	31.3	88.1%	338.0	28%	14%	0%	47%	39%	0%
2.4	28.2	30.0	84.6%	328.4	23%	9%	0%	45%	35%	0%
3.4	40.8	28.7	80.9%	318.4	18%	4%	0%	42%	25%	0%
4.8	57.6	27.4	77.3%	308.8	13%	0%	0%	39%	9%	0%
6.7	80.4	26.2	73.7%	298.8	8%	0%	0%	33%	0%	0%
9.1	109.2	24.9	70.2%	288.8	2%	0%	0%	21%	0%	0%

Figure 57 shows the cladding temperature histograms of a) total cladding temperature at the design basis heat load, b) PCT containing assembly at the design basis heat load, c) total cladding temperature at coldest simulated heat load, and d) coldest average assembly at the design basis heat load for the MAGNASTOR HLZC 1 from the STAR-CCM+ model.

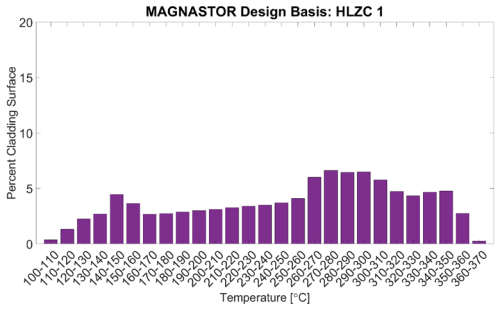

a) Total cladding temperature histogram for design basis heat load (35.5 kW)

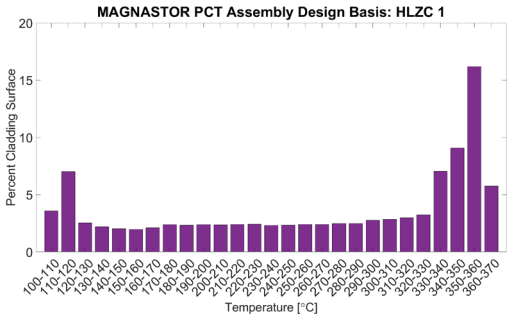

b) PCT assembly cladding temperature histogram for design basis heat load (35.5 kW)

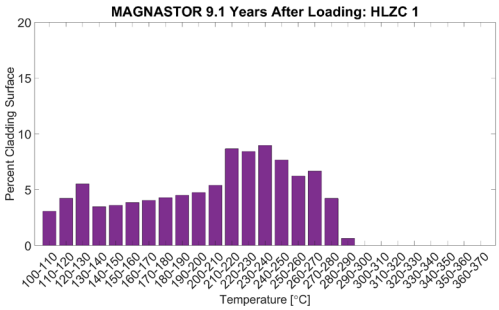

c) Total cladding temperature histogram for final simulated heat load (24.9 kW)

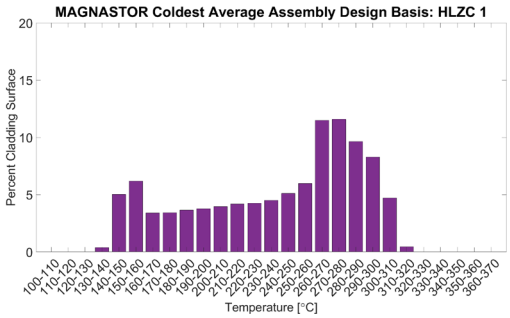

d) Coldest average assembly cladding temperature histogram for design basis heat load (35.5 kW)

Figure 57. Total and select assembly cladding temperature histograms at design basis heat load (35.5 kW) and final simulated heat load (24.9 kW) for the MAGNASTOR HLZC 1 from the STAR-CCM+ model

Figure 58 shows box plots for all the loadings. These plots summarize the maximum (PCT), 75th percentile, median, 25th percentile, and minimum cladding temperatures. Dashed lines for the 275°C, 300°C, and 350°C limits are also shown.

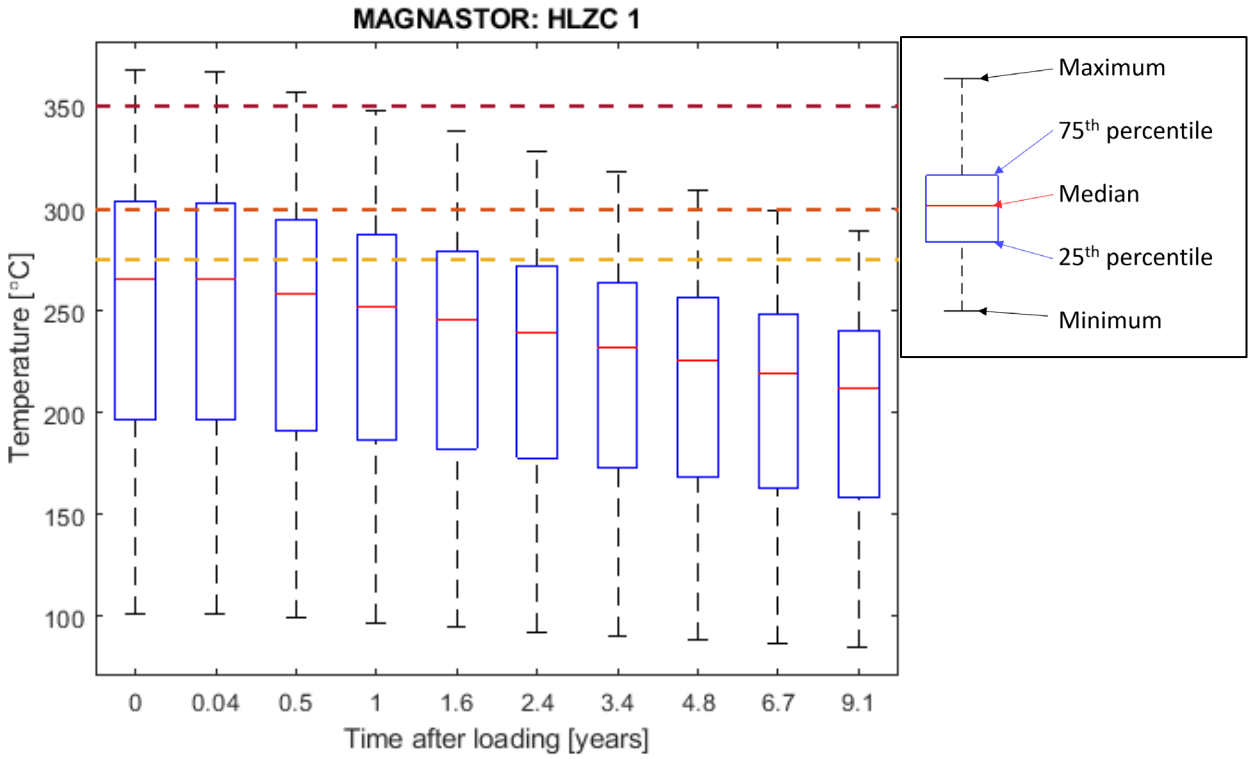

Figure 58. Box plot of HLZC 1 STAR-CCM+ MAGNASTOR HLZC 1 model with temperature limits identified with dashed lines

Figure 59 shows a map of locations of the assemblies in the MAGNASTOR model. Each assembly is labeled with its local PCT, and the local percentage of cladding above 275°C, 300°C, and 350°C for the design basis HLZC 1 heat load.

PCT [°C]
Percent above 275°C
Percent above 300°C
Percent above 350°C

		315 28% 5% 0%	323 33% 14% 0%	316 29% 6% 0%		
	329 44% 17% 0%	348 51% 38% 0%	355 53% 45% 2%	348 51% 38% 0%	328 43% 16% 0%	
316 29% 6% 0%	348 51% 37% 0%	359 53% 46% 8%	363 53% 46% 14%	359 54% 46% 8%	348 51% 38% 0%	315 29% 5% 0%
323 32% 14% 0%	355 54% 45% 1%	363 53% 46% 14%	368 54% 47% 22%	363 53% 45% 14%	355 53% 45% 2%	323 33% 15% 0%
315 30% 6% 0%	348 50% 37% 0%	359 54% 46% 8%	363 53% 46% 14%	359 53% 46% 8%	348 51% 38% 0%	316 28% 5% 0%
	328 43% 16% 0%	348 50% 37% 0%	355 53% 45% 2%	348 51% 37% 0%	328 43% 15% 0%	
		316 29% 6% 0%	323 32% 14% 0%	316 28% 5% 0%		

Figure 59. Assembly map with PCT and percent of cladding in each assembly above 275°C, 300°C, and 350°C for the design basis loading (35.5 kW) of the MAGNASTOR HLZC 1 from the STAR-CCM+ model.

Figure 60 shows the axial temperature profiles at the PCT location for the design basis and lowest simulated heat load.

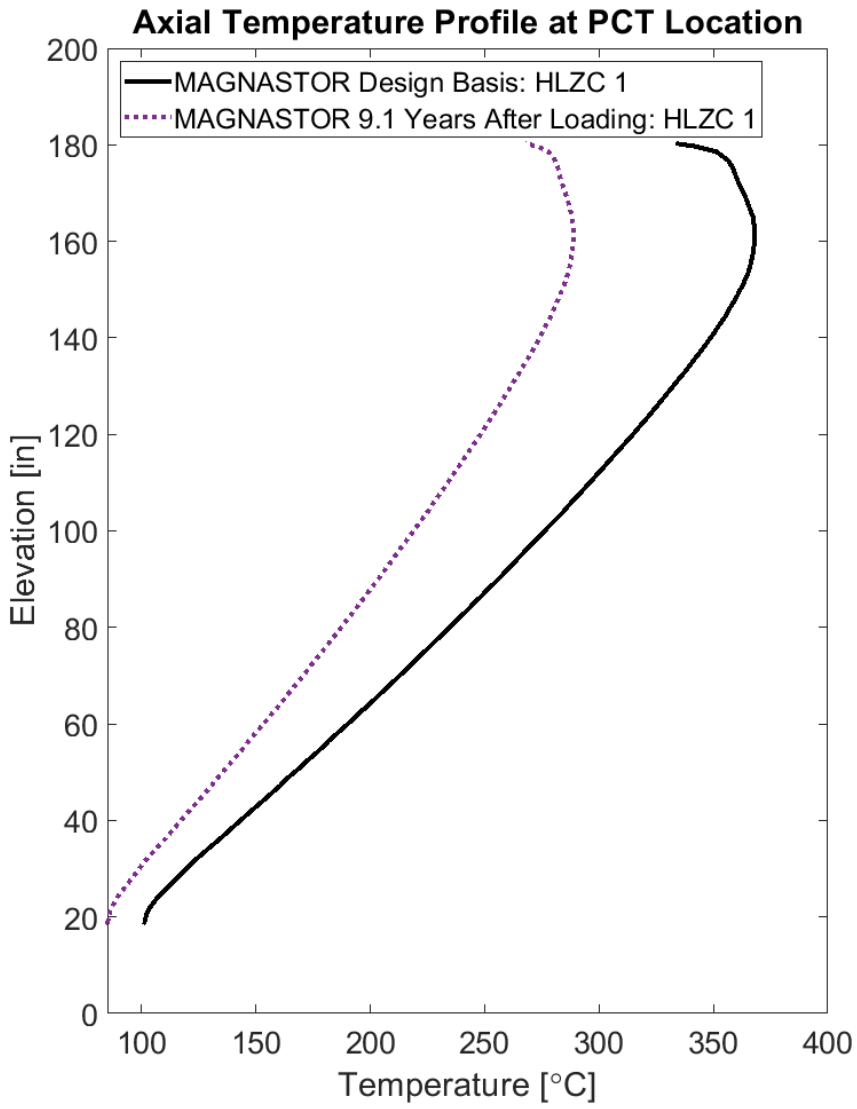

Figure 60. Temperature profiles of rods with PCT for design basis (35.5 kW) and final simulated heat loads (24.9 kW) from STAR-CCM+ MAGNASTOR HLZC 1model.

3.2.2.3 HLZC 2

Table 11 lists the STAR-CCM+ results for the MAGNASTOR system for the HLZC 2 loading at several storage times. The storage times were chosen as a subset of the COBRA-SFS storage times to produce ~10°C temperature intervals in PCT. The system heat load, the heat load as a percentage of the design basis, the predicted PCT of the loading, the percentage of total cladding above 275°C, 300°C, and 350°C, and the percentage of cladding in the assembly containing the predicted PCT above 275°C, 300°C, and 350°C are listed.

Table 11. MAGNASTOR HLZC 2 tabular data from STAR-CCM+ model

Time in Storage		Heat Load		PCT	% Total Cladding Above			PCT Assembly % Cladding Above		
[years]	[months]	[kW]	[% DB]	[°C]	275°C	300°C	350°C	275°C	300°C	350°C
0.0	0.0	35.5	100.0%	369.4	44%	28%	1%	55%	48%	8%
0.1	1.2	35.0	98.6%	365.1	43%	27%	1%	54%	47%	5%
0.2	2.4	34.5	97.2%	361.0	41%	25%	0%	54%	46%	2%
0.4	5.0	33.4	94.2%	351.7	38%	21%	0%	52%	42%	0%
0.7	8.4	32.3	91.1%	342.3	34%	18%	0%	50%	37%	0%
1.1	12.6	31.2	87.9%	332.3	29%	13%	0%	47%	29%	0%
1.5	17.4	30.2	85.0%	323.0	25%	9%	0%	44%	19%	0%
2.0	24.0	29.0	81.6%	312.6	19%	3%	0%	38%	7%	0%
2.7	31.8	27.9	78.7%	303.4	15%	0%	0%	30%	1%	0%
3.6	42.6	26.8	75.5%	293.6	9%	0%	0%	18%	0%	0%
4.8	57.0	25.68	72.3%	284.9	3%	0%	0%	18%	0%	0%
6.6	79.2	24.47	68.9%	276.3	0%	0%	0%	0%	0%	0%

Figure 61 shows the cladding temperature histograms of a) total cladding temperature at the design basis heat load, b) PCT containing assembly at the design basis heat load, c) total cladding temperature at coldest simulated heat load, and d) coldest average assembly at the design basis heat load for the MAGNASTOR HLZC 2 from the STAR-CCM+ model.

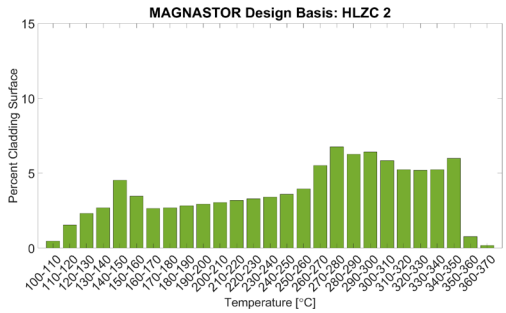

a) Total cladding temperature histogram for design basis heat load (35.5 kW)

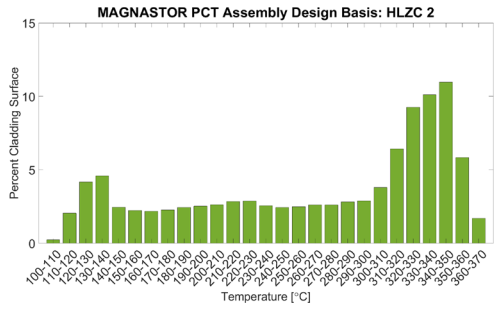

b) PCT assembly cladding temperature histogram for design basis heat load (35.5 kW)

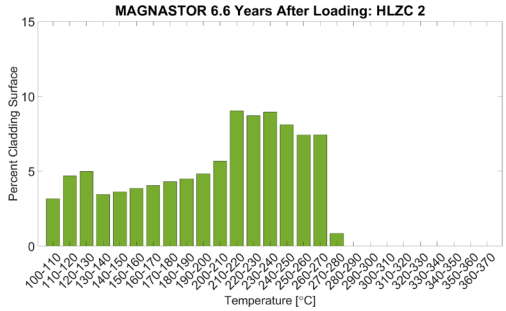

c) Total cladding temperature histogram for final simulated heat load (24.47 kW)

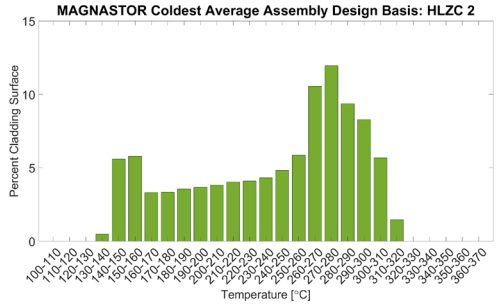

d) Coldest average assembly cladding temperature histogram for design basis heat load (35.5 kW)

Figure 61. Total and select assembly cladding temperature histograms at design basis heat load (35.5 kW) and final simulated heat load (24.47 kW) for the MAGNASTOR HLZC 2 from the STAR-CCM+ model

Figure 62 shows box plots for all the loadings. These plots summarize the maximum (PCT), 75th percentile, median, 25th percentile, and minimum cladding temperatures. Dashed lines for the 275°C, 300°C, and 350°C limits are also shown.

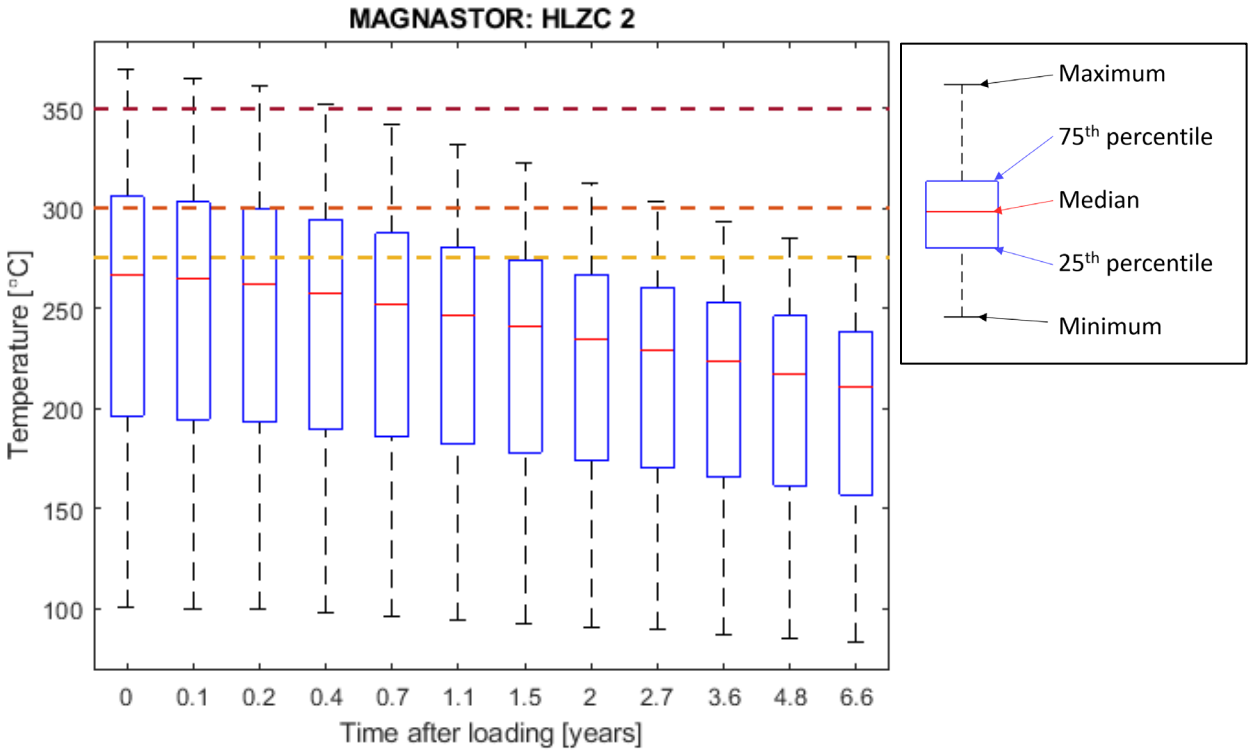

Figure 62. Box and whisker plots for each of the simulated loadings of the MAGNASTOR HLZC 2 loading from the STAR-CCM+ model.

Figure 63 shows a map of locations of the assemblies in the MAGNASTOR model. Each assembly is labeled with its local PCT, and the local percentage of cladding above 275°C, 300°C, and 350°C for the design basis HLZC 2 heat load.

PCT [°C]
Percent above 275°C
Percent above 300°C
Percent above 350°C

		320 30% 7% 0%	329 35% 17% 0%	321 31% 8% 0%		
	329 44% 18% 0%	349 52% 39% 0%	368 55% 48% 7%	349 52% 40% 0%	328 44% 18% 0%	
320 31% 8% 0%	349 51% 39% 0%	349 52% 44% 0%	352 51% 44% 1%	349 52% 44% 0%	349 52% 40% 0%	320 31% 8% 0%
329 34% 17% 0%	368 56% 48% 7%	352 51% 44% 1%	352 51% 44% 1%	352 51% 44% 1%	369 55% 48% 7%	329 35% 17% 0%
320 32% 8% 0%	349 51% 39% 0%	349 52% 45% 0%	352 51% 44% 1%	349 52% 45% 0%	349 52% 39% 0%	320 30% 7% 0%
	329 44% 17% 0%	349 51% 39% 0%	369 55% 48% 8%	349 51% 39% 0%	328 43% 16% 0%	
		321 31% 8% 0%	329 34% 17% 0%	320 30% 7% 0%		

Figure 63. Assembly map with PCT and percent of cladding in each assembly above 275°C, 300°C, and 350°C for the design basis loading (35.5 kW) of the MAGNASTOR HLZC 2 from the STAR-CCM+ model.

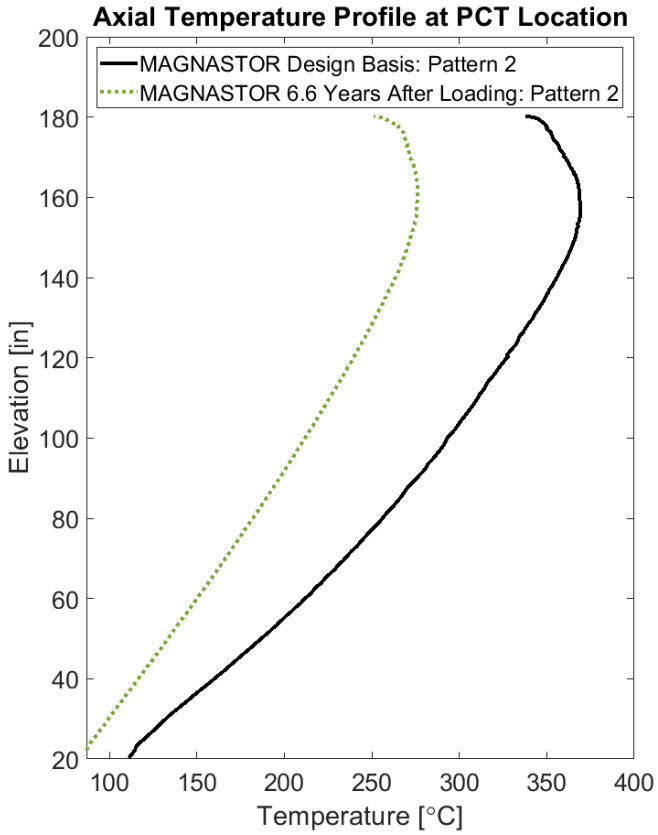

Figure 64. Temperature profiles of rods with PCT for design basis (35.5 kW) and final simulated heat loads (24.47 kW) from STAR-CCM+ MAGNASTOR HLZC 2model.

3.3 NUHOMS 32PTH2

3.3.1 Uniform HLZC

Table 12 lists the STAR-CCM+ results for the NUHOMS system for the uniform HLZC loading at several storage times. The system heat load, the heat load as a percentage of the design basis, the predicted PCT of the loading, the percentage of total cladding above 275°C, 300°C, and 350°C, and the percentage of cladding in the assembly containing the predicted PCT above 275°C, 300°C, and 350°C are listed.

Table 12. NUHOMS uniform HLZC tabular data from STAR-CCM+ model

Time in Storage		Heat Load		PCT	% Total Cladding Above			PCT Assembly % Cladding Above		
[years]	[months]	[kW]	[% DB]	[°C]	275°C	300°C	350°C	275°C	300°C	350°C
0.0	0.0	32.0	100.0%	362.6	43%	24%	1%	66%	58%	7%
0.1	1.0	31.7	99.0%	360.0	41%	22%	0%	65%	57%	5%
0.5	6.3	30.4	95.0%	350.0	36%	17%	0%	63%	53%	0%
1.0	12.1	29.2	91.1%	339.9	29%	12%	0%	60%	47%	0%
1.6	19.7	27.9	87.3%	330.0	23%	7%	0%	57%	38%	0%
2.4	28.9	26.7	83.6%	319.9	17%	3%	0%	52%	19%	0%
3.4	41.0	25.5	79.8%	309.9	11%	1%	0%	45%	6%	0%
4.8	57.8	24.4	76.2%	299.8	5%	0%	0%	32%	0%	0%
6.6	78.8	23.2	72.6%	289.9	1%	0%	0%	12%	0%	0%
8.9	106.8	22.1	69.0%	279.8	0%	0%	0%	2%	0%	0%

Figure 65 shows the cladding temperature histograms of a) total cladding temperature at the design basis heat load, b) PCT containing assembly at the design basis heat load, c) total cladding temperature at coldest simulated heat load, and d) coldest average assembly at the design basis heat load for the NUHOMS uniform HLZC from the STAR-CCM+ model.

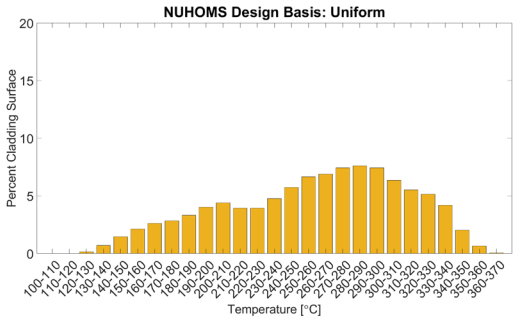

a) Total cladding temperature histogram for design basis heat load (32.0 kW)

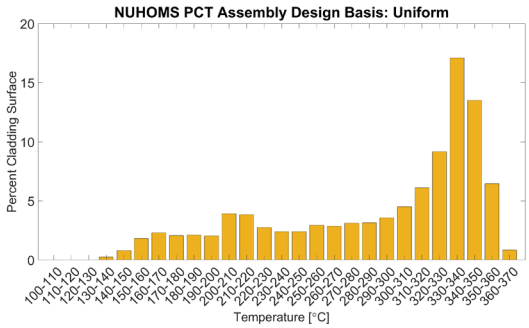

b) PCT assembly cladding temperature histogram for design basis heat load (32.0 kW)

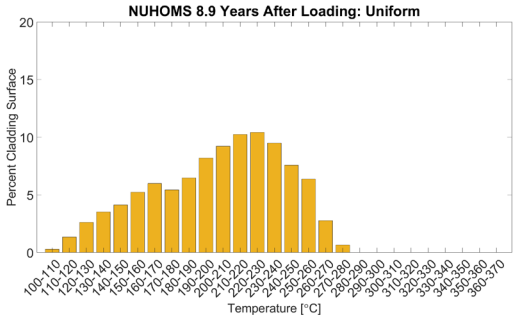

c) Total cladding temperature histogram for final simulated heat load (22.1 kW)

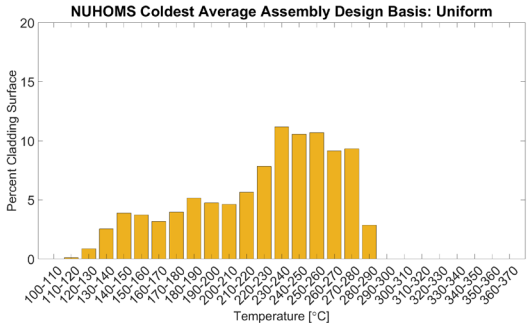

d) Coldest average assembly cladding temperature histogram for design basis heat load (32.0 kW)

Figure 65. Total and select assembly cladding temperature histograms at design basis heat load (32.0 kW) and final simulated heat load (22.1 kW) for the NUHOMS uniform HLZC from the STAR-CCM+ model

Figure 66 shows box plots for all the simulated loadings. These plots summarize the maximum (PCT), 75th percentile, median, 25th percentile, and minimum cladding temperatures. Dashed lines for the 275°C, 300°C, and 350°C limits are also shown.

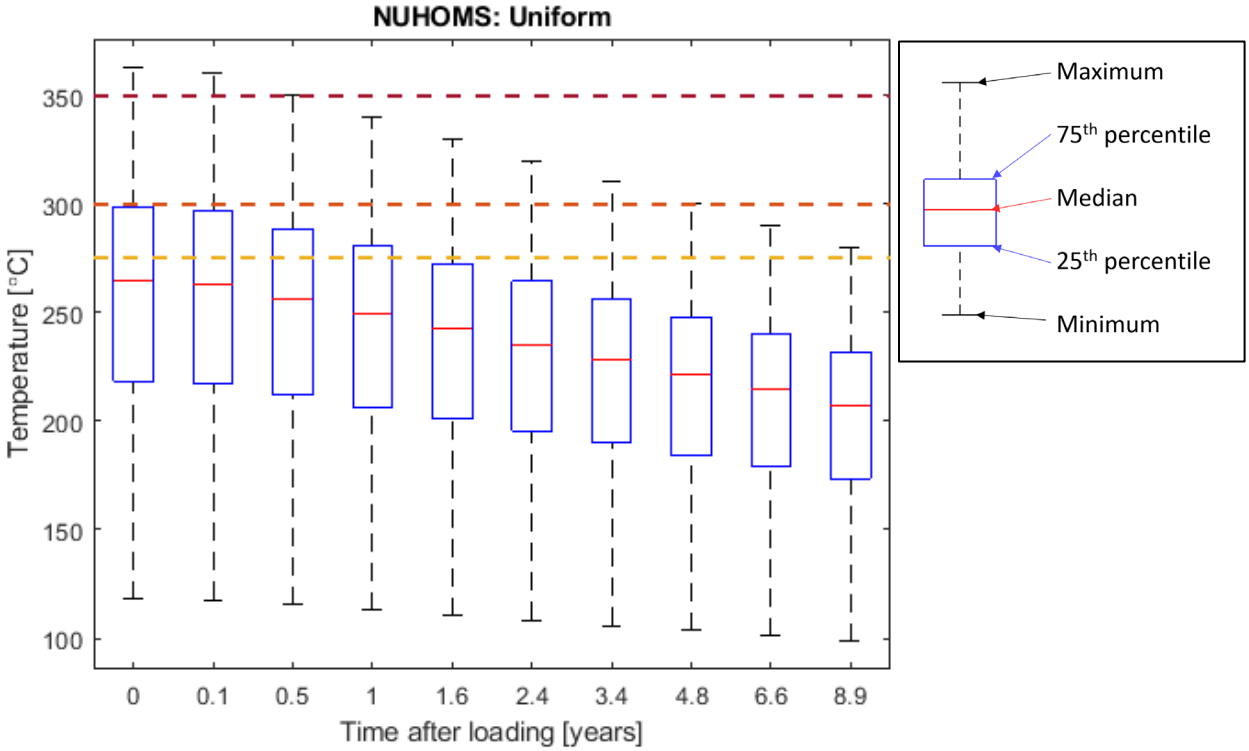

Figure 66. Box plot of uniform HLZC STAR-CCM+ NUHOMS model with temperature limits identified with dashed lines

Figure 67 shows a map of locations of the assemblies in the NUHOMS model. Each assembly is labeled with its local PCT, and the local percentage of cladding above 275°C, 300°C, and 350°C for the design basis uniform HLZC heat load.

PCT [°C]
Percent above 275°C
Percent above 300°C
Percent above 350°C

	306	319	319	307	
	29%	43%	44%	30%	
	3%	18%	18%	3%	
	0%	0%	0%	0%	
301	333	350	350	334	302
24%	57%	64%	64%	57%	25%
0%	34%	53%	53%	34%	0%
0%	0%	0%	0%	0%	0%
311	346	362	363	346	311
35%	63%	66%	66%	63%	35%
7%	49%	58%	58%	49%	7%
0%	0%	7%	7%	0%	0%
308	342	359	359	342	309
32%	61%	65%	65%	61%	32%
4%	45%	56%	56%	45%	4%
0%	0%	4%	4%	0%	0%
291	322	339	338	322	291
12%	45%	58%	59%	46%	13%
0%	19%	39%	39%	19%	0%
0%	0%	0%	0%	0%	0%
	286	301	300	287	
	7%	23%	23%	8%	
	0%	0%	0%	0%	
	0%	0%	0%	0%	

Figure 67. Assembly map with PCT and percent of cladding in each assembly above 275°C, 300°C, and 350°C for the design basis loading (32.0 kW) of the NUHOMS uniform HLZC from the STAR-CCM+ model.

Figure 68 shows the axial temperature profiles at the PCT location for the design basis and lowest simulated heat load.

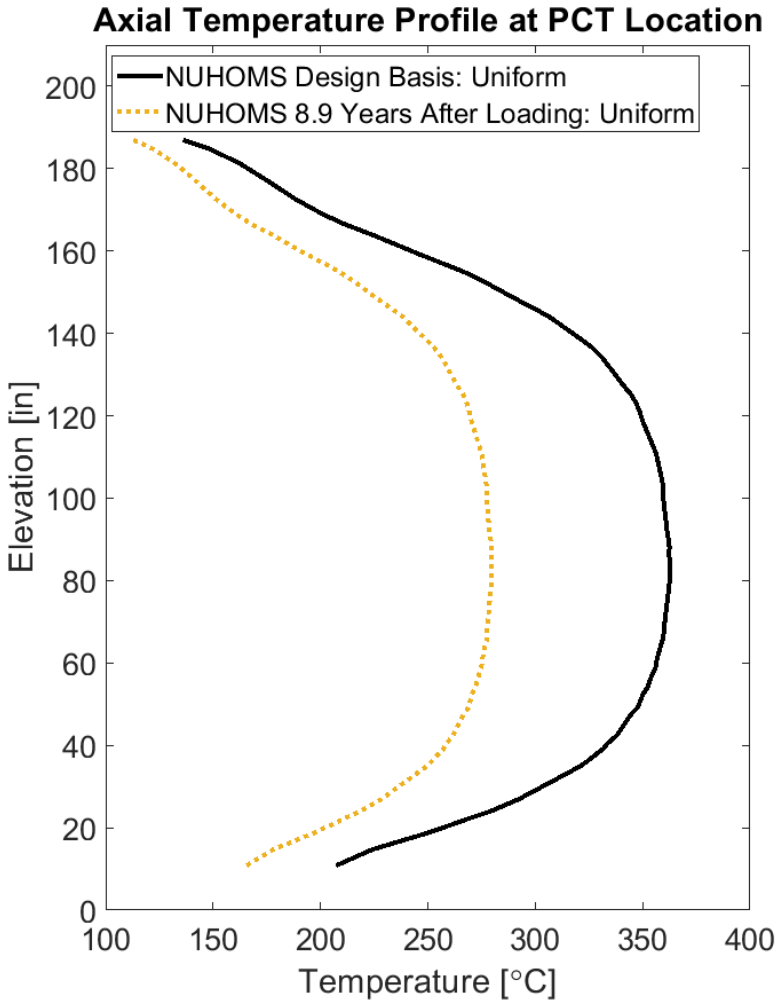

Figure 68. Temperature profiles of rods with PCT for design basis (32.0 kW) and final simulated heat loads (22.1 kW) from STAR-CCM+ NUHOMS uniform HLZC model.

3.3.2 HLZC 1

Table 13 lists the STAR-CCM+ results for the NUHOMS system for the HLZC 1 loading at several storage times. The storage times were chosen as a subset of the COBRA-SFS storage times to produce ~10°C temperature intervals in PCT. The system heat load, the heat load as a percentage of the design basis, the predicted PCT of the loading, the percentage of total cladding above 275°C, 300°C, and 350°C, and the percentage of cladding in the assembly containing the predicted PCT above 275°C, 300°C, and 350°C are listed.

Table 13. NUHOMS HLZC 1 tabular data from STAR-CCM+ model

Time in Storage		Heat Load		PCT	% Total Cladding Above			PCT Assembly % Cladding Above		
[years]	[months]	[kW]	[% DB]	[°C]	275°C	300°C	350°C	275°C	300°C	350°C
0.0	0.0	37.2	100.0%	399.6	60%	45%	17%	73%	67%	44%
0.1	1.0	36.7	98.6%	395.7	59%	44%	16%	73%	66%	41%
0.3	3.6	35.3	95.0%	384.7	55%	39%	11%	71%	64%	30%
0.5	6.5	34.0	91.5%	373.7	50%	34%	6%	69%	61%	17%
0.8	9.8	32.7	88.0%	363.2	46%	28%	2%	67%	58%	6%
1.1	13.7	31.5	84.6%	352.7	41%	23%	0%	64%	53%	1%
1.5	18.5	30.3	81.3%	343.3	35%	18%	0%	62%	51%	0%
2.1	25.2	28.8	77.5%	332.6	28%	12%	0%	59%	44%	0%
2.6	30.6	27.9	74.9%	325.0	23%	7%	0%	56%	35%	0%
3.2	38.9	26.7	71.9%	316.1	17%	2%	0%	51%	15%	0%
4.1	49.2	25.65	69.0%	307.6	12%	0%	0%	45%	5%	0%
5.3	63.6	24.53	65.9%	298.3	6%	0%	0%	32%	0%	0%
6.7	80.4	23.52	63.2%	290.0	2%	0%	0%	13%	0%	0%
8.7	104.5	22.43	60.3%	280.8	0%	0%	0%	3%	0%	0%

Figure 69 shows the cladding temperature histograms of a) total cladding temperature at the design basis heat load, b) PCT containing assembly at the design basis heat load, c) total cladding temperature at coldest simulated heat load, and d) coldest average assembly at the design basis heat load for the NUHOMS HLZC 1 from the STAR-CCM+ model.

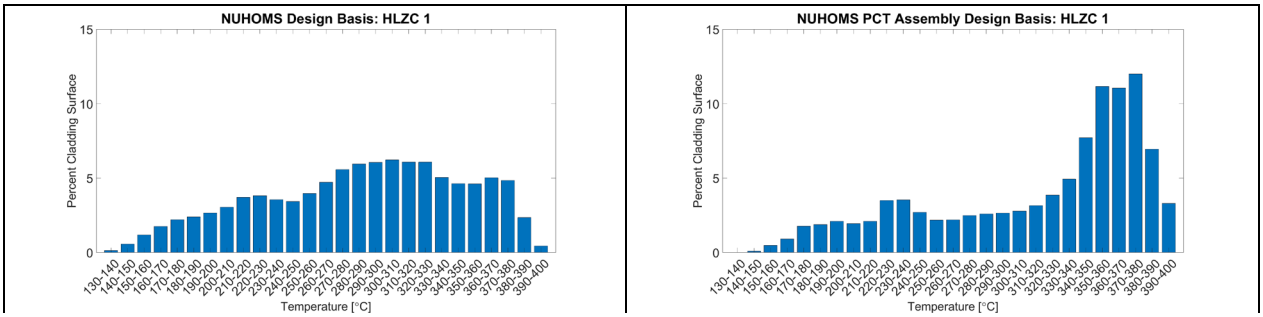

a) Total cladding temperature histogram for design basis heat load (37.2 kW)

b) PCT assembly cladding temperature histogram for design basis heat load (37.2 kW)

c) Total cladding temperature histogram for final simulated heat load (22.43 kW)

d) Coldest average assembly cladding temperature histogram for design basis heat load (37.2 kW)

Figure 69. Total and select assembly cladding temperature histograms at design basis heat load (37.2 kW) and final simulated heat load (22.43 kW) for the NUHOMS HLZC 1 from the STAR-CCM+ model

Figure 70 shows box plots for all the loadings. These plots summarize the maximum (PCT), 75th percentile, median, 25th percentile, and minimum cladding temperatures. Dashed lines for the 275°C, 300°C, and 350°C limits are also shown.

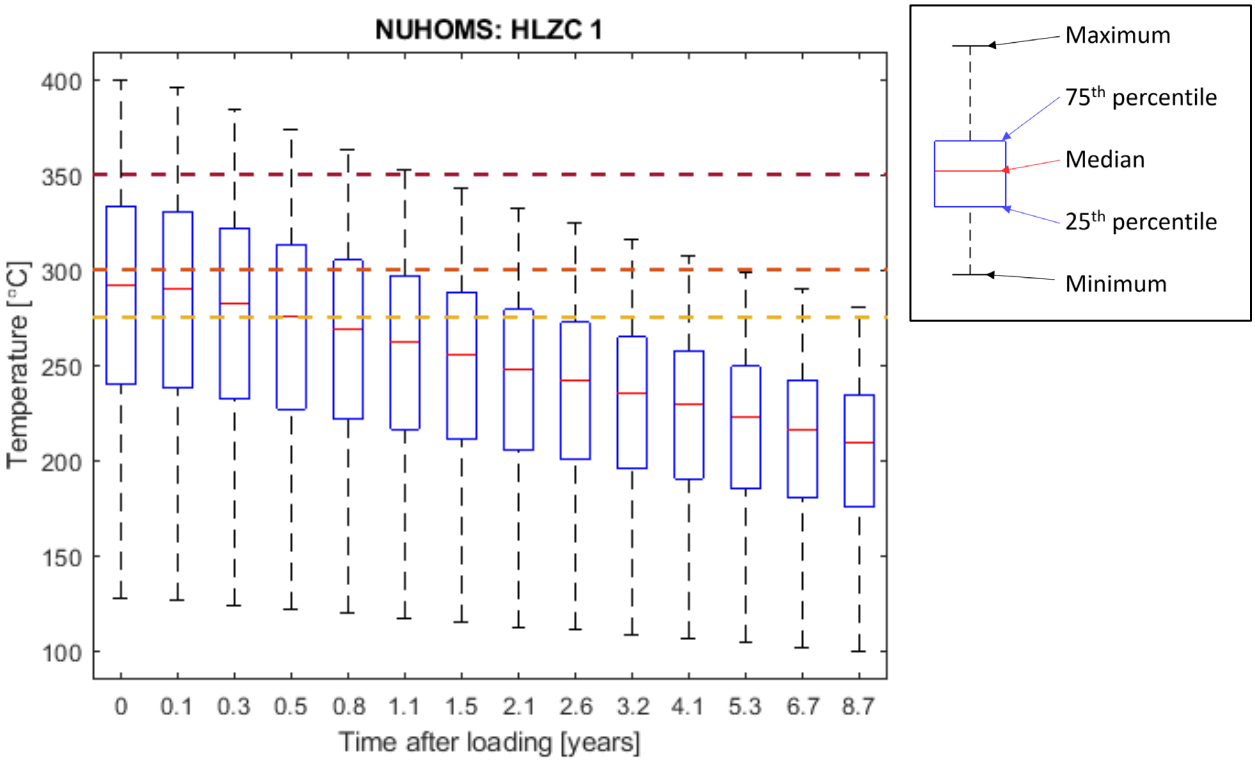

Figure 70. Box plot of HLZC 1 STAR-CCM+ NUHOMS model with temperature limits identified with dashed lines

Figure 71 shows a map of locations of the assemblies in the NUHOMS model. Each assembly is labeled with its local PCT, and the local percentage of cladding above 275°C, 300°C, and 350°C for the design basis HLZC 1 heat load.

PCT [°C]
Percent above 275°C
Percent above 300°C
Percent above 350°C

	334	350	350	335	
	56%	64%	64%	57%	
	30%	44%	45%	31%	
	0%	0%	0%	0%	
329	380	400	399	381	329
50%	70%	73%	73%	70%	51%
26%	62%	67%	67%	61%	26%
0%	23%	44%	45%	22%	0%
341	395	394	394	396	342
58%	73%	73%	73%	72%	58%
36%	66%	67%	66%	66%	36%
0%	39%	49%	49%	39%	0%
338	391	390	390	392	339
55%	71%	72%	72%	71%	56%
34%	64%	66%	66%	64%	34%
0%	34%	47%	47%	34%	0%
318	368	388	388	368	318
37%	65%	70%	70%	65%	37%
13%	53%	62%	63%	54%	14%
0%	11%	30%	30%	11%	0%
	313	331	331	314	
	31%	44%	45%	32%	
	9%	26%	26%	10%	
	0%	0%	0%	0%	

Figure 71. Assembly map with PCT and percent of cladding in each assembly above 275°C, 300°C, and 350°C for the design basis loading (37.2 kW) of the NUHOMS HLZC 1 from the STAR-CCM+ model.

Figure 72 shows the axial temperature profiles at the PCT location for the design basis and lowest simulated heat load.

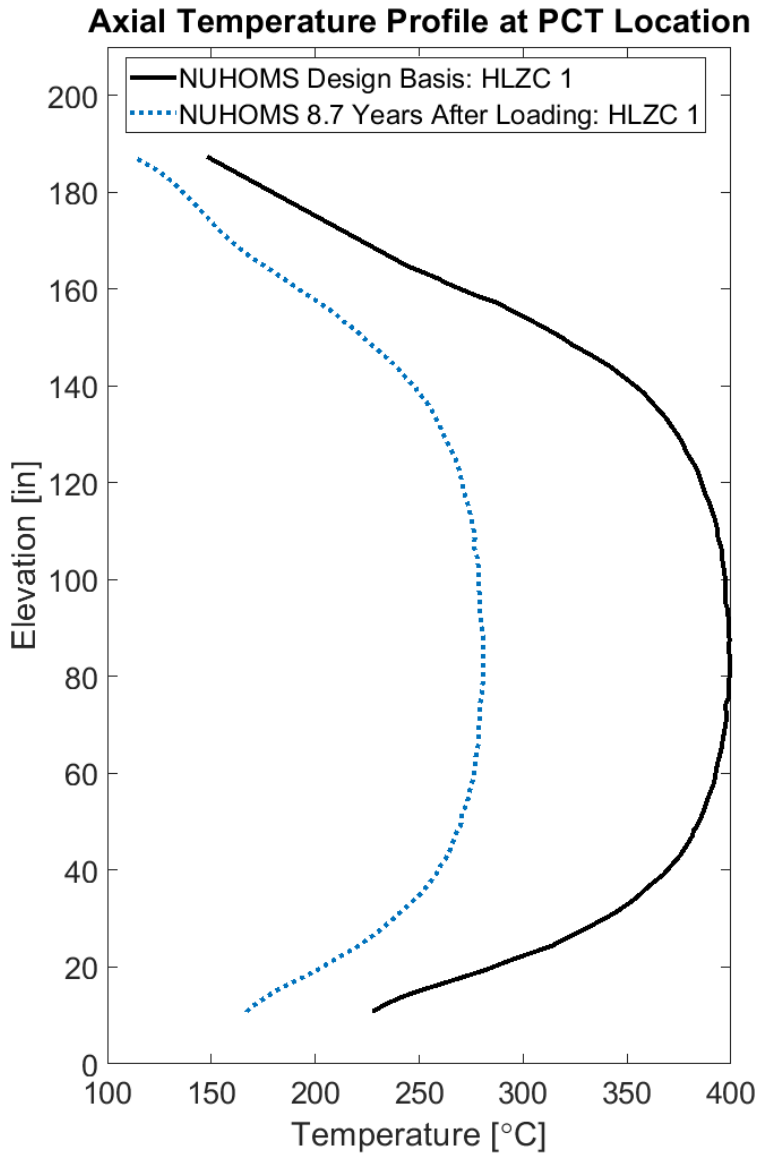

Figure 72. Temperature profiles of rods with PCT for design basis (37.2 kW) and final simulated heat loads (22.43 kW) from STAR-CCM+ NUHOMS HLZC 1model.

3.3.3 HLZC 2

Table 14 lists the STAR-CCM+ results for the NUHOMS system for the HLZC 2 loading at several storage times. The storage times were chosen as a subset of the COBRA-SFS storage times to produce ~10°C temperature intervals in PCT. The system heat load, the heat load as a percentage of the design basis, the predicted PCT of the loading, the percentage of total cladding above 275°C, 300°C, and 350°C, and the percentage of cladding in the assembly containing the predicted PCT above 275°C, 300°C, and 350°C are listed.

Table 14. NUHOMS HLZC 2 tabular data from STAR-CCM+ model

Time in Storage		Heat Load		PCT	% Total Cladding Above			PCT Assembly % Cladding Above		
[years]	[months]	[kW]	[% DB]	[°C]	275°C	300°C	350°C	275°C	300°C	350°C
0.0	0.0	35.2	100.0%	383.2	54%	38%	10%	71%	64%	40%
0.4	4.7	33.3	94.5%	368.9	48%	30%	3%	68%	60%	18%
0.7	8.2	32.2	91.4%	360.6	44%	26%	1%	66%	58%	7%
1.0	11.8	31.1	88.4%	352.6	39%	21%	0%	64%	55%	1%
1.4	16.4	30.1	85.4%	344.5	34%	17%	0%	62%	51%	0%
1.9	22.3	28.8	81.8%	334.6	28%	11%	0%	59%	44%	0%
2.4	28.7	27.8	79.0%	326.7	23%	7%	0%	56%	35%	0%
3.1	37.3	26.6	75.7%	317.5	17%	2%	0%	51%	16%	0%
4.0	48.5	25.5	72.6%	308.6	12%	0%	0%	45%	5%	0%
5.3	63.7	24.4	69.4%	299.3	6%	0%	0%	33%	0%	0%
7.0	83.8	23.32	66.2%	289.7	2%	0%	0%	12%	0%	0%
9.2	110.4	22.19	63.1%	280.0	0%	0%	0%	2%	0%	0%

Figure 73 shows the cladding temperature histograms of a) total cladding temperature at the design basis heat load, b) PCT containing assembly at the design basis heat load, c) total cladding temperature at coldest simulated heat load, and d) coldest average assembly at the design basis heat load for the NUHOMS HLZC 2 from the STAR-CCM+ model.

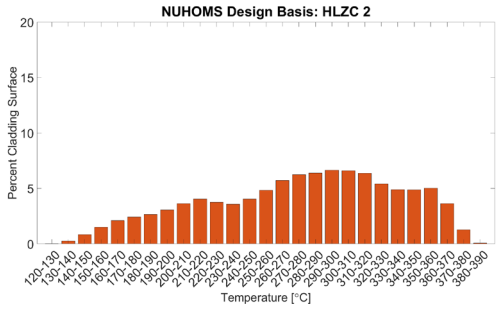

a) Total cladding temperature histogram for design basis heat load (35.2 kW)

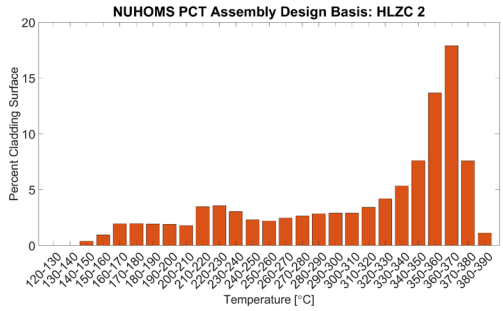

b) PCT assembly cladding temperature histogram for design basis heat load (35.2 kW)

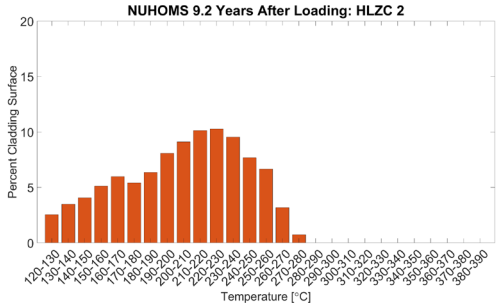

c) Total cladding temperature histogram for final simulated heat load (22.19 kW)

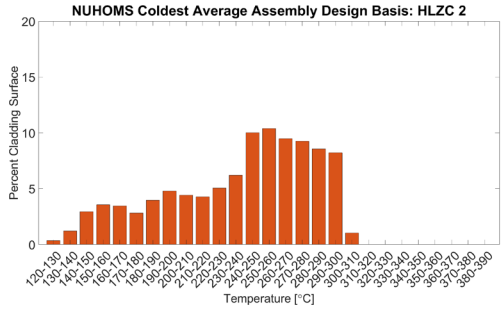

d) Coldest average assembly cladding temperature histogram for design basis heat load (35.2 kW)

Figure 73. Total and select assembly cladding temperature histograms at design basis heat load (35.2 kW) and final simulated heat load (22.19 kW) for the NUHOMS HLZC 2 from the STAR-CCM+ model

Figure 74 shows box plots for all the loadings. These plots summarize the maximum (PCT), 75th percentile, median, 25th percentile, and minimum cladding temperatures. Dashed lines for the 275°C, 300°C, and 350°C limits are also shown.

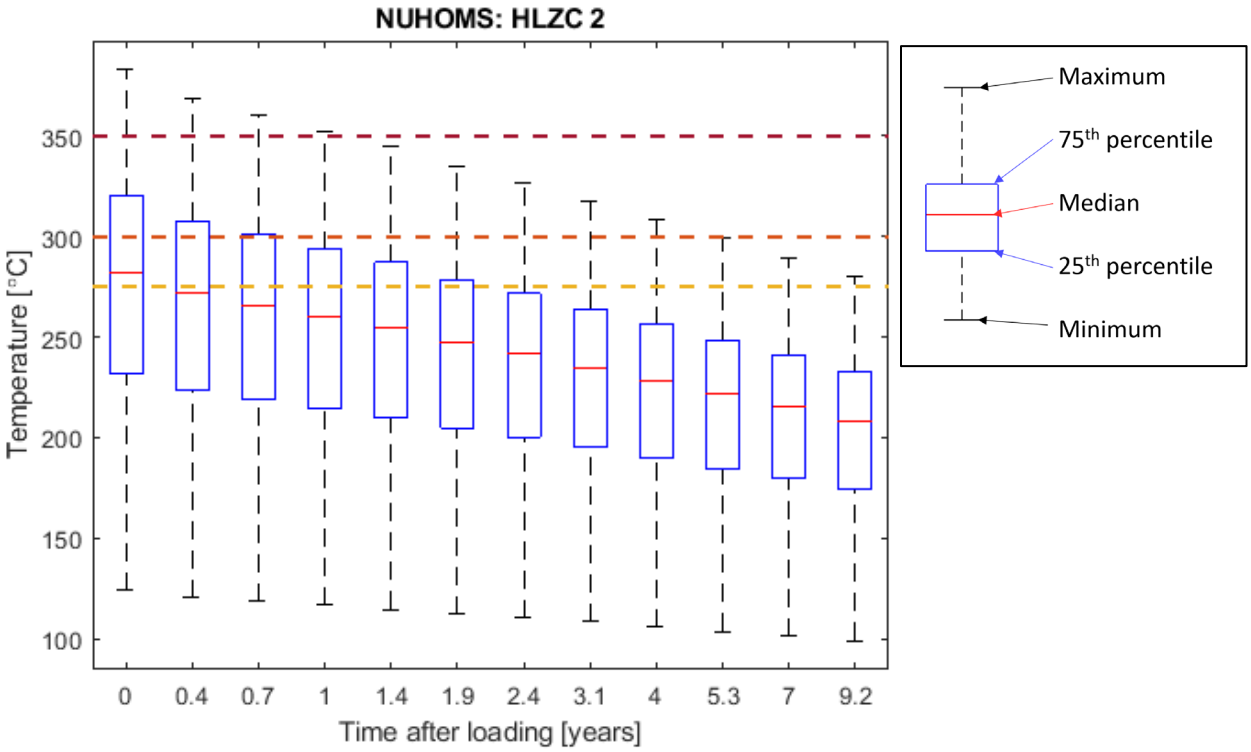

Figure 74. Box and whisker plots for each of the simulated loadings of the NUHOMS HLZC 2 loading from the STAR-CCM+ model.

Figure 75 shows a map of locations of the assemblies in the NUHOMS model. Each assembly is labeled with its local PCT, and the local percentage of cladding above 275°C, 300°C, and 350°C for the design basis HLZC 2 heat load.

PCT [°C]
Percent above 275°C
Percent above 300°C
Percent above 350°C

	324 48% 20% 0%	338 59% 36% 0%	338 59% 36% 0%	324 48% 20% 0%	
319 41% 16% 0%	363 66% 55% 6%	381 71% 63% 27%	381 70% 63% 27%	363 66% 55% 6%	319 41% 16% 0%
330 49% 28% 0%	377 69% 62% 22%	383 71% 64% 40%	383 71% 64% 40%	377 69% 61% 22%	330 49% 27% 0%
327 46% 25% 0%	373 68% 60% 17%	379 70% 63% 35%	379 70% 63% 35%	373 68% 60% 17%	327 46% 25% 0%
308 27% 5% 0%	350 60% 43% 0%	369 66% 57% 12%	369 66% 58% 12%	351 60% 44% 0%	308 27% 4% 0%
	303 22% 1% 0%	319 38% 16% 0%	319 38% 16% 0%	304 22% 1% 0%	

Figure 75. Assembly map with PCT and percent of cladding in each assembly above 275°C, 300°C, and 350°C for the design basis loading (35.2 kW) of the NUHOMS HLZC 2 from the STAR-CCM+ model.

Figure 76 shows the axial temperature profiles at the PCT location for the design basis and lowest simulated heat load.

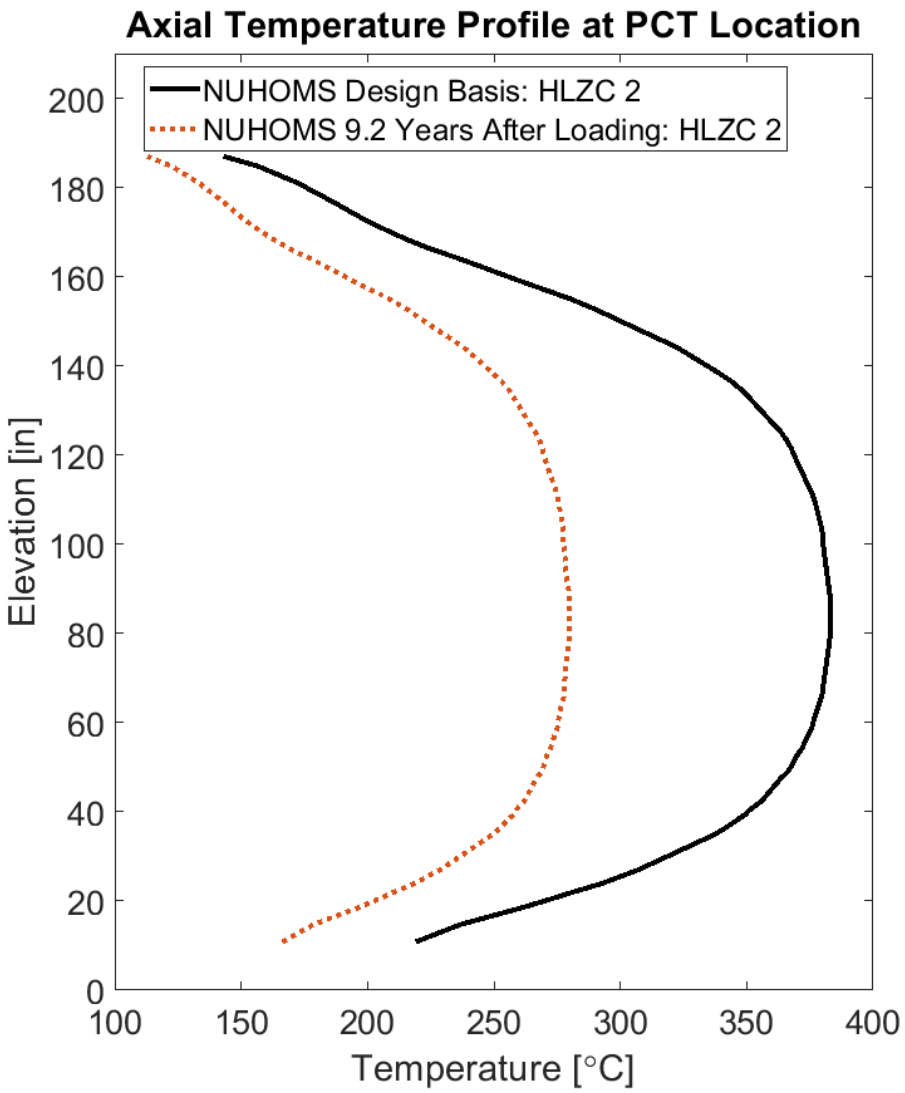

Figure 76. Temperature profiles of rods with PCT for design basis (35.2 kW) and final simulated heat loads (22.19 kW) from STAR-CCM+ NUHOMS HLZC 2 model.

This page is intentionally left blank.

4. DISCUSSION

This section discusses the results presented in Section 3 in comparison to each other and the temperature cutoffs studied. The TN-32 model is not included here because the PCT modeled was 265.7 °C, which is below the 275 °C temperature cutoff. Therefore, all of the cladding surface area is well below a temperature that would potentially cause annealing.

The most impactful comparisons to draw conclusions about the U.S. fleet are provided by Figure 77 through Figure 84 which show how two completely different storage system designs provide relatively similar thermal performance through the entire storage lifecycle. Although the PCT is different between the two casks, the cladding temperature percent cutoff plots are within 10-15% at most time periods and heat loads. This shows that broad conclusions about fuel performance can likely be drawn from analyzing a relatively small number of cask designs. It is noted that the total decay heat varies between the two systems as well as between loading patterns (HLZC).

The effect of loading pattern is clearly shown by examining the differences in the plots of percentage through time vs the plots of percentage against heat load. When plotted through time the temperature results show a clear difference relative to loading pattern. This is due to the differential cooling rate of the preferential assemblies. In the temperature against heat load plots, although the codes predict different temperatures there is no significant difference between cladding temperatures of different patterns at the same heat load. This result also indicates a fundamental thermal performance property of the cask. Although PCT may be well correlated to loading pattern, average cladding temperatures are far more strongly correlated to total heat load.

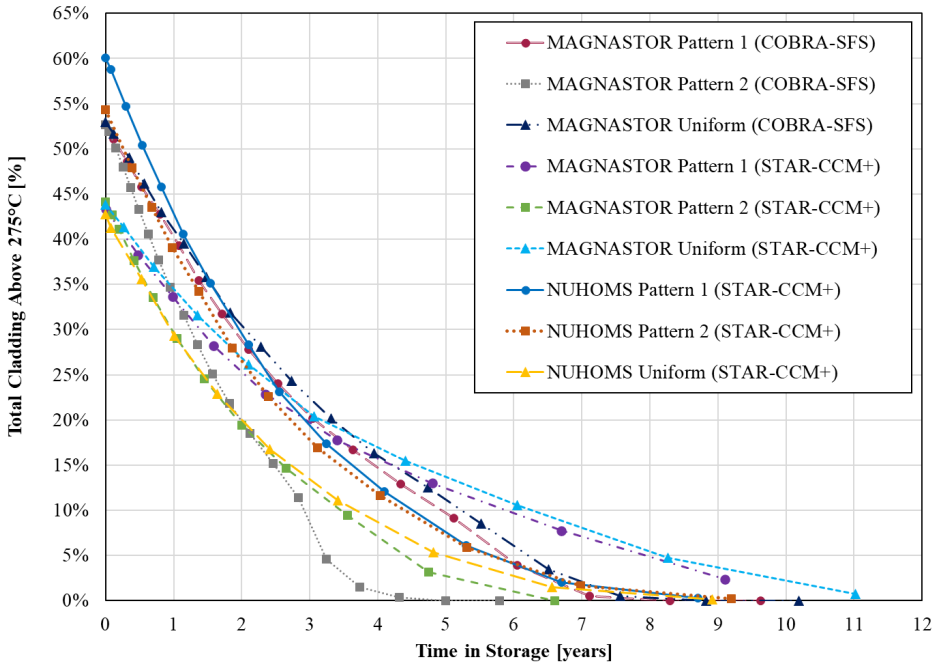

Figure 77. Time in Storage vs. Percent Clad Surface Area above 275 °C for MAGNASTOR and NUHOMS

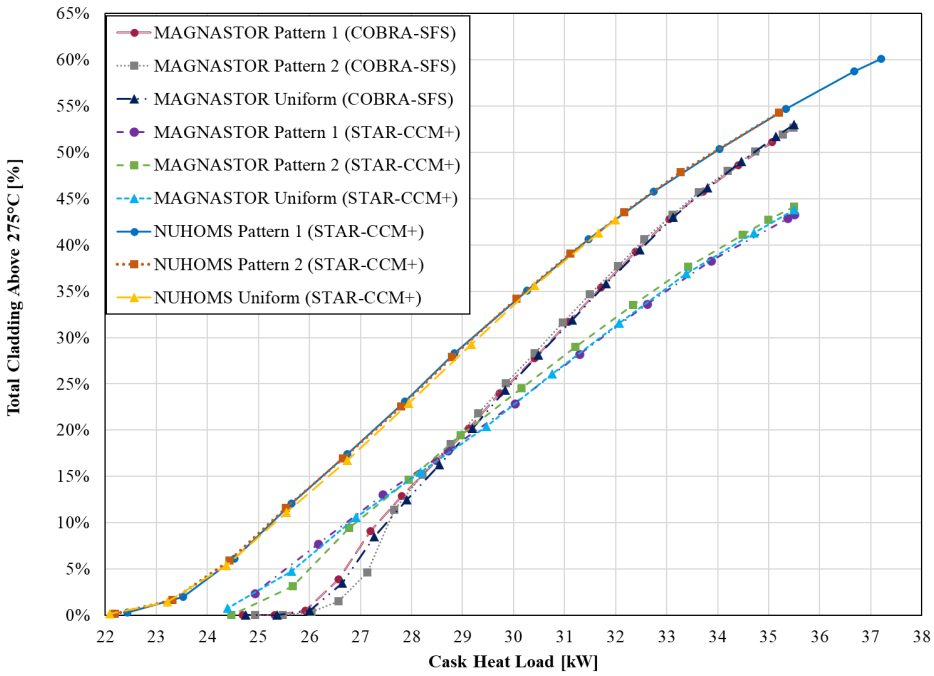

Figure 78. Heat Load vs. Percent Clad Surface Area above 275 °C for MAGNASTOR and NUHOMS

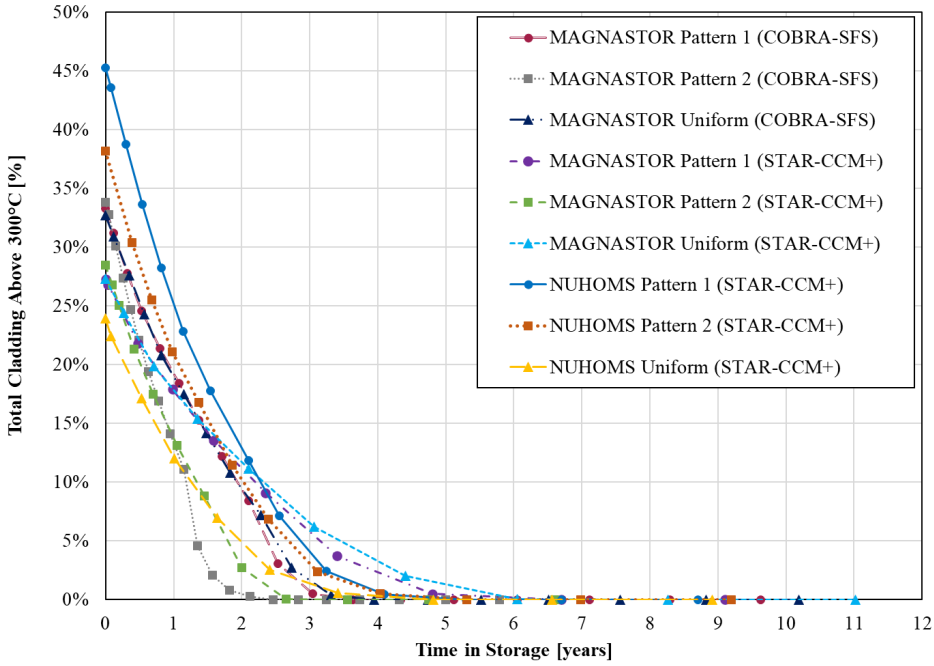

Figure 79. Time in Storage vs. Percent Clad Surface Area above 300 °C for MAGNASTOR and NUHOMS

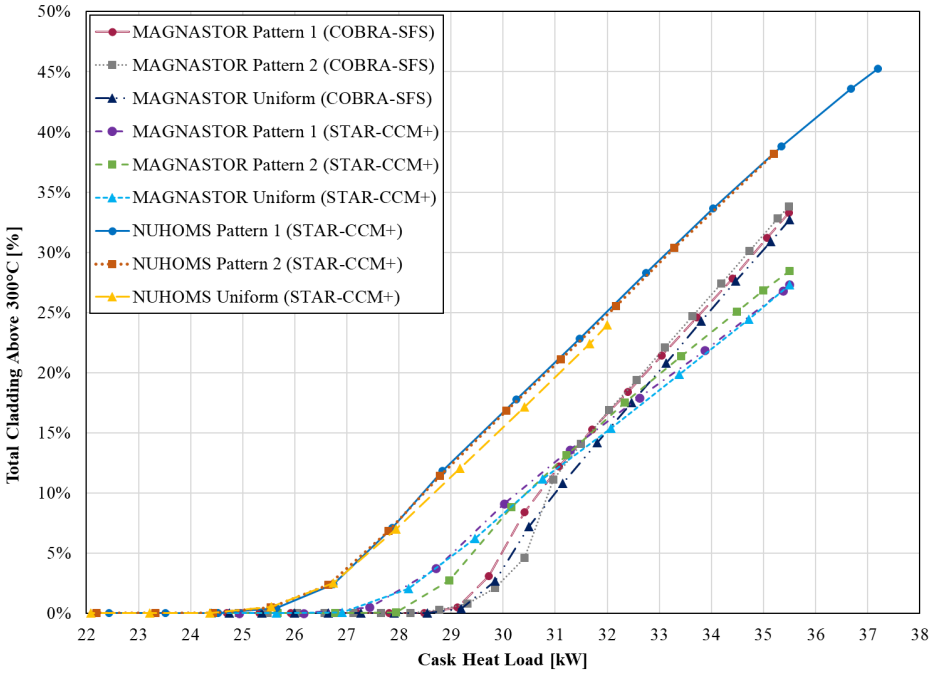

Figure 80. Heat Load vs. Percent Clad Surface Area above 300 °C for MAGNASTOR and NUHOMS

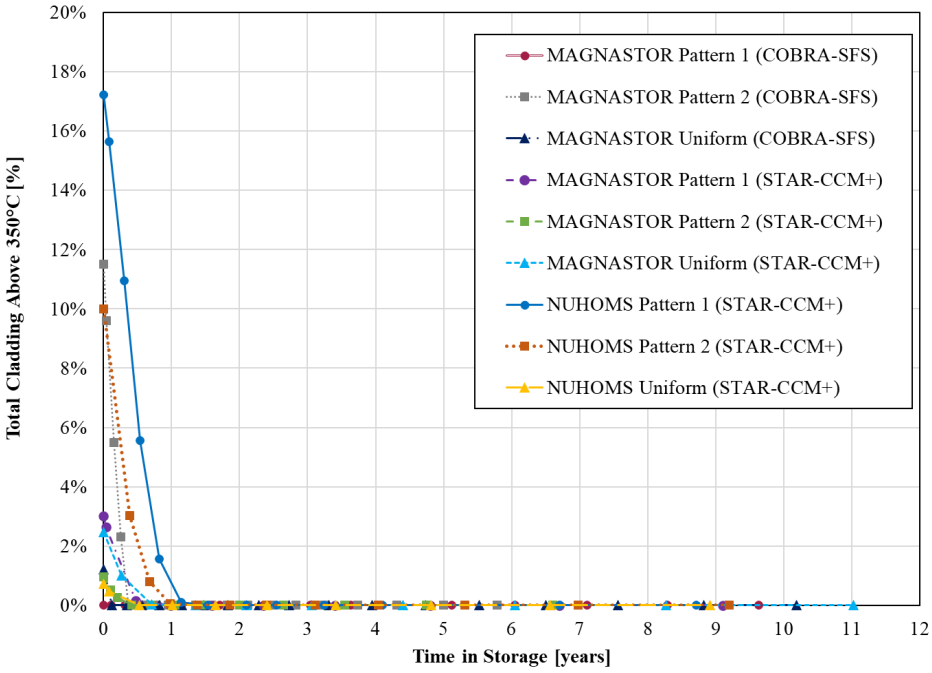

Figure 81. Time in Storage vs. Percent Clad Surface Area above 350 °C for MAGNASTOR and NUHOMS

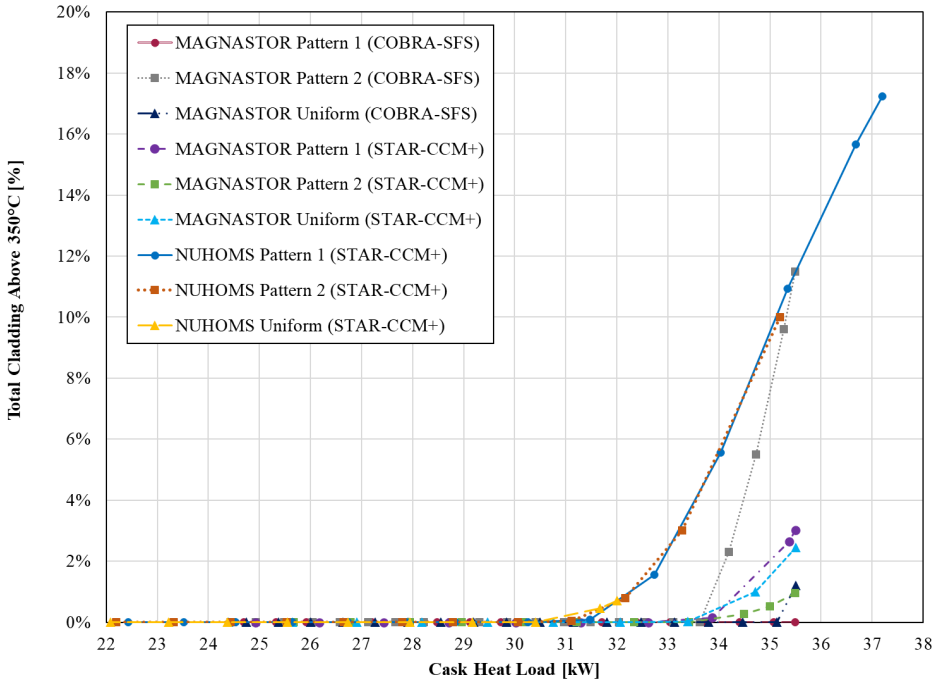

Figure 82. Heat Load vs. Percent Clad Surface Area above 350 °C for MAGNASTOR and NUHOMS

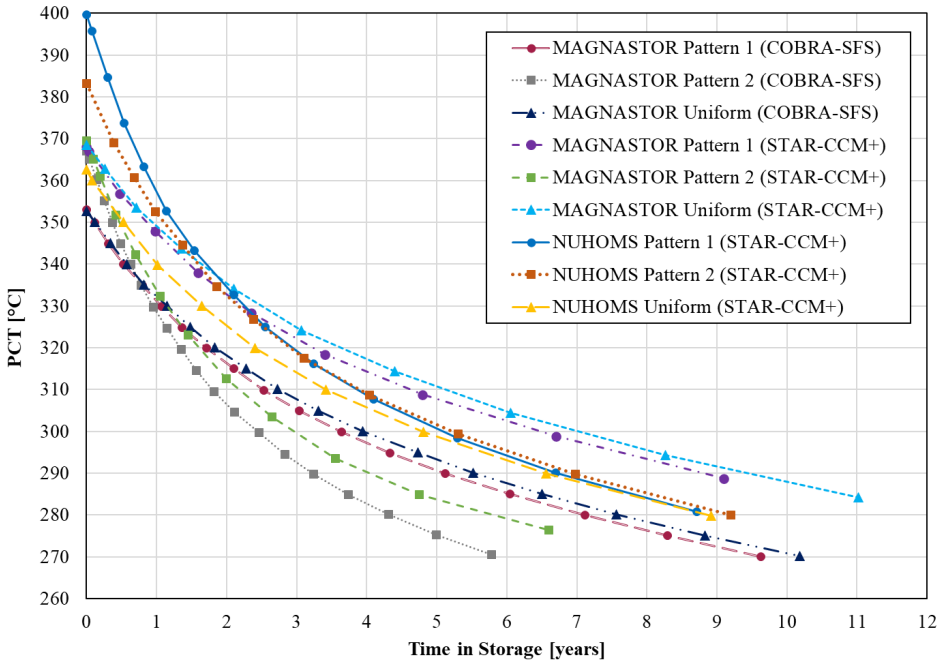

Figure 83. Time in Storage vs. PCT for MAGNASTOR and NUHOMS

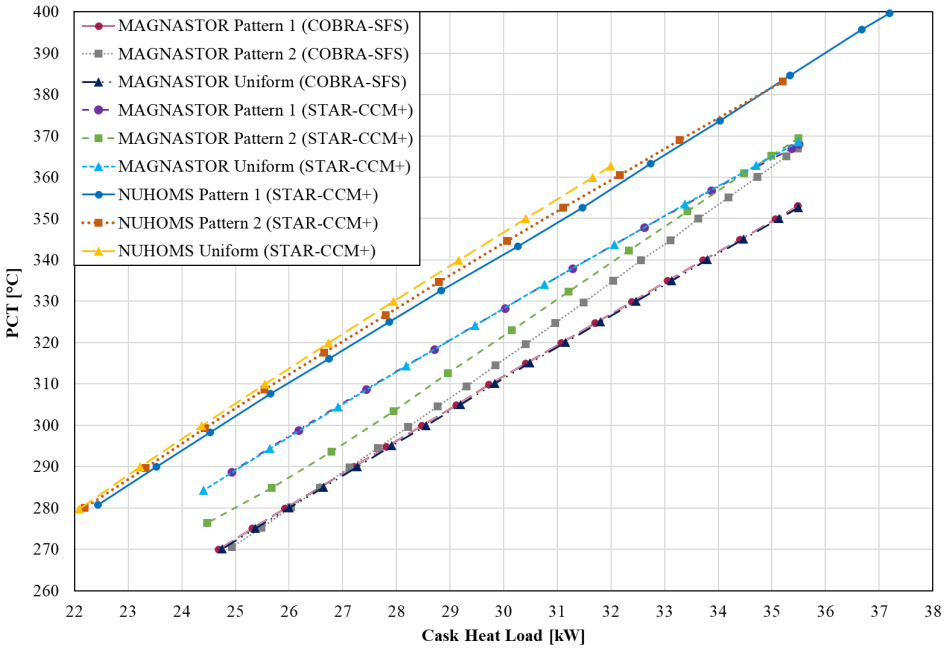

Figure 84. Heat Load vs. PCT for MAGNASTOR and NUHOMS

Figure 87 through Figure 92 show results separated by cask design. This allows a better comparison between codes in the case of the MAGNASTOR. Relatively good agreement between the COBRA-SFS and STAR-CCM+ models is shown for the PCT with an approximately 15 °C difference. The STAR-CCM+ model is consistently hotter than the COBRA-SFS model. This result is expected due to the porous media fuel representation, which is designed to be inherently conservative, although the entire difference cannot be accounted for solely by that factor. There are differences in the STAR-CCM+ and COBRA-SFS modeling of both the internal and external fluid flow. Because there is no validation data specific to the MAGNASTOR cask. it is not possible to isolate the effects of these differences. This result supports the decision to use multiple codes for higher assurance that results are reasonable. One specific difference in the COBRA-SFS model is that there is no adjustment for pressure drop in the canister as the heat load goes down which would tend to model internal convective cooling as stronger than reality at low heat loads.

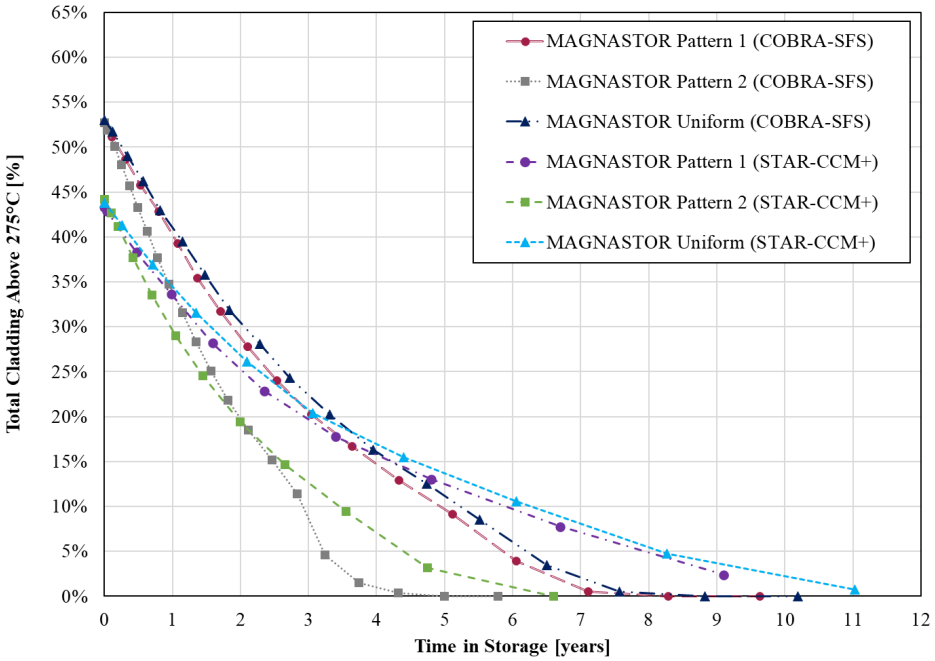

Figure 85. Time in Storage vs. Percent Cladding above 275 °C for MAGNASTOR

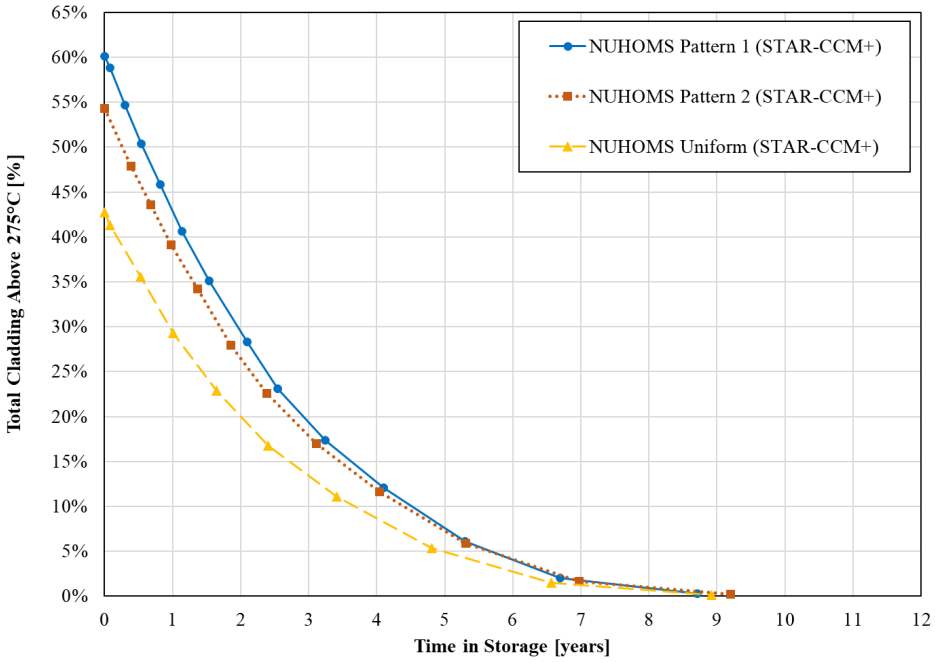

Figure 86. Time in Storage vs. Percent Cladding Above 275 °C for NUHOMS

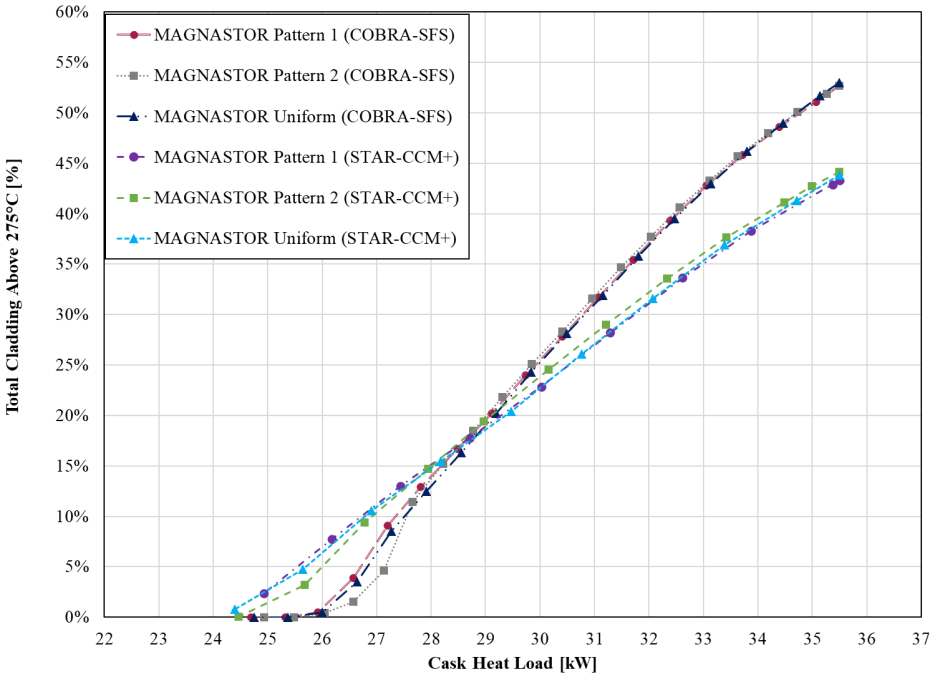

Figure 87. Heat Load vs. Percent Cladding above 275 °C for MAGNASTOR

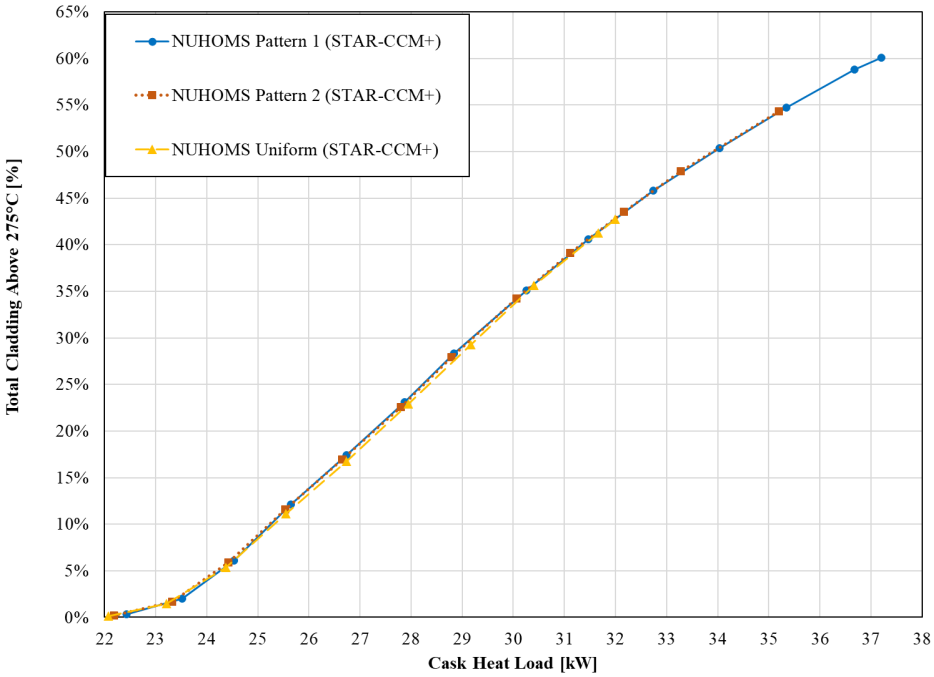

Figure 88. Heat Load vs. Percent Cladding above 275 °C for NUHOMS

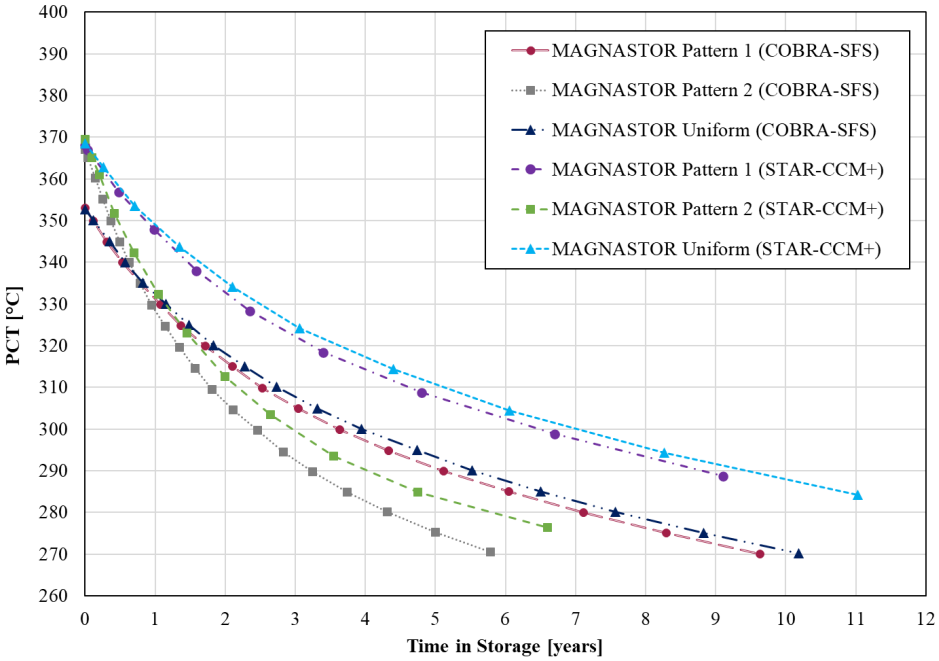

Figure 89. Time in Storage vs. PCT for MAGNASTOR

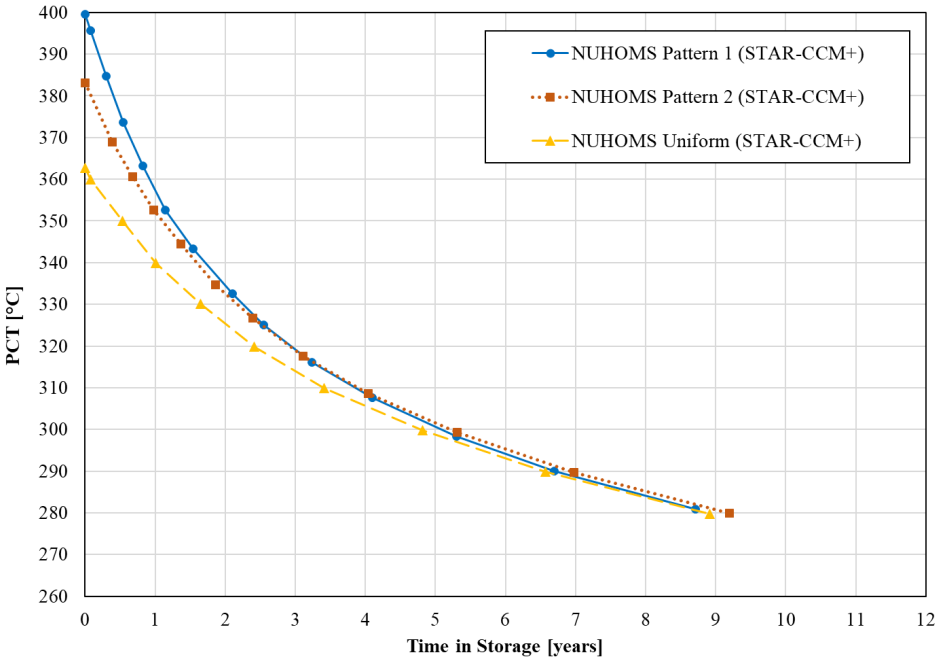

Figure 90. Time in Storage vs. PCT for NUHOMS

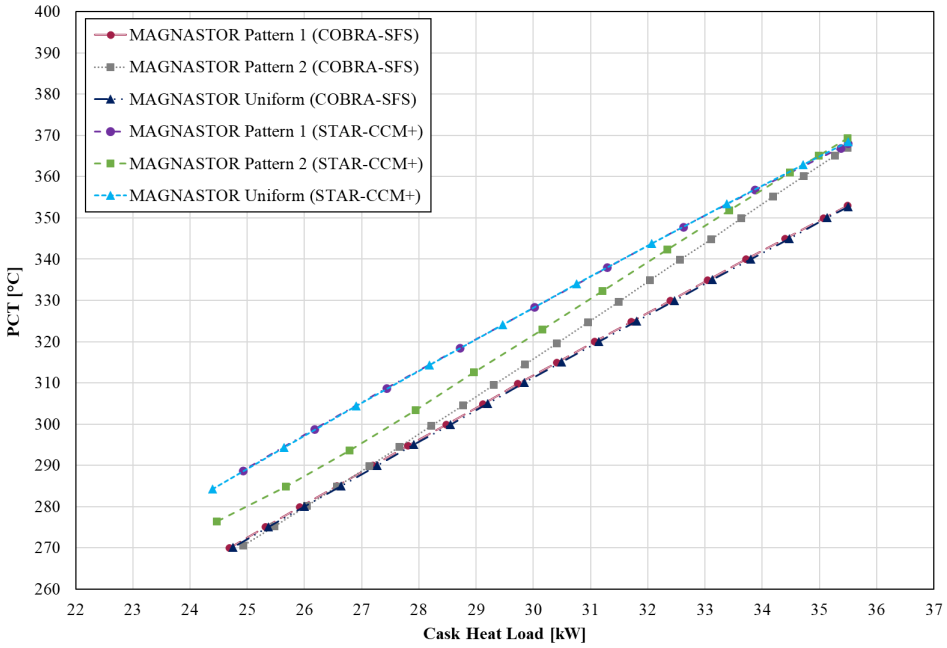

Figure 91. Heat Load vs. PCT for MAGNASTOR

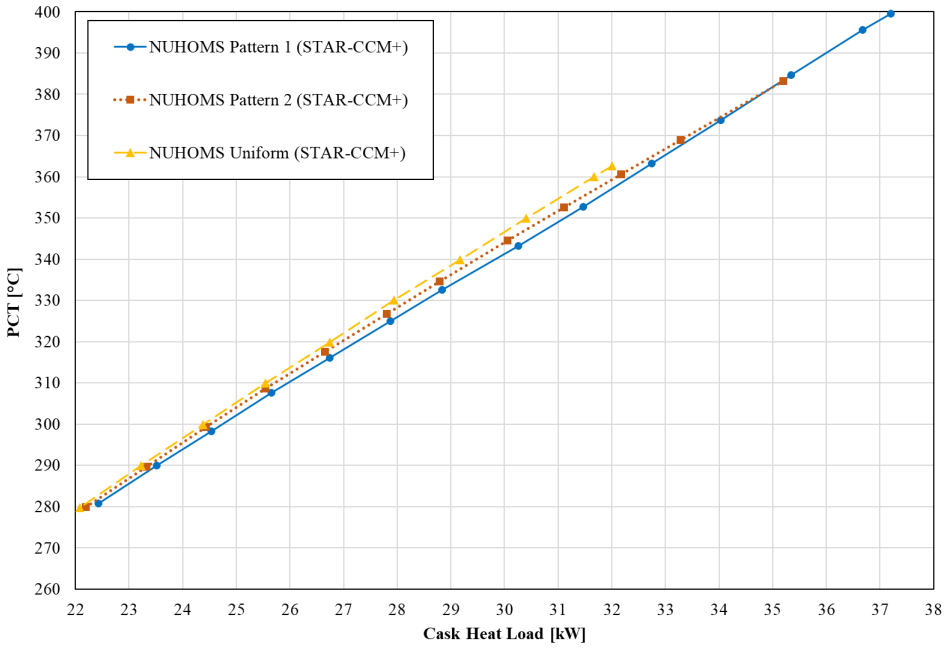

Figure 92. Heat Load vs. PCT for NUHOMS

This page is intentionally left blank.

5. CONCLUSIONS

This report shows the process of modeling SNF cladding temperatures through time in three different storage cask designs to support understanding of the extent of SNF cladding annealing that may occur in representative systems. The modeling required examination of decay heat and thermal performance. The three casks modeled (TN-32, MAGNASTOR, and NUHOMS) encompass the wide range of cask design types in use in the U.S. fleet. These are vertical dual-purpose, vertical ventilated, and horizontal ventilated designs. The decay heats modeled were conservative relative to in service casks, however, they still fall within a realistic range of what might be loaded in the U.S. contemporaneously to this report. Two different thermal analysis codes were used to provide better assurance of reasonable results. The results presented focused on percentage of cladding surface temperature above proposed cutoff points that may be relevant to cladding annealing. These results show a clear dependence on heat load pattern in time, however when compared to across total heat load, there is little difference at a consistent heat load. One area for future work would be to confirm these results with more casks designs such as the HOLTEC HI-STORM FW or a NUHOMS module using the EOS canister. These are two PWR systems that also hold 37 assemblies. In the case of the EOS canister is has a higher design basis heat load, however for all designs cladding temperatures are still ultimately limited by the NRC guidance limit of 400 °C. The PWR results are generally applicable to BWR fuel, however, BWR casks tend to be cooler, even at design basis heat load. A BWR cask design would be a useful model to understand and potentially rule out the potential for annealing and other thermally driven fuel performance issues in BWR cladding.

This page is intentionally left blank.

6. REFERENCES

Banerjee, K., et al. (2023). The Data And Analyses Needed to Support Large-Scale Spent Nuclear Fuel Transportation in the United States. Proceedings of the 20th International Symposium on the Packaging and Transportation of Radioactive Materials. Juan-les-Pins, France.

Fort, J., et al. (2016). Thermal Modeling of a Loaded Storage System at Catawba Nuclear Station, PNNL. PNNL-25871.

NAC International (2015). MAGNASTOR Final Safety Analysis Report. Norcoss, GA.

Richmond, D. J., et al. (2023). COBRA-SFS Version 6.2.1. Richland, WA, PNNL.

Richmond, D. J. and B. J. Jensen (2022). Environmental Impacts on Thermal Performance of Spent Fuel Storage Systems. International High Level Radioactive Waste Management, American Nuclear Society.

Richmond, D. J., et al. (2022). Uncertainty in Thermal Modeling of Spent Nuclear Fuel Casks. Richland, WA, PNNL.

Siemens Industries Digital Software (2022). Simcenter STAR-CCM+ Version 2210, Siemens.

Stefanovic, P., et al. (2023). STANDARDS 5.0. Richland, WA, PNNL.

Transnuclear Inc. (2006). Updated Final Safety Analysis Report For the Standardized NUHOMS Horizontal Modular Storage System of Irradiated Nuclear Fuel. Columbia, MD.

Transnuclear Inc. (2012). TN-32 Updated Final Safety Analysis Report Revision 5. Columbia, MD.

Wieselquist, W. A., et al. (2020). SCALE 6.2.4. Oak Ridge, TN.